Assessment of Integrated Multi-Product Biorefineries

by

Temitayo Giwa

A thesis submitted in partial fulfillment of the requirements for the degree of

Master of Science
in
Engineering Management

Department of Mechanical Engineering
University of Alberta

Abstract

Concerns about the climate and the need for energy security motivate the shift towards sustainable means of energy production. Biorefineries are facilities that convert biomass into material and energy products. Biorefineries are a key component of ensuring increased sustainability of the global energy mix and for decarbonization of demand sectors such as transportation and power generation. However, economic viability have hampered commercial adoption of biorefineries. There have been efforts to improve the economics of biorefineries, but more efforts are needed.

The traditional approach in biorefining focuses on the production of one product or material path at a time. This approach limits the opportunity to fully use the original feedstock and thus derive maximum value. A multi-product approach, wherein multiple material paths are valorized to produce multiple products from a biorefinery, has been the subject of interest recently. This approach encourages the full use of the original feedstock and increases the revenue stream of the biorefinery. Hence, it has the potential to improve the economics of a biorefinery. The multi-product approach has been applied to various biomass valorization technologies like fast-pyrolysis. However, the application of this approach to the fast-pyrolysis process has been limited to the bio-oil material flow path, with the biochar and non-condensable gases material flow paths being ignored and used for less valuable applications like combustion.

The aim of this research is to investigate the economic and environmental implications of additional products produced through the valorization of biochar and hydrogen-rich non-condensable gases in a fast-pyrolysis biorefinery. Simulation models were developed for six different scenarios of modified biorefineries for value-adding to biochar and non-condensable gases and were compared to a conventional fast pyrolysis biorefinery. The scenarios differ by three proposed uses of the non-condensable gases and two types of external fuel, namely, natural gas

and woodchips. It is assumed that ethanol is produced from both biochar and non-condensable gases and hydrogen from the non-condensable gases, depending on the scenario. The economic performance of the biorefineries was assessed using the internal rate of return, while the environmental performance was measured using the life cycle net energy ratio and greenhouse gas emissions of the biorefineries and their products.

The research findings show that multi-product approach improves the economic performance of biorefineries compared to the conventional fast pyrolysis process. The conventional fast pyrolysis process, the base case, has a rate of return of 7%, while the assessed scenarios have rate of return values in the range of 7.5 – 13%. However, the conversion of the original feedstock, in the assessed scenarios, did not show marked improvement relative to the conventional fast pyrolysis process. Generally, the products of the biorefineries showed lower greenhouse gas emissions intensity than their fossil counterparts. The results of this research will be of value to decision-makers in the public and private sectors.

Preface

This thesis is an original work by Temitayo Giwa under the supervision of Dr. Amit Kumar. Chapter 2 and Chapter 3 will be submitted for publication in peer-reviewed journals as "Techno-economic assessment of an integrated biorefinery producing bio-oil, ethanol, and hydrogen" and "Life cycle net energy ratio and greenhouse gas emissions assessments of an integrated biorefinery producing bio-oil, ethanol, and hydrogen" by Temitayo Giwa, Maryam Akbari, and Amit Kumar. Chapter 4, titled "Analysis of the GHG abatement cost of biorefinery products," builds on the assessment and results of Chapters 2 and 3.

I was responsible for the research conceptualization, model development, analysis, and manuscript composition. Dr. Maryam Akbari contributed by providing research guidance, assistance with model development, and manuscript review. Dr. Amit Kumar was involved in idea conceptualization, guidance on research direction, and support with the manuscript composition and review.

For

Olufunke and Molayo

Acknowledgements

My Master's program has been a life-changing opportunity in my career journey. It would not have been possible without Dr. Amit Kumar, my supervisor. I want to thank Dr. Kumar for creating a space where careers are built. I admire his hard work, intelligence, and diligence in all he does. I am grateful for the growth and lessons learned and opportunities throughout the program.

I appreciate the financial support provided by the NSERC/Cenovus/Alberta Innovates Associate Industrial Research Chair in Energy and Environmental Systems Engineering and the Cenovus Energy Endowed Chair in Environmental Engineering for this research.

I would like to thank Dr. Maryam Akbari for her unceasing support from the first day. Thank you for not just being a superior but also being a friend. Her kindness and encouragement sustained my effort to push to the end. I would also like to thank Astrid Blodgett for her editorial assistance.

I am grateful to Dr. Abayomi Oni for his belief in me, mentorship, and guidance. I am thankful to his family for their support and making my transition and living in Canada a smooth one. I would also like to extend my gratitude to my friends Mubarak and Yusuf for making Canada a memorable experience. I also appreciate my friends and colleagues at the University of Alberta that made the journey a memorable one for me.

Special thanks to my mother, Olufunke, and brother, Molayo, for their moral support throughout my life's journey. They have both been my inspiration to continue to strive for the better.

Above all, to God almighty, the one who orders my steps.

Table of Contents

List of Tables

List of Figures

Chaper 1 Introduction

1.1 Background

The rise in prosperity correlates with the rise in energy use in the development of most nations [1]. Currently, most of this energy consumption is met by fossil fuels. Fossil fuels still play an important role in the global economy, as about 85% of the 173,340 terawatt-hours of energy consumed in 2019 came from fossil fuel sources [2]. However, there are concerns about the environmental impact of burning fossil fuels, and more energy supply security assurance is needed in the face of volatile oil prices [3] and increasing energy demand [4]. It is therefore imperative to find ways to reduce our dependence on fossil fuel consumption and increase the security of energy supply.

Alternative energy sources are being introduced. The bulk of renewable energy deployments is limited to solar and wind power. The electricity sector has seen an impressive amount of solar and wind technology penetration in recent years. Between 2010 and 2020, there was a 10% net increase in the contribution of renewables to the global electricity mix [5]. However, there are drawbacks to these renewable sources such as intermittency and uneven geographical distribution, thus demand is met by fossil resources.

While electricity generation benefits from solar and wind technologies, some sectors are difficult to decarbonize with solar and wind power. The transportation sector, for instance, relies heavily on liquid fuels (about 95%), and about 55% of global liquid fuel is consumed in this sector [6]. Liquid fuels are preferred in the transportation sector because of their availability, high volumetric energy density, convenience of use, and affordability [7, 8]. Moreover, in recent years, most transportation infrastructure has been designed for internal combustion engines, which use liquid

fuel, mostly gasoline and diesel; it would take many years and considerable cost to replace these [8]. And, while alternative vehicles are being developed, they have drawbacks, including higher costs and a shorter driving range [9]. The petrochemical sector is an important industry whose products are ubiquitous. Aside from its use in transportation, petroleum is used in petrochemical feedstock production. The chemical and petrochemical sector is a large greenhouse gas (GHG) emitter. In 2010, this sector emitted about 1.24 Gt CO_2eq [10]. The emissions intensity of the sector is not surprising given its high energy intensity and reliance on petroleum. A shift away from the petroleum-based petrochemical precursors would require an equivalent replacement from cleaner sources. Besides the transportation and petrochemical sector, the industrial sector, is also difficult to decarbonize.

Biorefineries can meet the needs of these hard-to-decarbonize sectors as many of the materials, chemicals, and fuels produced from fossil resources can be produced from biomass using the appropriate technology. Today, the main products of biorefineries are bio-fuels, primarily bio-ethanol and bio-diesel, which are produced from food-based biomass. The production of bio-fuel from food crops has raised concerns about the sustainability of these bio-fuels because of their potential impact on food prices. Consequently, there have been many studies on the use of non-food-based biomass as feedstock in biorefineries. The studied feedstocks include forest biomass [11], agricultural residue [12], herbaceous crops [13], and algae [14]. Many products have been identified as outputs of the biorefining of these feedstocks, i.e., ethanol [15], renewable diesel [11], renewable natural gas [16], hydrogen [17], butanol [18], benzene [19], and asphalt [19].

Biorefineries can satisfy our demand for material and energy and play a role in the global energy transition and thereafter. Despite the potential, high costs (along with low technology readiness levels) have impeded large-scale commercialization needed to meet the growing demand for

renewable fuels and materials [20]. Traditional approaches to biorefining, moreover, focus on a single product or material flow path at a time. These approaches result in by-products and side streams that are used for less valuable applications (such as combustion) to satisfy the heat demand of the biorefinery. Hence, the potential to gain the maximum value from a feedstock is limited. The challenge arising from the combination of the sparse distribution of biomass resources, long travel distance from biorefineries, and large amounts of biomass required at the high capacity needed for widespread commercialization is high feedstock cost [21]. Several studies [22-24] have found that the feedstock cost has an important role in the overall economics of the biorefinery. It is, therefore, essential that attempts are made to completely valorize biomass feedstocks by exploiting every material stream in the biorefinery.

A multi-product approach to biorefining encourages the full use of the original feedstock and has the potential to improve the economics. Establishing biorefineries that produce multiple products ensures that investments are hedged against uncertain market events, that is, every product in the biorefinery portfolio can protect the other products [25]. Besides this, many studies show that there is economic benefit in having multiple products in a biorefinery. For instance, Zhao and Liu [26] conducted the comparative economic assessment of producing only ethanol and of producing ethanol with furfural and high-purity lignin. They found that the minimum selling price of ethanol when these other products are co-produced with ethanol was 12% of the price when only ethanol was produced. The multi-product concept can benefit both the biochemical and the thermochemical processing of biomass. Therefore, the multi-product approach can use either of these platforms or their combination.

Common thermochemical processes for biomass valorization are gasification and pyrolysis. Through gasification, opportunities for multiple products rely on a single stream of an intermediate

product, syngas. The syngas can be synthesized into a final product. Multiple products from the syngas are usually achieved through the Fischer-Tropsch synthesis, wherein hydrocarbons are produced, and then fractionated into different individual products [27]. Unlike the gasification process, in which a single intermediate is produced, in pyrolysis, multiple intermediates are produced. These intermediates are bio-oil, biochar, and non-condensable gases [12, 28] . The simultaneous production of multiple products in the pyrolysis process has been studied. Yuan and Eden [29] simulated a multi-product biorefinery based on a fast pyrolysis process that integrates gasification. The biorefinery produced liquid fuels and propylene simultaneously. These products were produced by hydrotreating bio-oil and synthesizing (using Fischer-Tropsch synthesis) both the non-condensable gases and the syngas; the syngas was derived from the gasification process. The biochar from the process was combusted to produce process heat. The study demonstrated that the co-production of multiple products is a viable approach to improve economics. Jones et al. [30] also conducted an economic analysis of the production of gasoline and diesel blendstocks from woody biomass from fast pyrolysis bio-oil. Both biochar and non-condensable gases were used to supply process heat. The production of commodity chemicals from fast pyrolysis has also been studied. Hu et al. [19] fractionated bio-oil into various fractions based on the functional groups, and the fractions were upgraded into different end products including fuels and chemicals. This study also used biochar and non-condensable gases for process heat generation.

Despite the simultaneous production of many products from fast pyrolysis, existing studies usually ignore the use of biochar and non-condensable gases for purposes other than combustion. To address this oversight, this study propose the use of biochar to produce ethanol and non-condensable gases to produce either ethanol or hydrogen. This represents an opportunity to improve the original biomass valorization and the process economics. Hydrogen is considered the

future energy vector because of the cleanliness during energy release, especially in fuel cell applications. It is expected that the demand for hydrogen will grow rapidly in the coming years, as various jurisdictions have acknowledged the role of hydrogen in decarbonizing their economies [31]. Some valuable biochar applications have been considered in the literature. Singh et al. [32] characterized and evaluated the use of biochar produced from various feedstocks for soil amendment. Tan et al. [33] reviewed the methods of activated carbon production from biochar and the application of the derived activated carbon in water treatment, carbon dioxide capture, and energy storage. Hildago-Oporto et al. [34] demonstrated the production of carbon nanotubes from biochar. Although these applications represent potential revenue sources for the biorefinery, the products are not strategically integrated into the product portfolio of the fast pyrolysis biorefinery. Products such as ethanol have a better strategic position in the biorefinery given the potential to share the existing infrastructure and serve a similar customer base.

Ethanol, moreover, has myriad applications. The use of ethanol as fuel is perhaps the most important. As a replacement for tetraethyl lead, ethanol is blended with gasoline. Canada's gasoline pool was made up of around 6% ethanol in 2018 (18). Ethanol demand is growing following the implementation of the blending mandate in various jurisdictions to decarbonize the transportation sector. Today, bio-ethanol production is primarily from food crops [35], a use that has caused food versus fuel debates [36]. The shift to a more sustainable and ethical production method is required. Hence, the production of ethanol from a fast pyrolysis by-product, biochar, not only represents the potential to maximize the use of the original feedstock but also alleviates the food versus fuel issue. To produce bio-ethanol from bio-biochar, the conventional sugar fermentation approach is not applicable. Instead, bio-biochar must be processed into a synthesizable intermediate like syngas. The synthesis of ethanol from syngas can then be carried

out using a thermochemical or biochemical process. Mixed alcohol synthesis is the thermochemical route for ethanol production [37]. This process requires catalysts and operates at a specific hydrogen-to-carbon monoxide ratio, which requires the water-gas shift process. To prevent fouling and deactivation of the catalyst, syngas cleaning is also required. However, in the biochemical ethanol production from syngas, no specific ratio of these gases [38] or syngas cleaning is required [39], and microbes are able to tolerate higher levels of impurities than catalysts [40]. Hence, this study considered the production of ethanol through the fermentation of the syngas produced from the gasification of the biochar produced in a fast pyrolysis process.

There are a few studies in the literature that assess the production of ethanol through syngas fermentation. De Medeiros et al. [41] conducted a simulation and cost assessment of ethanol production from sugarcane bagasse through syngas fermentation. Modisha et al. [42] conducted a cost analysis of various biomass feedstocks. Roy et al. [40] compared the cost and GHG emissions implications of producing ethanol through syngas fermentation from treated (torrefied) and untreated miscanthus. Benalcazar et al. [43] assessed the potential of producing ethanol through syngas fermentation from various biomass feedstocks in three countries: the Netherlands, Brazil, and the United States of America. Existing studies considered several feedstocks and addresses the technical, economic, and environmental aspects of the syngas fermentation process. However, these studies assessed only standalone systems with biomass and not biochar as the feedstock. Hence, this study proposed the integration of gasification and syngas fermentation into a fast pyrolysis biorefinery for the valorization of biochar into ethanol. To the best of the author's knowledge, this is the first attempt of such kind.

The integration of new technologies to valorize the side streams of a fast pyrolysis biorefinery adds to the complexity of the biorefinery and increases energy demand. In addition, since the side

steams that are generally used to satisfy the heat demand of the fast pyrolysis process are now being converted into material products, there is a need to satisfy the heat demand from other sources. This changes the energy and emissions profile of the biorefinery. Several studies have assessed the life cycle GHG emissions of biorefineries and their products. For instance, Pourbafrani et al. [44] investigated the life cycle GHG emissions of simultaneously producing ethanol, methane, and limonene from citrus waste and found that emissions were considerably lower than in the petroleum-based route. Several studies have assessed the life cycle GHG emissions intensities of bio-based ethanol. Kumar and Murthy [45] estimated the life cycle GHG emissions of ethanol production from straws. Also, there are a few studies that evaluated the life cycle GHG emissions of hydrogen. Amaya-Santos et al. [46] evaluated, among other environmental categories, the GHG emissions of hydrogen from a life cycle standpoint. Assessments of life cycle GHG emissions associated with fast pyrolysis-based biorefineries have also been conducted. The life cycle GHG emissions of bio-oil produced from various types of forest biomass were quantified by Fan et al. [28], while Peters et al. [47] considered the life cycle emissions from upgrading bio-oil into fungible fuels through fast pyrolysis. Zhang et al. [48] evaluated the life cycle GHG emissions in the production of commodity chemicals produced from pyrolysis.

There are studies that assess the life cycle GHG emissions of multi-product and fast pyrolysis biorefineries and their products, both simultaneously and individually. However, none of these studies, to the best of the author's knowledge, conduct a life cycle GHG emissions assessment of a multi-product biorefinery based on the fast pyrolysis process, integrating syngas fermentation for the valorization of biochar and producing hydrogen from non-condensable gases. Therefore, this research sets out to investigate the effect of implementing an integrated, multi-product

approach in a fast-pyrolysis biorefinery and determine the environmental implications of the added complexity arising from this integration.

1.2 Objectives of this research

The aim of this research is to investigate the energetic, economic, and environmental implications of an integrated, multi-product biorefining approach in a fast pyrolysis biorefinery. The premise of this research is anchored on the assumption that a multi-product approach has the potential to improve the economics of biorefining operations. Hence, alternative methods to valorize the by-products of the conventional fast pyrolysis biorefineries, biochar and non-condensable gases, are proposed and assessed. The following are the objectives of the study:

- To develop process models of a novel, integrated multi-product biorefinery producing bio-oil, ethanol, and hydrogen based on a conventional fast pyrolysis process.
- To develop and assess six scenarios that differ based on the use of the non-condensable gases and the type of external fuel used (natural gas or feedstock woodchips).
- To develop a techno-economic model to assess the economic performance of the integrated biorefinery scenarios and compare it with the conventional fast pyrolysis process, using the internal rate of return (IRR) as the performance metric.
- To develop life cycle cradle-to-gate and cradle-to-grave models to assess the energy consumption, net energy ratio (NER), and GHG emissions intensities of the biorefineries scenarios and the individual products.
- To determine the GHG abatement cost (the cost of GHG emissions avoided through the production of the products considered from the integrated biorefineries).

- To carry out sensitivity analyses to understand the effect of the input parameters on the assessed metrics.
- To perform uncertainty analyses to determine the implication of the probabilistic nature of input parameters on the output metrics.

1.3 Scope and limitation

The following are the limitations of the study:

- The modelling of the system studied and the analyses conducted were based on experimental data. It is assumed that this experimental data can be scaled to a large-scale plant, which is assessed in this study. However, such direct scaling of laboratory capacity to commercial capacity would not be linear in practice.
- The economic assumptions use Canadian data.
- Cost allocations are based on the ratio of the market prices of the product, which may not reflect the actual cost contribution of each product.

1.4 Organization of the thesis

This thesis consists of five chapters. Among these, Chapters 2 and 3 have been prepared to be published as academic papers in peer-reviewed journals. Both papers assess the performance of the biorefinery systems. Each paper focuses on a different performance metric. Consequently, the reader may find similar background information when reading both chapters. The chapters are as follows:

Chapter 1: This is the current and introductory chapter. It provides the foundation of the study (background), what the study intends to achieve (objectives), the scope and limitations, as well as the thesis organization.

Chapter 2: This chapter is titled "Techno-economic assessment of an integrated biorefinery producing bio-oil, ethanol, and hydrogen." It examines the economic performance of a modified biorefinery using the internal rate of return (IRR) and compares to a conventional fast pyrolysis biorefinery.

Chapter 3: This chapter is titled "Life cycle net energy ratio and greenhouse gas emissions assessments of an integrated biorefinery producing bio-oil, ethanol, and hydrogen." It examines the net energy ratio and life cycle GHG emissions of a biorefinery.

Chapter 4: This chapter is titled "Analysis of the GHG abatement cost of biorefinery products." It builds on the assessments and results of Chapters 2 and 3 to determine the cost penalty resulting from the emissions savings associated with renewable fuels relative to corresponding fossil equivalents.

Chapter 5: This is the concluding chapter. It includes recommendations for future work.

Chaper 2 Techno-economic assessment of an integrated biorefinery producing bio-oil, ethanol, and hydrogen.

2.1 Introduction

Petroleum has contributed immensely to the prosperity we experience today. A large portion of global energy demand is satisfied by petroleum [49, 50]. However, burning petroleum-based fuels has adverse effects on the climate. Moreover, petroleum resources are finite. A sustainable energy future requires supply security and CO_2 emissions reduction. Bio-fuels can play an important role in the global energy mix and are especially important for hard-to-decarbonize sectors, like the transportation and petrochemical sectors. Today, food-based biomass is the major source of commercially available bio-fuels. Using these food-based bio-fuels, mainly ethanol, challenges food security and raises ethical questions. Lignocellulosic biomass, the so-called second-generation biomass, which is used in this study, has been a major subject of research in the bio-energy domain as a potential solution to the problems of food-based bio-fuels. The production of bio-fuels from lignocellulosic feedstock is plagued by a lack of economic competitiveness, especially when compared with the petroleum-based fuels.

The traditional approach for biomass valorization focuses on producing a single product of interest [51], with by-products going to less valuable applications, the most common of which is combustion [52]. A potential solution is to follow an integrated, multi-product approach to add value to by-products or co-products. Having multiple value-added products increases the revenue of the biorefinery and thus can be a potential means to improve the economics of renewable fuels and chemicals production from lignocellulosic feedstocks. Moreover, adding more conversion technologies to a biorefinery to convert different material streams such as intermediate products

and/or by-products into more valuable and marketable products encourages the full use of the original feedstock. Hence, waste streams are channeled for valuable product production. This improves the overall rate of return from the investment. Moreover, having multiple products from a biorefinery ensures that investors are protected against market uncertainties. This is because the products serve as a hedge for each other against unfavourable market conditions. This is, in fact, the approach in the petroleum industry [25].

The multi-product concept can be based on both biochemical and thermochemical platforms or a combination [53]. Gasification and pyrolysis technologies are the two most common thermochemical technologies for biomass valorization. In gasification, the production of multiple products relies solely on the synthesis of the syngas generated from the gasification process. Multi-product opportunities from further processing the syngas are mainly Fischer-Tropsch synthesis and mixed alcohol synthesis [27], which are followed by fractionation.

In the case of pyrolysis (fast pyrolysis in particular), multiple products are derived from bio-oil. In the fast pyrolysis process, biomass is heated in an inert atmosphere to a temperature in the range of 400 - 550 ^{o}C, producing bio-oil, non-condensable gases and biochar [54]. Bio-oil, the major product of interest in the fast pyrolysis process, is usually likened to crude-oil and is subjected to further processing for the simultaneous production of gasoline and diesel [11, 55]. Another emerging approach is to fractionate the bio-oil into different fractions based on the functional groups and potential application and then further process each fraction into valuable end products [19]. Although this simultaneous production of gasoline and diesel from bio-oil is a multi-product approach, it focuses solely on bio-oil and neglects the potential to fully valorize the biomass into valuable end products. Instead, the non-condensable gases and, in most cases, biochar produced in the fast pyrolysis process, in addition to bio-oil, are usually used to generate process heat,

although there are other suggested uses for biochar such as soil amendment [56], activated carbon production [33], and carbon nanomaterial production [34, 57]. However, these applications are not strategically integrated into the existing biorefinery. Valuable products like ethanol, which fits strategically into the product portfolio of a biorefinery, can be produced from biochar. Hydrogen can be produced by purifying hydrogen-rich non-condensable gas streams.

Ethanol is commonly produced through the hydrolysis fermentation of biomass [35]; however, this approach cannot be used to produce ethanol from biochar. The gasification of biochar, however, allows ethanol to be produced from biochar. The syngas produced through biochar gasification can then be used for the synthesis of ethanol. This synthesis can be either thermochemical or biochemical. Biochemical processes like syngas fermentation have some advantages over the thermochemical process. While fermentation occurs at near ambient temperature and pressure, the thermochemical process requires elevated temperature and pressure [38, 40]. Also, stringent gas cleaning is required in the thermochemical process as the catalysts are prone to deactivation by even very small levels of impurities in the gas stream. Microbes, on the other hand, can cope under higher levels of impurities. Another advantage to the use microbes in general is that there is no fixed ratio for H_2/CO as there is in the catalytic process [38].

The gasification-syngas fermentation process has been modelled in the existing literature. Pardo-Planas et al. [58], using switchgrass as feedstock, studied the impacts of the gas uptake rate and ethanol concentration achieved in the fermentation unit on the volume of the fermenter and the energy requirement of the system, respectively. De Medeiros et al. [41] carried out the modelling and economic analysis of an energy self-sufficient gasification-syngas fermentation process with sugarcane bagasse as feedstock. Ro et al. [42] assessed the economics of ethanol production from syngas derived from wood chips, corn stover, wheat straw, swine manure mixed with wheat straw,

and oil seed rape meal. In addition to a techno-economic assessment, Roy et al. [40] calculated the GHG emissions of the process. They considered miscanthus as the feedstock with four pretreatment options for an ethanol production rate of 22 million liters per year. Benalcazar et al. [43] conducted environmental and techno-economic assessments of ethanol production from sugarcane bagasse, pine wood, corn stover, and eucalyptus wood in three countries, the Netherlands, Brazil, and the United States. Although these studies assessed the gasification-syngas fermentation process from technical, economic, and environmental perspectives, they all considered standalone systems. There is no study, to the best of the authors' knowledge, that has considered ethanol production from the fermentation of biochar-derived syngas integrated with fast pyrolysis.

In this study, biochemical and thermochemical technologies were integrated to increase the products in the portfolio of the fast pyrolysis biorefinery as a potential way to achieve more efficient use of the original biomass. Different scenarios of this integration were assessed to produce ethanol and hydrogen from the non-condensable gases and biochar, in addition to bio-oil, by evaluating the economic implications and comparing them with the conventional fast pyrolysis process. The following objectives were set:

- To develop process models of an integrated, multi-product biorefinery producing bio-oil, ethanol, and hydrogen.
- To develop a techno-economic model to assess the rate of return for each scenario and compare the results with conventional fast pyrolysis.
- To assess six scenarios that consider different uses of non-condensable gases (NCGs) and two types of external fuel (natural gas and woodchips).

- To perform sensitivity analysis to understand the impact of input parameters on the rate of return.
- To carry out uncertainty analysis to understand the effect of the variability of the most impactful parameters on the rate of return.

2.2 Method

This section discusses the approach used in this study. The scenarios and the unit processes involved in the process modelling are described.

2.2.1 Scenario description

This study examines the potential to improve the economics of the pyrolysis process. Six process scenarios (three major scenarios with two sub-scenarios each) were developed to carry out this assessment. The feedstock considered in this study is spruce woodchips and is processed at a rate of 2000 dry tonnes/day, in all cases. To have a good reference point for the comparison of the pathways developed, the conventional pyrolysis process (the base case) was also modelled. Figure 2-1 is a simplified process flow diagram of the base case. The feedstock is dried and ground to meet the requirements for pyrolysis. During pyrolysis, bio-oil, biochar, and NCGs are produced. Bio-oil is considered a final product. NCGs are burned to satisfy process heat requirements, and some of the produced biochar is used to supplement the heat demand. In scenario 1, the production of ethanol from biochar through gasification and subsequent syngas fermentation was assessed. NCGs are considered in this scenario as fuel, and an external fuel (either natural gas or woodchip) is used as a supplement. In every scenario, "a" indicates that natural gas is the supplemental fuel and "b" that woodchip is the supplemental fuel. The process flow diagram of scenario 1 is shown in Figure 2-2. Scenario 2 (see Figure 2-3) is like scenario 1 in terms of the use of biochar, but here, the NCGs are combined with the syngas generated from the gasification of biochar to produce more ethanol. Scenario 3 (see Figure 2-4) also uses biochar for ethanol production like scenarios 1 and 2; however, the NCGs are purified for hydrogen production. Table 2-1 summarizes the scenarios.

Table 2-1: Description of scenarios

Scenario ID	Description
Base case	Conventional fast pyrolysis process for production of bio-oil, biochar and NCGs
1a	NCGs are combusted to generate process heat, and natural gas is used as supplemental fuel
1b	NCGs are combusted to generate process heat, and biomass is used as supplemental fuel
2a	NCGs are converted to bioethanol, and natural gas is the sole fuel for process heat generation
2b	NCGs are converted to bioethanol, and biomass is the sole fuel for process heat generation
3a	Hydrogen is produced from the NCGs, and natural gas is the sole fuel for heat generation
3b	Hydrogen is produced from the NCGs, and biomass is the sole fuel for heat generation

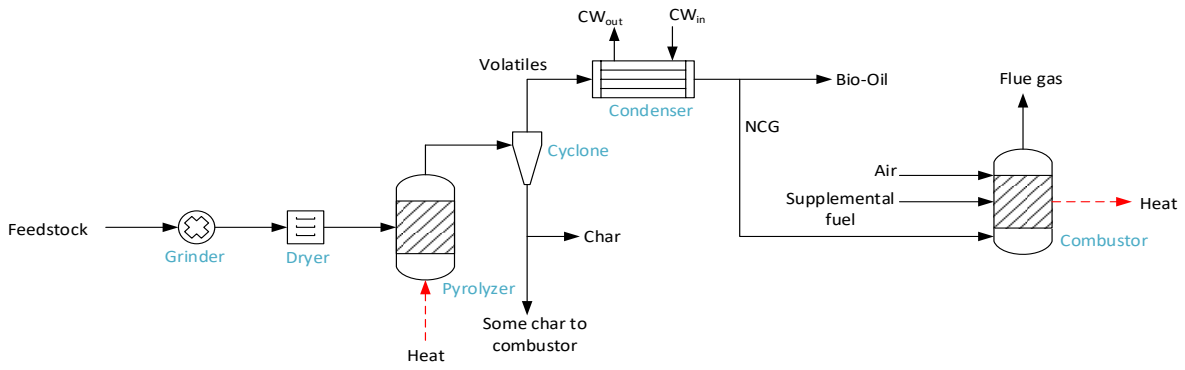

Figure 2-1: Simplified process flow diagram of the base case (conventional fast pyrolysis process)

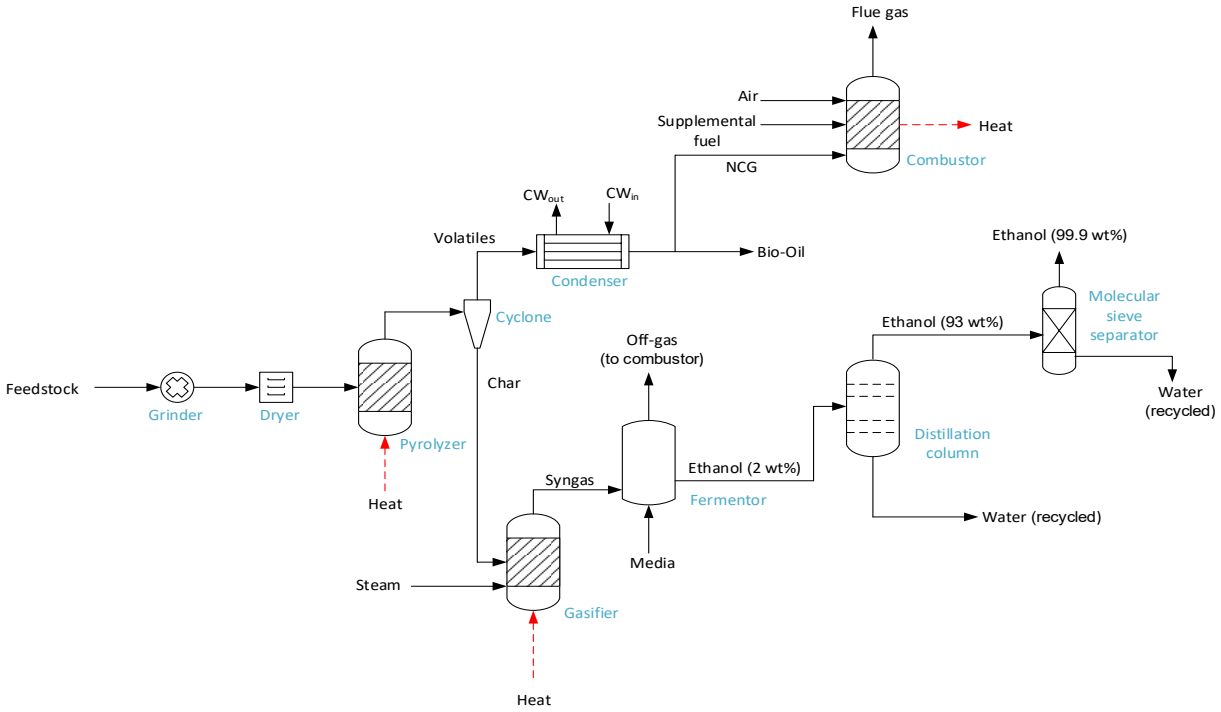

Figure 2-2: Simplified process flow diagram of scenario 1 (in addition to bio-oil, ethanol is produced from biochar)

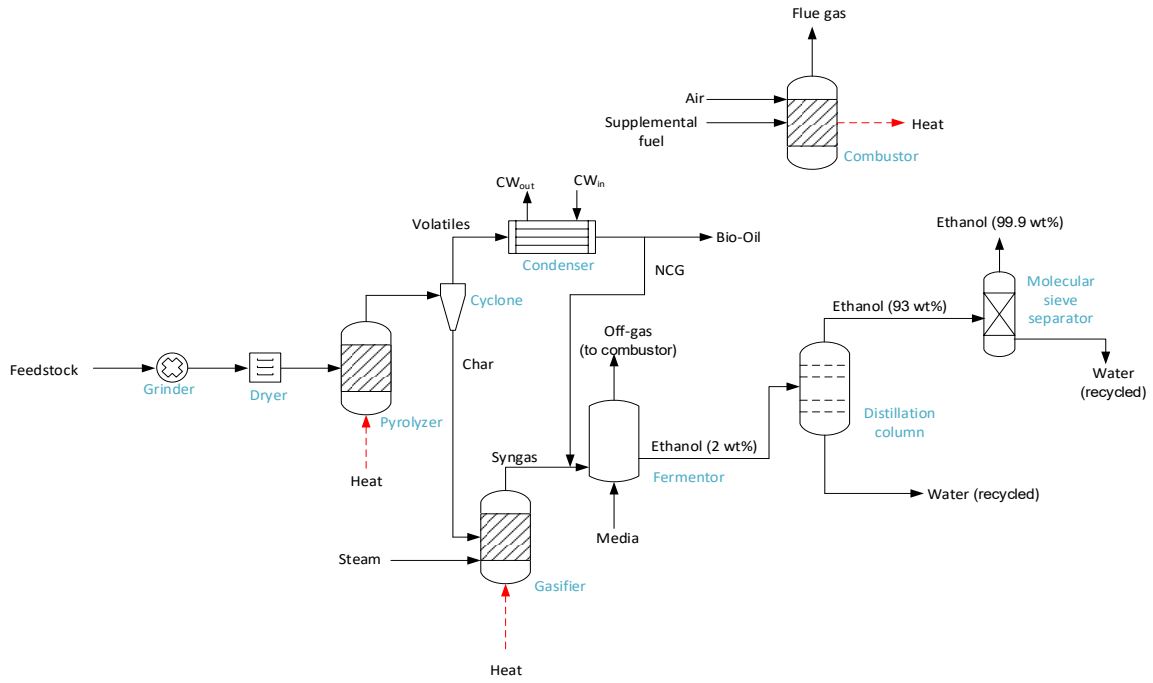

Figure 2-3: Simplified process flow diagram of scenario 2 (in addition to bio-oil, ethanol is produced from biochar and NCGs)

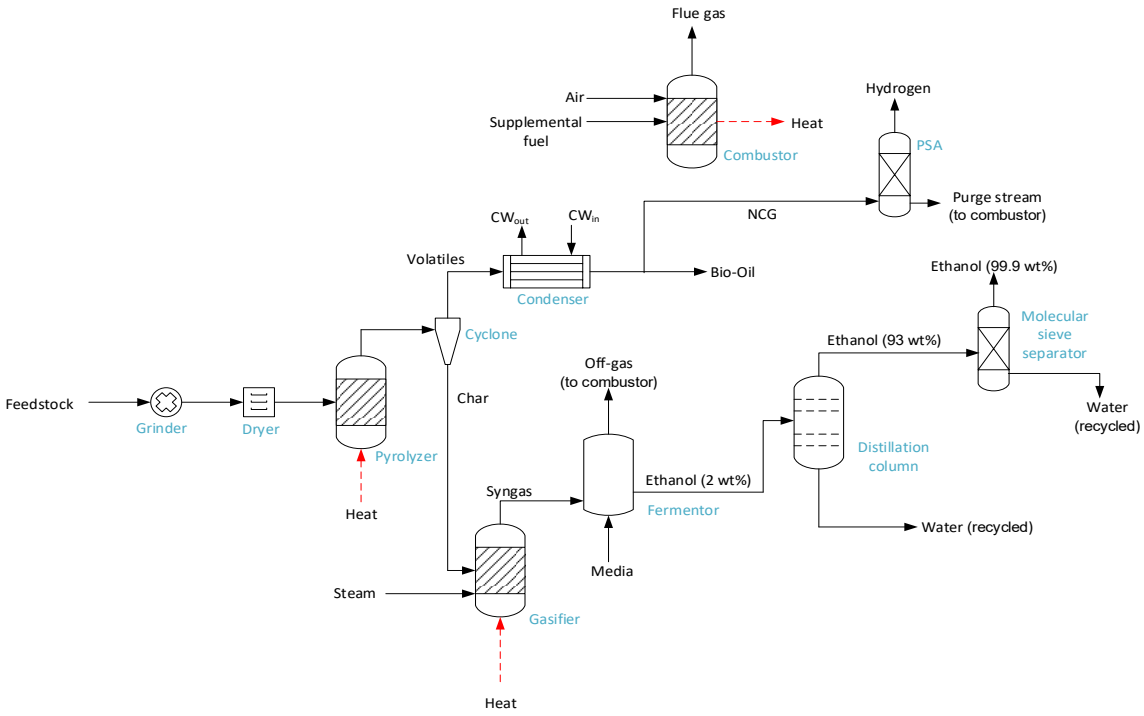

Figure 2-4: Simplified process flow diagram of scenario 3 (in addition to bio-oil, ethanol is produced from biochar and hydrogen is produced from NCGs)

2.2.1.1 Ethanol production model validation

To ensure that the modelling of ethanol production is accurate in this study, Medeiros et al.'s work [41] was first simulated. The simulation included biomass gasification, syngas fermentation, and ethanol purification and included all the process conditions of Medeiros et al.'s work. The model was validated using the ethanol production output. In Medeiros et al.'s work, 71,000 m^3/year of ethanol was produced. The output in this was close to the study by Medeiros et al., at 71,875 m^3/year. With the model now calibrated, process conditions specific to this study were subsequently used.

2.2.1.2 Description of process units and modelling

The process modelling carried out in this study has three sections. The first is the modelling of the conventional fast pyrolysis process to yield bio-oil (the main product), NCGs, and biochar. The pyrolysis section of the model, which is common to all scenarios, consists of feedstock pretreatment, the pyrolysis unit, and product separation. In this study, one of the major goals is to use the biochar to produce ethanol that can be sold, thereby improving the economics of bio-oil production. The production of ethanol from biochar is the second section of the modelling. This section, also common to all scenarios, consists of biochar gasification to produce syngas, syngas fermentation to produce ethanol, and product separation for the concentration of ethanol. The last section is the purification of pyrolysis gas or NCGs. For scenario 1, NCGs were burned in a combustor along with supplemental fuel to provide process heat. For scenario 2, NCGs were mixed with biochar syngas to be fermented. For scenario 3, the separation of hydrogen from the NCGs using a pressure swing adsorption system was considered. The following sections discuss the process units considered in this study.

2.2.1.3 Feedstock and pretreatment

The feedstock studied here is spruce wood chips. Spruce is an important tree species globally and in Canada; it makes up about 47% of Canada's total forest inventory [59]. The ultimate and proximate analyses of the feedstock are taken from an earlier study [12].

The particle sizes of the as-received feedstock is not suitable for the pyrolysis process and contains 50% moisture [12]. For fast pyrolysis, it is recommended that the particle size is at most 2 mm [60]; this size was adopted in this study. Consequently, the feedstock was ground in a mill to a particle size not more than 2 mm. The grinding operation was modelled using the crusher block in Aspen Plus. The grinding energy consumption was taken as 33 kWh/t [61]. The grinding operation

is followed by drying, modelled using a RStoic reactor and a flash separator. Rogers and Brammer recommend that the moisture content of the feed entering the pyrolysis reactor be less than 10 wt% [60]. Drying the feedstock using the heat recovered from the flue gas was done to a 7 wt. % moisture content.

2.2.1.4 Pyrolysis

The modelling of the pyrolysis process is based on previous experimental work conducted on the pyrolysis of spruce wood chips in a batch fluidized bed pyrolysis reactor [12]. The process was carried out at a temperature of 490^{o}C, under atmospheric pressure. The pyrolysis reactor was modelled using the RYield block. This block requires pyrolysis product yield and, with it, estimates process energy consumption. The experimental yields used for this model are taken from an earlier study [12]. The outputs of the pyrolyzer are volatile components and biochar. The volatile component contains bio-oil compounds, which are a liquid at room temperature, and NCGs, which are a gas at room temperature. These volatile compounds and the solid biochar particles were separated with the help of cyclones with a solid removal efficiency of 90%. To extract the bio-oil, the volatile stream first needs to be cooled. Cooling the volatiles from 490^{o}C to 50 ^{o}C condenses the bio-oil compounds. This extracted heat was used to generate some of the steam required for the gasification process. Bio-oil is collected and stored, and NCGs are used for heat generation, ethanol production, or hydrogen production, depending on the biorefinery scenario.

2.2.1.5 Biochar gasification

The gasification of biochar was modelled through Gibbs energy minimization. An RGibbs reactor was used to simulate the gasification process and predict syngas composition. The gasification

temperature was 800ºC and atmospheric pressure was considered [62]. The steam-to-char ratio was set such that biochar conversion was 80%, as reported by Chaudhari et al. [62]. Gasification was assumed to be carried out in an indirectly heated dual fluidized bed gasifier. This gasifier configuration has two reactors, a gasification reactor, and a combustion reactor. Steam gasification, an endothermic reaction, takes place in the gasification reactor. The heat required for steam gasification is supplied by the second reactor. A solid heat carrier, olivine, circulates between the two reactors. The olivine circulation rating was taken as 12.3 kg/kg of bone-dry feed (biochar), as reported in an earlier study [63]. Biochar is a non-conventional compound in Aspen Plus. Hence, it was specified as a non-conventional compound in the process model using its ultimate analysis as in an earlier study [64].

2.2.1.6 Syngas fermentation

Ethanol is versatile; it can serve as a solvent, beverage, antifreeze, and fuel. Perhaps the most important application is as fuel. Today ethanol serves as a blend for gasoline and improves its octane number, replacing tetraethyl lead. The production of ethanol from biomass sources is predominantly from grains [35], though lignocellulosic feedstock is also used. Both rely on the use of fermentable substrates derived from biomass. However, this approach cannot be used to derive ethanol from biochar. Biochar needs to be gasified before it is converted to fermentable gases. The derived syngas can then be used for the synthesis of ethanol. In this study, it was considered that the production of ethanol is through syngas fermentation, a biochemical process.

Microorganisms capable of fermenting syngas are known as acetogens [65]. Acetogens are anaerobic micro-organisms (including bacteria and archaea) that use the acetyl-CoA pathway to fix CO_2 [66] and other substrates like glucose [67]. The products from syngas fermentation generally fall into two major categories: carboxylic acids and corresponding alcohols. Usually,

carboxylic acid is readily produced, unlike alcohol. Acetic acid, ethanol, butyric acid, butanol, hexanoic acid, hexanol, and 2,3-butanediol can be produced from syngas fermentation [65]. Of these, acetic acid and ethanol are the prominent ones [65]; both are readily produced by many acetogens [67]. The production of ethanol from syngas is shown by Equations 1 and 2, as given by Pardo-Planas et al. [58].

$$6CO + 3H_2O = C_2H_5OH + 4CO_2 \quad (1)$$

$$6H_2 + 2CO_2 = C_2H_5OH + 3H_2O \quad (2)$$

The fermentation process was modelled, with Equations 1 and 2 as the stoichiometric equation inputs. The process conditions for syngas fermentation were based on experimental data from the work by Gaddy et al. [39], who used *Clostridium ljundhalii* as the acetogen. Their work considered 20 scenarios with different process conditions to see which process would produce the most ethanol. This study is based on the approach that recirculates the bottom product (i.e., acetic acid and water) of the ethanol purification stage into the fermenter, as demonstrated in earlier work by Gaddy et al. (38). This approach eliminated the need to separate the acetic acid produced during fermentation; the water stream containing acetic acid can be recycled. Recycling the acetic acid led to an equilibrium concentration in the system and thus the microbes did not produce more acetic acid. DeMedeiros et al. [41] used a similar approach. Off-gas from the fermentation unit was combusted to generate process heat.

2.2.1.7 Ethanol separation and purification

The ethanol produced in the fermentation reactor is highly diluted (2 wt%). This stream must be concentrated to a purity of 99.9% if the ethanol is to be used as fuel. The separation and purification of ethanol occur in two different units to achieve the purity specified. First, the broth from the

fermentation unit is concentrated to 93 wt% in the distillation column. The distillation column was simulated. The column has 25 stages and the feed to the column enters at stage 11. A reflux ratio of 5 (on a mole basis) was specified. Second, the concentrated ethanol stream exiting the distillation column was sent into a molecular sieve separation unit. Purification of ethanol beyond 93 wt% could not be achieved because of the azeotropic nature of the ethanol-water mixture [68]. In the molecular sieve separation unit, ethanol was further purified to a purity of 99.9%. The molecular sieve separation dehydrates the ethanol through adsorption. This system consists of packed columns of adsorption materials. The molecular sieve separation process was modelled using a separator block in the process model.

2.2.1.8 Hydrogen production

Hydrogen was produced only in scenario 3 and was done in a pressure swing adsorption (PSA) unit to separate hydrogen from the NCG stream. The PSA is a commonly used technology for the separation of hydrogen from other gases [69, 70]. One of the advantages of the PSA process is that it can achieve high purity hydrogen, as high as 99.9% [71]. In this study, the hydrogen content in the NCG stream was about 75% by volume. The PSA functions through adsorption, which occurs in the PSA beds. These beds consist of solid adsorption materials like zeolite and activated carbon [72]. The type of adsorbents used depends on the composition of the hydrogen stream that needs to be purified. This is because the affinity for each impurity differs with the type of adsorbent [72]. Separating hydrogen from the impure hydrogen stream is possible because the desirable adsorbent has less affinity for hydrogen.

The adsorption of impurities within the beds occurs at high pressure, in the range of 10-50 bar [73, 74]. A pressure of 30 bar was selected in this study. The NCGs are thus compressed from atmospheric pressure to 30 bar. A compression ratio of 2.8 was selected for each compressor. The

PSA process, however, works near ambient temperature [74]. Once a bed of adsorbent becomes saturated with impurities, it is taken offline for regeneration (desorption) using purge gases such as nitrogen [75]. The desorption process takes place at low pressure. Hence, the pressure in the bed must be lowered to near atmospheric pressure. The desorbed impurities' stream is also used for combustion. To ensure continuous operation, several PSA beds are used in the PSA process [74]. Hydrogen recovery in the PSA process has been reported to be between 80 and 90% [74]. A hydrogen recovery of 90% was adopted in this study.

2.2.2 Techno-economics assessment

2.2.2.1 Base economic evaluation

The assessment of the profitability of each scenario developed in this study was based on the internal rate of return (IRR) generated by the scenario. This rate of return is the minimum return that the plant must generate for the investors to just recuperate all their expenses. The expenses are twofold: the capital expenditure (CAPEX) and the operating expenditure (OPEX). A discounted cash flow model was used to assess the rate of return from the combined CAPEX and OPEX. The assumptions for our discounted cash flow analysis are given in Table 2-2.

Table 2-2: Economic parameters

Parameter	Value	Source
Base year	2019	
Currency	USD	
Plant characteristics		
Lifetime	20 years	
Location	Alberta, Canada	
Operating hours	8,000 hr/yr	
Material Market prices		
Hydrogen	1.50 $/kg	[76]
Bio-oil	0.32 $/L	[77]
Ethanol	0.36 $/L	[78, 79]
Electricity	0.068 $/kWh	[80]
Natural gas	1.51 $/GJ	[81]
Spruce woodchips	43.23 $/t	[12]
Olivine	232.70 $/t	[15, 82]
Labour rate		
Operator labour	30.77 $/hr	[83, 84]
Supervisor labour	38.46 $/hr	[83, 84]

The capital expenditure is estimated from the cost of each piece of equipment used with the plant. The purchase equipment costs for conventional equipment were determined using the process

model, and the purchase equipment costs of other non-conventional equipment were taken from published sources.

Table 2-3 gives the base equipment cost derived from the literature.

Table 2-3: Base purchase equipment cost

Unit	**Base equipment cost ($k)**	**Scaling parameter**	**Base capacity**	**Scale factor**	**Source**
Gasification	$4,760	Solid flow rate	500 tonne/day	0.60	[63]
Fermentation	$1,759	NA*	1000 m^3	NA	[39, 85]
Molecular sieve	$2,987	Purge stream flow rate	22,687 kg/hr	0.60	[63]
PSA bed	$7,063	Impurities stream flow rate	0.294 kmol/s	0.74	[86, 87]

* A bubble column reactor is assumed. The given cost is the cost of one reactor of 1000 m^3 volume, which is the practical maximum volume currently (58). The number of vessels was determined by combining the maximum reactor volume, this study's syngas flow rate, and reaction residence time.

In addition to the purchase equipment cost, costs are incurred to put the equipment in place at the plant site. Table 2-4 gives the breakdown of the factors used in estimating the CAPEX from the equipment purchase cost.

Table 2-4: Cost component of capital investment

Component	Formula
Total equipment cost (TEC)	Obtained from equipment sizing
Total installed cost (TIC)	302 % of TEC
Indirect cost (IC)	89% of TEC
Total direct and indirect cost (TDIC)	TIC + IC
Contingency (Con.)	20% of TDIC
Fixed capital investment (FCI)	TDIC + contingency
Location factor (LF)	10% of FCI
Total capital investment (TCI)	FCI + LF

The OPEX has two parts: the variable operating cost and the fixed operating cost. The variable operating cost includes the costs of the feedstock, utilities, and raw materials. The fixed operating cost includes labour and supervision, maintenance, and other general and administrative costs.

Table 2-5 gives the fixed operating cost schedule used in this study.

Table 2-5: Operating cost schedule

Component	Formular
Maintenance cost (M)	3% of TCI
Operating charges (OC)	25% of labour cost
Plant overhead (PO)	50% of (labour cost + maintenance cost)
Sub-total operating cost	M + OC + PO + labour cost + raw materials cost + utilities cost
General and administration (G & A)	8% of sub-total operating cost
Total operating cost	G & A + sub-total operating cost

2.2.2.2 Sensitivity and uncertainty analysis

A Morris sensitivity analysis was conducted to determine the input parameters that have the most impact on the rate of return of the process. The sensitivity analysis was done using the Regression, Uncertainty and Sensitivity Tool (RUST) [88]. RUST was further used with the parameters of greatest influence to carry out a Monte Carlo simulation to determine the uncertainty in the profitability of the processes.

2.3 Results

2.3.1 Production rates and energy consumption.

Table 2-6 presents the production rate of the three final products and the amount of external fuel required for each scenario. This study considered a fast pyrolysis plant processing 4000 tonnes/day of biomass with 50% moisture which was reduced to 7% by drying. This is equivalent to 2000 dry tonnes of biomass/day. The production rates of bio-oil, biochar, and NCGs in the pyrolysis unit are 1023, 303, and 718 tonnes/day, respectively. In all three scenarios, ethanol is produced from biochar through biochar gasification with a syngas production rate of 555 tonnes/day.

The production rate of ethanol is the same in scenarios 1 and 3. This is because they process syngas derived from biochar gasification only. Scenario 2 processes more gases (NCGs from pyrolysis + syngas from biochar gasification) and produces nearly double the amount of ethanol produced in scenarios 1 and 3. The ethanol yield in scenarios 1 and 3 was derived to be 857 L/tonne of biochar and in scenario 743 L/tonne of biochar plus NCGs. The existing literature on syngas fermentation reports ethanol yields of 212-546 L/tonne of biomass feedstock [40-43, 58, 89, 90]. The relatively higher yield reported in this study is due to the higher carbon content of biochar compared to whole biomass. The carbon content of spruce woodchips biochar considered in this study is 92%, while in the cited literature, the carbon content of the feedstocks is between 45% and 53%. Hydrogen production is only possible in scenario 3 at about 18,000 tonnes/year. The overall mass yields were 61%, 69%, and 64% in scenarios 1, 2, and 3, respectively. Meanwhile, the base case has an overall mass yield of 64%. Hence, only scenario 2 has a better feedstock conversion compared to the base case. However, the market outlook of ethanol and hydrogen is better than biochar. Hence, from an economic standpoint, if biochar is excluded, the mass yield of the base case is about 52%.

Energy consumption for the major process units is given in Table 2-7. The energy consumption values shown for the common process units are the same in all scenarios, except for the drying and distillation unit. In the case of drying, the calculated energy demand is about 60.8 MW in all cases where natural gas is combusted. However, in the cases where woodchips are combusted, additional woodchips, hence additional drying energy, are required. These additional energies are about 10.6, 22.4, and 20.7 MW more than the base drying requirement of 60.8 MW for just the feedstock. The distillation operation consumes more energy in scenario 2 than in scenarios 1 and 3 because it processes a larger amount of ethanol. In the base case, all the NCGs are consumed to satisfy 86% of the heat demand, with supplemental heat being satisfied by 16% of the biochar generated. In scenario 1, 68% of the heat requirement is met by combusting all the NCGs and the off-gas (produced at the rate of 375 tonnes/day) from the syngas fermenter. In scenario 2, off-gas from the fermenter produced at the rate of 421 tonnes/day satisfies 38% of the heat demand, while in scenario 3, off-gas from the PSA and the fermenter is combined to satisfy 37% of the heat demand. The amount of external fuel used to satisfy the energy balance in all the scenarios is shown in

Table 2-6.

Table 2-6: Production rates and external fuel consumption

	Bio-oil (m^3/yr)	**Ethanol (m^3/yr)**	**H_2 (tonne/yr)**	**Ext. fuel (tonne/yr)**	**Fuel type**
Scenario 1a	289,000	85,000	-	45,504	NG
Scenario 1b	289,000	85,000	-	231,647	Biomass
Scenario 2a	289,000	158,860	-	97,848	NG
Scenario 2b	289,000	158,860	-	492,557	Biomass

	Bio-oil (m^3/yr)	Ethanol (m^3/yr)	H_2 (tonne/yr)	Ext. fuel (tonne/yr)	Fuel type
Scenario 3a	289,000	85,000	18,170	90,608	NG
Scenario 3b	289,000	85,000	18,170	454,667	Biomass

Table 2-7: Energy consumption of major unit operations

Unit	Energy consumption (MW)
Heat	
Biomass drying	60.80$^{\alpha}$
Pyrolysis	60.45
Gasification	42.01
Distillation	39.73* (74.00**)
Electricity	
PSA compression unit	6.19
Grinding	5.5

α This the energy consumption for scenarios consuming natural gas. An additional 10.6, 22.4 and 20.7 should be added to scenarios 1b, 2b, and 3b, respectively (when woodchips are the external fuel).

* This is the distillation unit energy consumption associated with scenarios 1 and 3.

** This is the distillation unit energy consumption associated with scenario 2.

2.3.2 Techno-economic assessment

2.3.2.1 Capital cost

The capital costs of the base case and scenarios 1, 2, and 3 are broken down in Table 2-8 by capital cost categories. As expected, the capital costs of the scenarios are higher than those of the base case because of the additional capital investment in the extra equipment in all three scenarios. Scenario 2 is the most capital-intensive plant, with a cost that is about 2.6 times that of the base case. However, scenario 3 is only slightly less costly than scenario 2. Scenario 1, the least costly among the scenarios, is also almost double the base case. Scenario 1 is the least costly of all the scenarios because it processes a lesser amount of gas, and thus produces lesser amount of ethanol than scenario 2. Also, in addition to bio-oil, scenario 1 produces only ethanol. Meanwhile, scenario 3 produces ethanol and hydrogen in addition to bio-oil. For these mentioned reasons, scenario 1 has correspondingly smaller and fewer equipment than scenarios 2 and 3, respectively.

Table 2-8: Capital cost (costs are in million $) for a 2000 tonne per day biorefineries.

	Base case	**Scenario 1a**	**Scenario 1b**	**Scenario 2a**	**Scenario 2b**	**Scenario 3a**	**Scenario 3b**
Total equipment cost	$27.95	$54.19	$54.75	$72.08	$73.23	$71.72	$72.78
Total installed cost	$84.41	$163.65	$165.34	$217.67	$221.14	$216.59	$219.80
Indirect cost	$24.88	$48.23	$48.73	$64.15	$65.17	$63.83	$64.78
Total indirect cost	$109.28	$211.88	$214.07	$281.82	$286.31	$280.41	$284.58
Contingency	$21.86	$42.38	$42.81	$56.36	$57.26	$56.08	$56.92
Fixed capital investment	$131.14	$254.26	$256.88	$338.18	$343.57	$336.50	$341.50
Location cost	$13.11	$25.43	$25.69	$33.82	$34.36	$33.65	$34.15

	Base case	Scenario 1a	Scenario 1b	Scenario 2a	Scenario 2b	Scenario 3a	Scenario 3b
Total capital investment	**$144.25**	**$279.69**	**$282.57**	**$372.00**	**$377.93**	**$370.15**	**$375.65**

Figure 2-5 presents the breakdown of the capital cost for the base case and the scenarios considered, according to the major processing units in the biorefineries. The difference between the capital cost of the biorefinery scenarios and the base case has been established. Hence, the capital cost breakdown discussed hereafter is focused on the biorefinery scenarios. In every scenario, the pyrolysis plant accounts for a significant share of the total capital cost and the largest share in both scenarios 1 and 3, at about 39% and 30%, respectively. It also accounts for about 30% of the total capital cost in scenario 2. However, in scenario 2, the cost of the fermentation unit is the largest cost contributor at about 42%. The cost of the fermentation unit is also significant in scenarios 1 and 3, accounting for 28% and 21%, respectively. The fermentation cost is higher (double) in scenario 2 than in scenarios 1 and 3 because a larger amount of gases is processed into ethanol. Both scenarios 1 and 3 have a gas input of 648 m^3/min compared to 1323 m^3/min in scenario 2. However, for scenario 3, the cost of the PSA unit is higher than that of the fermentation unit, constituting nearly 24% of the capital cost of scenario 3. This high cost of the PSA unit is largely caused by the compression requirement of the PSA process, which needs expensive compressors.

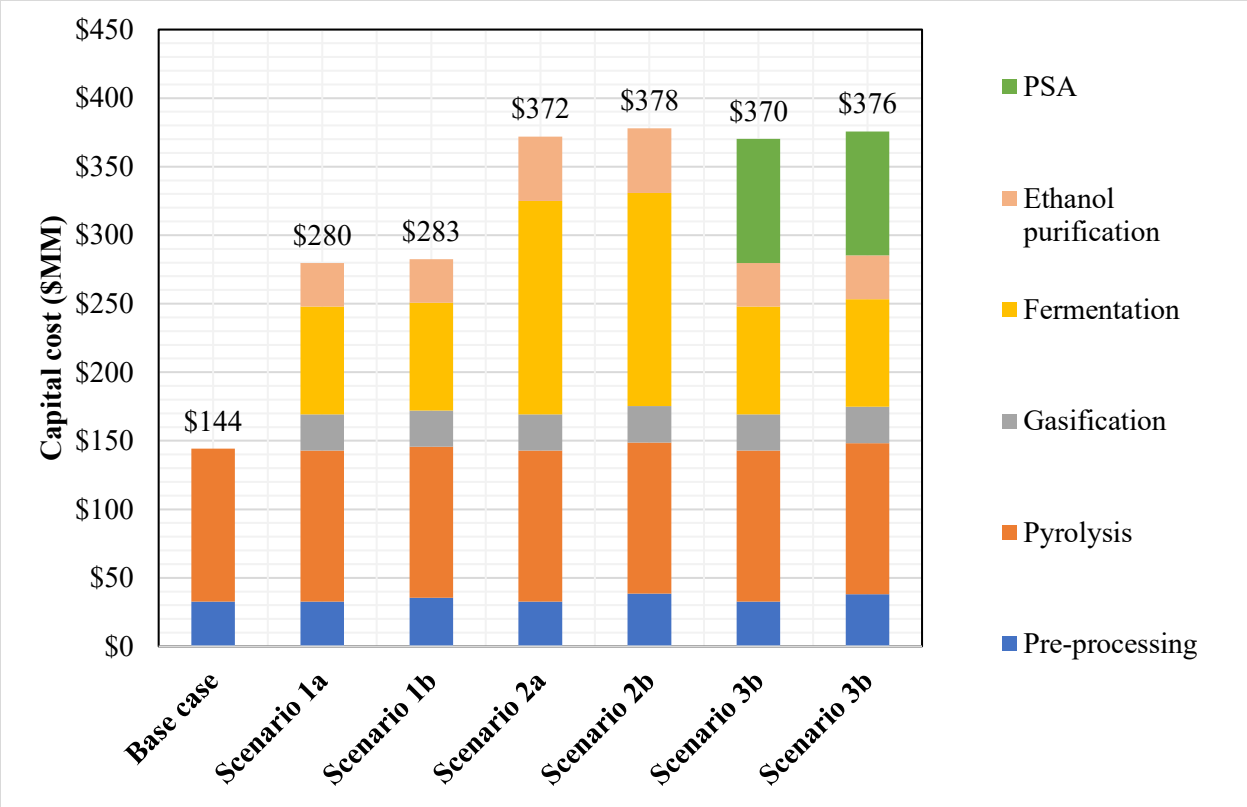

Figure 2-5: Capital cost distribution of the base case and biorefinery scenarios (Scenario 1a: Ethanol from biochar; natural gas for supplementary heat | Scenario 1b: Ethanol from biochar; woodchips for supplementary heat | Scenario 2a: Ethanol from biochar and NCG; natural gas for supplementary heat | Scenario 2b: Ethanol from biochar and NCG; woodchips for supplementary heat | Scenario 3a: Ethanol from biochar; Hydrogen from NCG; natural gas for supplementary heat | Scenario 3b: Ethanol from biochar; Hydrogen from NCG; woodchips for supplementary heat)

It is important to note the cost similarities and differences in the scenarios. As shown in Figure 2-5, the dollar contribution values of the pyrolysis and gasification units are the same in all scenarios. The preprocessing cost values are the same in all cases where natural gas is burnt; however, it is slightly higher in the scenarios where woodchips are burnt instead. Furthermore, scenarios 1 and 3 share similar dollar values for the fermentation and ethanol purification units

(because they process the same amount of syngas), while those of scenario 2 are about double the costs of scenarios 1 and 3.

2.3.2.2 Operating cost

The total operating cost for each case is constituted by fixed and variable operating costs. Figure 2-6 gives the operating costs of the scenarios and base case. It should be noted that the operating costs presented are for the first year of biorefinery operation. However, a yearly escalation in each operating cost category was considered in the discounted cash flow analysis.

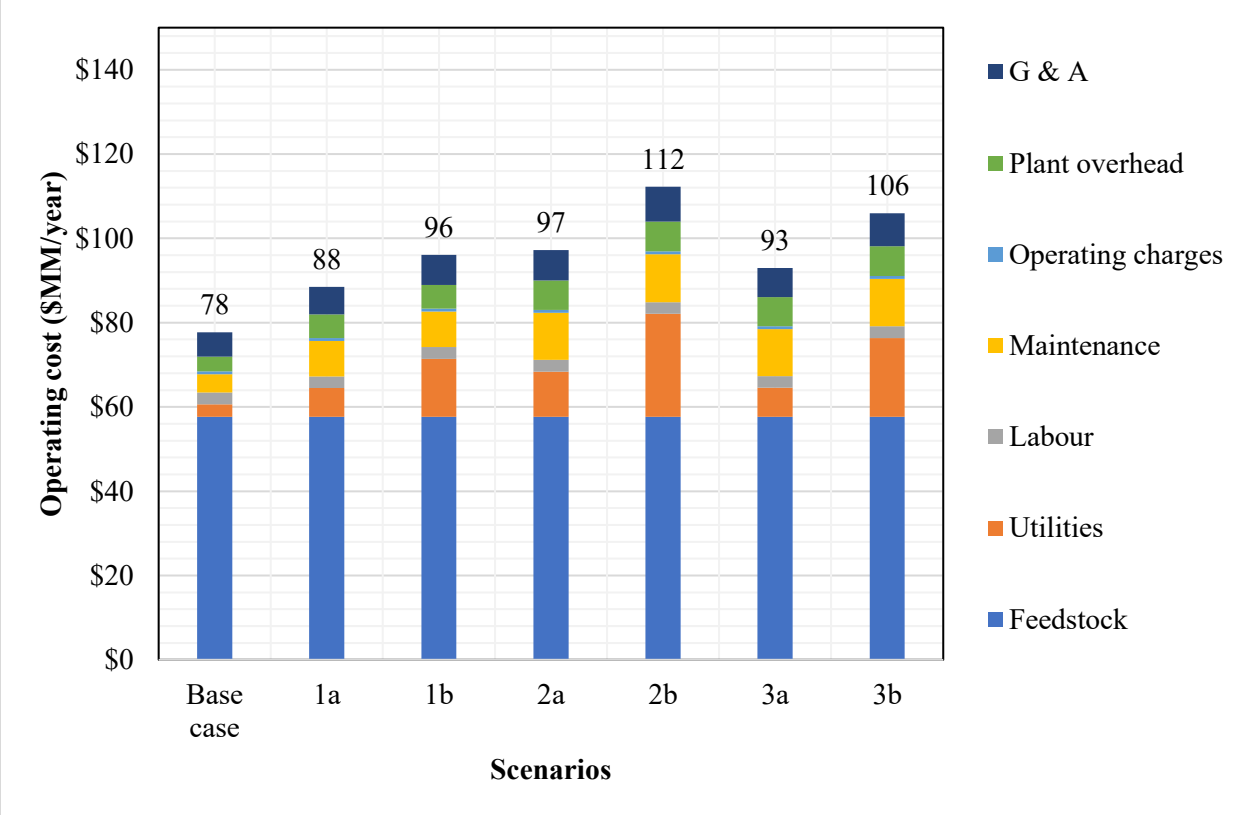

Figure 2-6: Base case and scenarios operating costs (Scenario 1a: Ethanol from biochar; natural gas for supplementary heat | Scenario 1b: Ethanol from biochar; woodchips for supplementary heat

| Scenario 2a: Ethanol from biochar and NCG; natural gas for supplementary heat | Scenario 2b: Ethanol from biochar and NCG; woodchips for supplementary heat | Scenario 3a: Ethanol from biochar; Hydrogen from NCG; natural gas for supplementary heat | Scenario 3b: Ethanol from biochar; Hydrogen from NCG; woodchips for supplementary heat)

As shown in Figure 2-6, the base case has the lowest operating cost. This is because in the six biorefinery scenarios there are additional costs to operate the extra equipment. The total delivered feedstock cost is the parameter that most influences the operating cost; it is responsible for about 74% of the base case. The percentage contribution of the feedstock cost in the operating cost is between 51% and 64% in the biorefinery scenarios. Following the feedstock cost, the costs of maintenance and utilities are influential. The maintenance cost is more significant than the utility cost in the cases where natural gas is burnt, while the cost of utilities is more significant when the fuel of choice is biomass.

The lower operating cost of the "a" sub-scenarios compared to the "b" sub-scenarios is because natural gas is cheaper and has a higher heating value than biomass. The difference in operating costs for sub-scenarios "a" and "b" for all the scenarios considered is less pronounced for scenario 1 than scenarios 2 and 3. The cost differences between "a" and "b" in all scenarios are about \$7.61M, \$15.08M, and \$13.01M, for scenarios 1, 2, and 3, respectively. This cost difference is more pronounced in scenarios 2 and 3 because both cases are more energy-intensive than scenario 1.

2.3.2.3 Rate of return

The profitability of each scenario was also studied using rate of return as the metric. The rate of return for each scenario is presented in Figure 2-7. Generally, compared to the base case, the

scenarios studied are more profitable. This indicates that there is an economic benefit to producing valuable products from non-condensable gases and biochar. It is important to point out the trend related to the fuel type. As shown, the "a" scenarios, which use natural gas as a fuel, are more profitable than the "b" scenarios, in which woodchips are used as fuel. This difference in profitability between the "a" and "b" scenarios is an indication of the lower projected net income (before taxes and depreciation) associated with the use of woodchips for the same projected revenue. For instance, the second year's projected net incomes (before taxes and depreciation) for scenario 1 with natural gas and woodchips as fuel are $12.5 and $4.6 million, respectively. It was also seen that the difference in the profitability of the "a" and "b" scenarios is higher in scenarios 2 and 3. These differences stem from the higher operating cost associated with burning woodchips than natural gas, as pointed out in Section 2.3.2.2.

Furthermore, when natural gas is burnt, scenario 3 is the most profitable scenario, with a return of about 13%. Likewise, when woodchips are burnt, scenario 3 is the most profitable scenario. The higher profitability of scenario 3 over scenario 2 is because scenario 3 has slightly lower capital and operating costs and higher revenue than scenario 2. However, both scenarios 2 and 3 have higher profitability than 1, despite having higher capital and operating costs. This higher profitability is a result of higher net revenue.

The potential of the base case fast pyrolysis process matching the return rate of scenario 3a, in which ethanol and hydrogen were produced in addition to bio-oil, was assessed, based on the sales of biochar. It was derived that the base case could match this profitability of 13.01% if biochar could be sold at $236/tonne. Hence, at this price point and above, the base case fast pyrolysis process is preferable to scenario 3a. Shabangu et al. [91] reported a breakeven selling price for biochar of $280/tonne for a slow pyrolysis plant co-producing methanol at a discount rate of 10%.

Although this was slow pyrolysis, their product distribution is near that of fast pyrolysis. It could be expected that at a similar product distribution and discount rate, the result obtained in this study is reasonably within Shabangu et al.'s reported cost. Dickson et al. [92] also cited biochar breakeven prices of $173-$320/tonne. The biochar market price is between $726 and $3,080 in the US market, the European market, and globally [93-95]. These high prices seem attractive and suggest that biochar should be sold instead of further processing it. However, the market for biochar is small. Market research puts the 2018 global demand for biochar at about 350 kt per year [96], which could be easily met by four fast pyrolysis plants of the capacity assumed in this study. The high market price may be due to the lower scale of production, and prices should decline as supply gets higher.

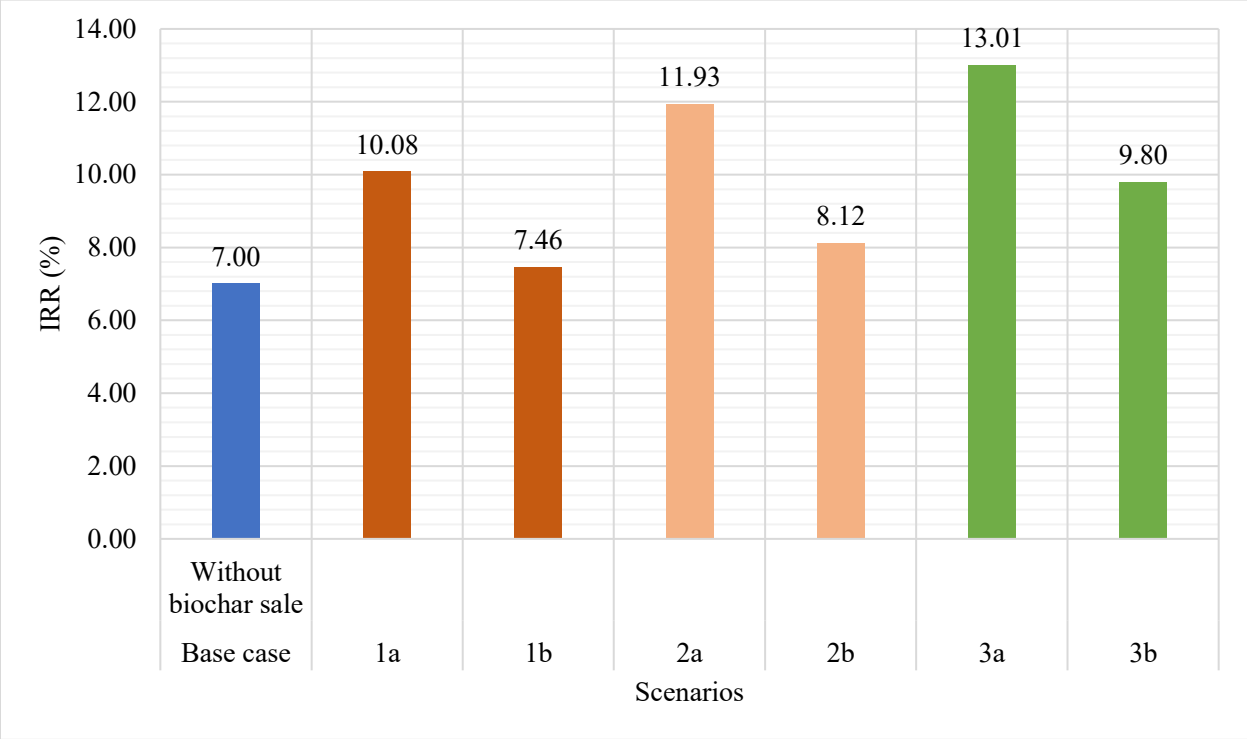

Figure 2-7: Internal rate of return of biorefinery scenarios (Scenario 1a: Ethanol from biochar; natural gas for supplementary heat | Scenario 1b: Ethanol from biochar; woodchips for supplementary heat | Scenario 2a: Ethanol from biochar and NCG; natural gas for supplementary heat | Scenario 2b: Ethanol from biochar and NCG; woodchips for supplementary heat | Scenario 3a: Ethanol from biochar; Hydrogen from NCG; natural gas for supplementary heat | Scenario 3b: Ethanol from biochar; Hydrogen from NCG; woodchips for supplementary heat)

2.3.2.4 Influence of scale on the capital cost per unit of processed biomass

The effect of capacity on the capital cost per unit of biomass processed was assessed in this study. Figure 2-8 gives the plot of the capital cost as a function of plant capacity for scenario 3a. Scenario 3a was chosen for brevity as it is the most profitable scenario. The capital cost increases with capacity, as expected. However, a diminishing trend in the increase was observed at a scale factor

of 0.598. This diminishing trend is seen in the plot of capital cost per unit of processed biomass vs capacity, as shown in Figure 2-9. The capital cost per unit capacity reduces as the capacity increases, showing the presence of economies of scale. However, the slope of the curve decreases as the capacity is increased, indicating a diminishing return with added capacity.

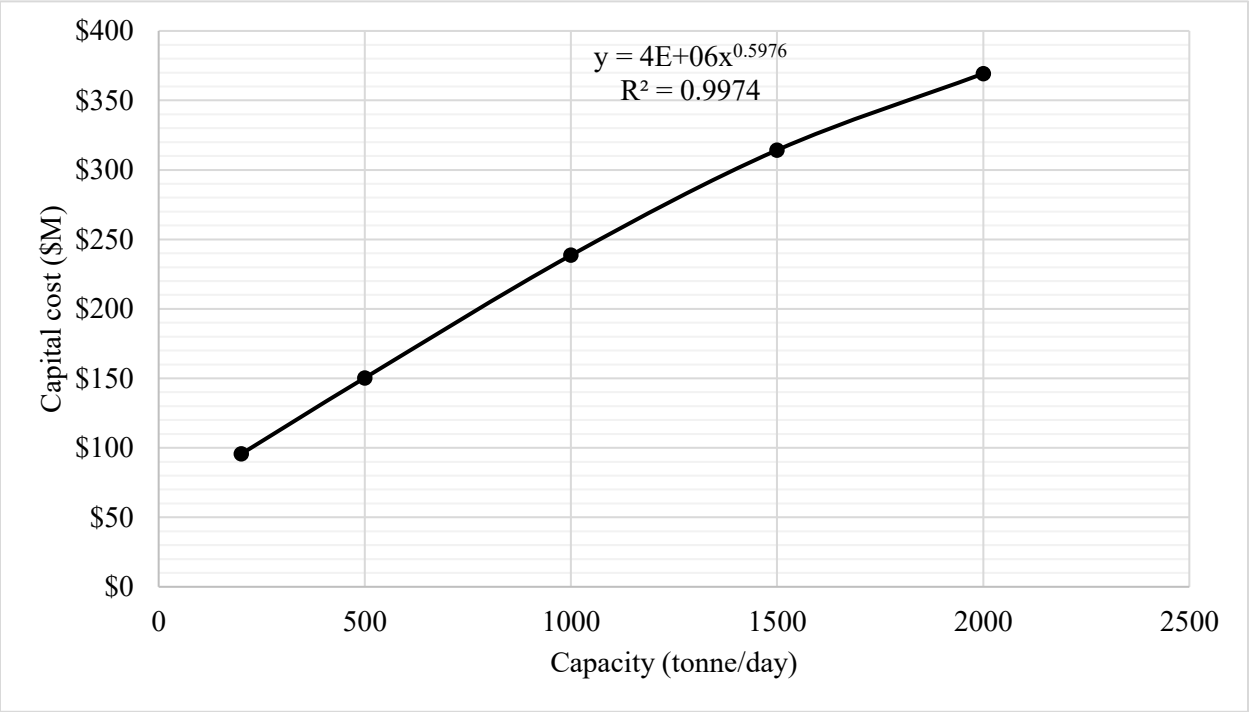

Figure 2-8: Determination of scale factor for scenario 3a (scenario where ethanol is produced from biochar, hydrogen is produced from NCG, and woodchips is used for supplementary heat supply)

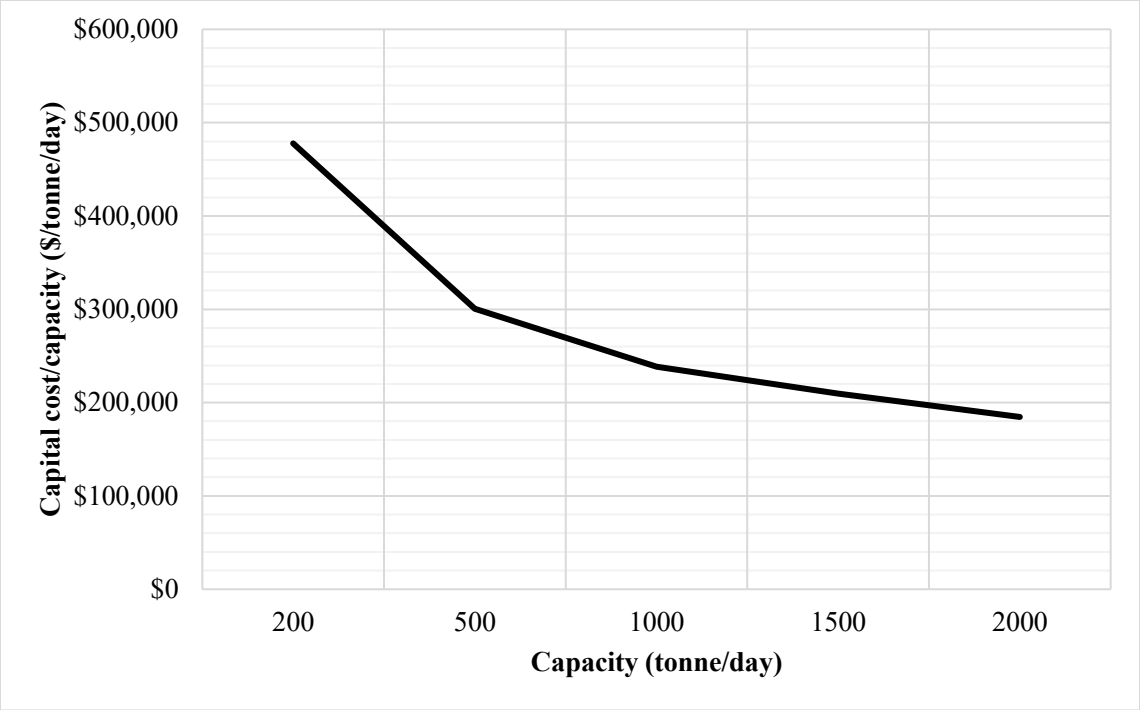

Figure 2-9: Influence of capacity on capital cost for scenario 3a (scenario where ethanol is produced from biochar, hydrogen is produced from NCG, and woodchips is used for supplementary heat supply)

2.3.3 Sensitivity analysis and uncertainty analysis

Sensitivity analysis was conducted for scenario 3a for brevity and because it was the most profitable among the scenarios studied. The profitability was assessed by varying most of the input parameters by +/- 30% of their base values, except the market prices of bio-oil and ethanol. This range was chosen as preliminary estimates are reported to be in this range [97]. A range of +/-50% was used for the market prices of bio-oil and ethanol because of the high uncertainty in the market prices. Figure 2-10 presents the results of the Morris sensitivity analysis. The horizontal axis of the plot gives the mean of the change in the rate of return as the input parameters change from their minimum to maximum values [88]. The higher a parameter's mean, the greater its impact on the rate of return. The standard deviation on the vertical axis indicates the interaction of a

parameter with other parameters or a nonlinear influence on the rate of return [98]. As shown, bio-oil price, capital cost, hydrogen price, feedstock cost, and ethanol price are the most important parameters, in that order. The importance of the prices of the products emphasizes the importance of having a good market price for the products, notwithstanding any process improvement. However, the market for bio-oil is not yet established. Meanwhile, the hydrogen market has gained traction recently. Compared to bio-oil and hydrogen, the market for ethanol is well established and can be expected to grow in future. Focus should be given in improving the yield of ethanol from the fermentation process as ethanol sales will also boost revenue. Further improvements in biomass harvesting and transportation are needed to reduce the delivered cost of the feedstock. For the capital investment, the pyrolysis, fermentation, and PSA units contribute significantly to capital cost. As more pyrolysis projects are built and the learning rate increases, the capital investment in the pyrolysis reactor is expected to decrease. The maximum practical volume of a 1000 m^3 fermentation reactor does not show economies of scale. Increasing ethanol yield from the fermentation process and better reactor design to allow for a high volume inside a single reactor are essential. In the case of the PSA unit, the high cost is largely from the compression needed for the purification process.

The analysis carried out in this study is deterministic in nature. In reality, the values of the input parameters would vary and are unpredictable and will result in variation in the output parameter (the rate of return in this case). To determine the variability of the rate of return due to the potential variation in the input parameter, an uncertainty analysis was conducted. 10,000 Monte Carlo simulations to derive the uncertainty in the rate of return of scenario 3a were run. Uncertainty analysis was also conducted for the input parameters identified in the previous section as having

the most impact on the rate of return. Figure 2-11 is a histogram plot showing the range of the rate of return (between -9% and 33%).

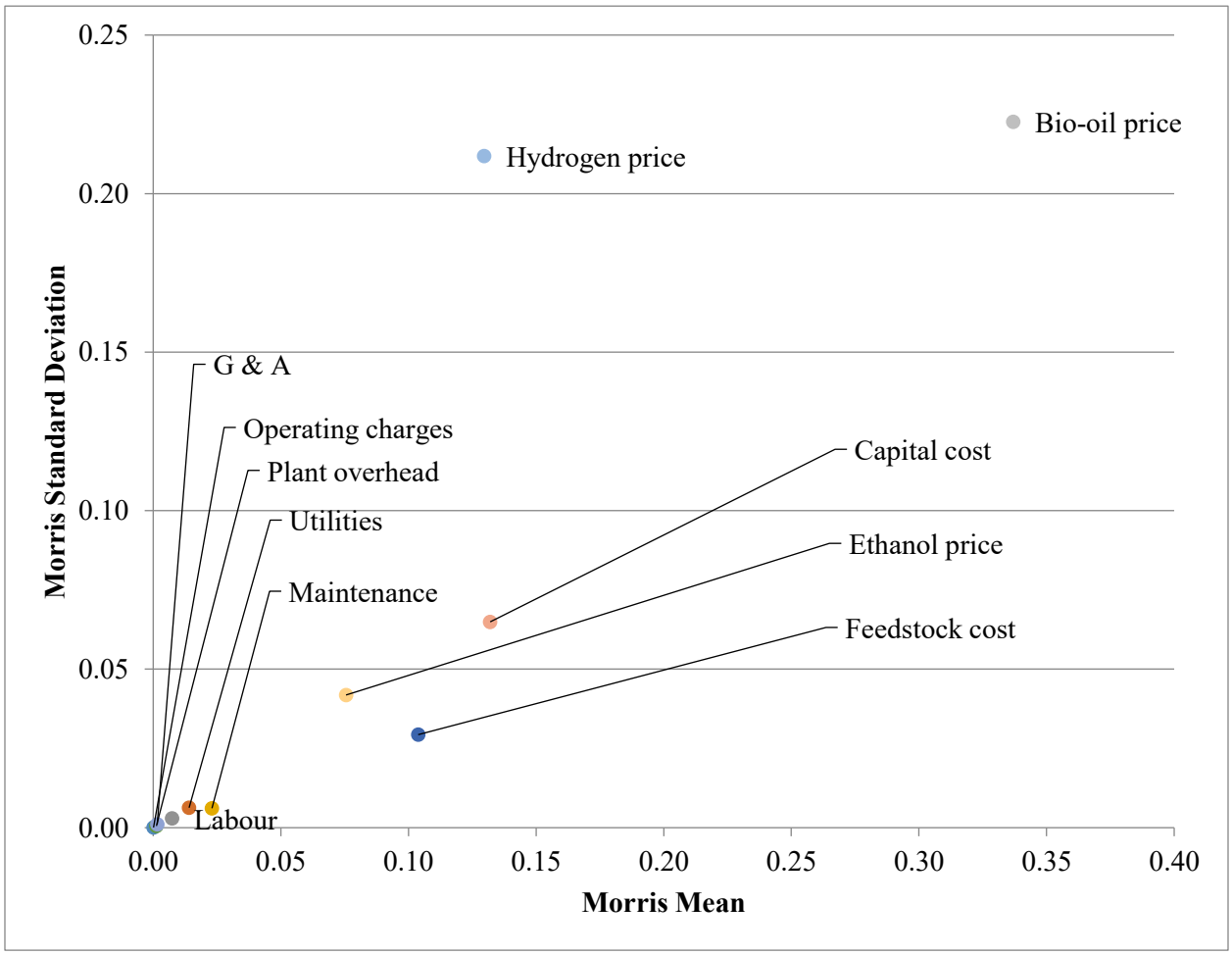

Figure 2-10: Sensitivity analysis of scenario 3a (scenario where ethanol is produced from biochar, hydrogen is produced from NCG, and woodchips is used for supplementary heat supply)

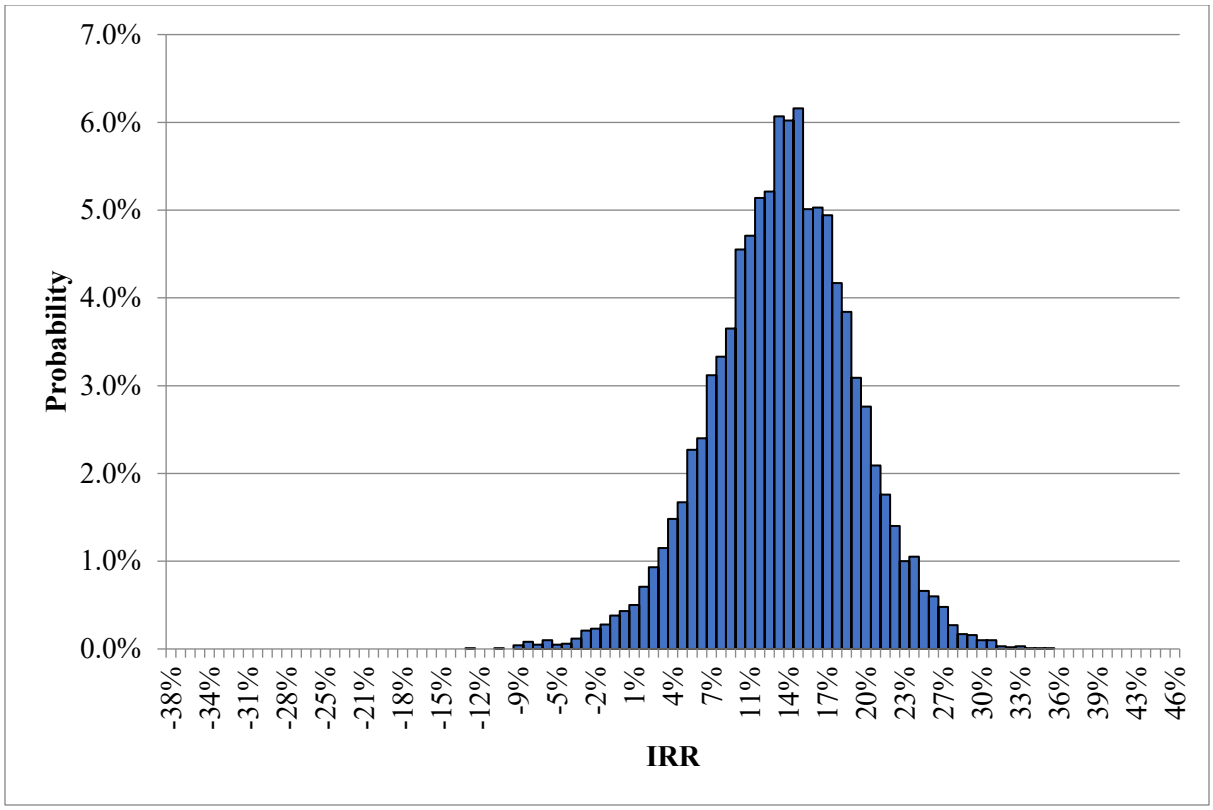

Figure 2-11: Uncertainty analysis of scenario 3a (scenario where ethanol is produced from biochar, hydrogen is produced from NCG, and woodchips is used for supplementary heat supply)

2.4 Conclusion

In this study, the prospect of improving the profitability of biorefineries was assessed through an integrated, multi-product approach, where valuable products, ethanol and hydrogen, were produced from the by-products (biochar and non-condensable gases) of a traditional fast pyrolysis biorefinery. Six scenarios, based on the NCG stream and the type of external fuel (natural gas or biomass) used to supplement heat, were assessed. A fast pyrolysis biorefinery processing biomass at a rate of 2000 dry tonne/day was considered. A data-intensive techno-economic model was developed to assess the internal rate of return of the scenarios relative to the base fast pyrolysis plant.

It was observed that the production of valuable products like ethanol and hydrogen from the by-products of fast pyrolysis is a profitable venture, especially in an uncertain biochar market. This is because if biochar cannot be sold, the six scenarios assessed show a higher rate of return than the base case, which has a rate of return of 7.00%. When natural gas is the external fuel, the internal rate of return is between 10 and 13%. When woodchips are burnt, the internal rate of return is between 7.46 and 9.80%. In every scenario, it is most profitable to use biochar for ethanol production and the hydrogen-rich non-condensable gases stream for hydrogen production. Overall, using natural gas as the external fuel is cheaper than burning woodchips because of the higher heating value and lower cost of natural gas. Although scenario 3a, in which both ethanol and hydrogen were produced in addition to bio-oil, has the highest return rate (13%), this rate of return could be matched by the fast pyrolysis plant if biochar can be sold at $236/tonne. The assessment of the influence of capacity shows that higher capacities are favoured. However, fluctuating feedstock supply and high transportation distances may limit plant capacities. Sensitivity analysis conducted on scenario 3a (the most profitable scenario) showed that the price of the products is a

very important parameter affecting the profitability, in addition to feedstock prices and capital investment. The results of this study provide helpful insights on the potential of improving the economics of the fast pyrolysis process by producing value-added products from the by-products. Overall, from these analyses, there is an indication that an integrated, multi-product concept, has the potential to improve the economic outlook of biorefining processes.

Chaper 3 Life cycle assessment of an integrated biorefinery producing bio-oil, ethanol, and hydrogen

3.1 Introduction

The world has experienced tremendous growth between the last century and now, due to the easy accessibility of energy. Today, the main source of our energy supply is fossil fuels [50, 99]. Because of the effect of burning fossil fuels on our climate, interest in renewable energy sources continues to grow, and great strides have been made in the last decade, as is evident in the decreasing cost of renewable sources like solar power [100]. However, besides the un-dispatchability of the major renewable energy sources, not all sectors of the global economy can be easily decarbonized using these renewable sources. These sectors – transportation, for example – typically rely heavily on non-electrical sources of energy and materials to operate. Biomass resources are well positioned to produce products that are fungible with those from fossil resources. Over the years, there has been considerable interest in biomass valorization, in both the academic and commercial communities. However, progress in the commercialization of biomass valorization has been within the sphere of food-based biomass, which challenges food security and raises social questions. The use of so-called second-generation biomass, however, can ameliorate the potential consequences of using food-based biomass.

Poor economics has been a major hindrance for the commercialization of second-generation biomass valorization. Both thermochemical and biochemical technologies have been used and researched for the valorization of second-generation biomass. In both cases, the traditional approach is to target one product of interest [51] or a material flow path that relies on only one intermediate of interest [23]. This implies that side streams or other material flow paths are rejected

and processed for less valuable applications or, in some cases, are considered waste. As an example, in the biochemical approach, bio-ethanol is a common product of interest. In the traditional production of ethanol from lignocellulosic biomass, cellulose is extracted and, usually, the remaining biomass constituents are combusted. Such single product or single path approaches do not encourage the full use of the original feedstock. The full use of the original feedstock for more valuable applications is a potential way to improve the economics of the process.

Multi-product biorefining is an approach that continues to gain interest for the full valorization of biomass [101-103]. In a multi-product biorefinery, different material paths and technologies are integrated in a deliberate attempt to add value to every unit mass of the original feedstock. With the multi-product approach, the revenue stream of the biorefinery is increased and so the approach has the potential to improve the economics of the biorefinery. Moreover, increasing the product offering of a biorefinery increases the hedge for investors in case of negative market events [25].

The multi-product approach can and has been applied to various technologies for valorizing biomass. One technology to which this approach may be applied is fast pyrolysis. Fast pyrolysis produces bio-oil, non-condensable gases (NCGs), and biochar as products, though the main interest of many studies is bio-oil. Bio-oil is a renewable substance that can serve both as a fuel and as raw material for the production of other fuels and chemical substances [104]. Bio-oil is considered to be analogous to crude-oil. That is, it can be further processed to derive a range of hydrocarbon liquids that are fungible with petroleum-based hydrocarbons [11]. This is often followed by fractionation into different ranges that match those of gasoline, diesel, and jet fuel. While this approach makes this fast pyrolysis biorefinery a multi-product one in nature, it focuses on a single path and neglects the potential of using the NCGs and biochar for more valuable applications than combustion. Hydrogen has gained considerable attention as the energy vector of

the future and much interest has been shown in its adoption [105]. Hydrogen can be produced from hydrogen-rich NCGs. Meanwhile, biochar can be valorized to produce ethanol. Although biochar has been conceived for other valuable applications such as activated carbon [33], soil amendment [106], adsorbent [107], and carbon nanomaterial production [34, 57], unlike ethanol, these applications are not directly or strategically integrated into the biorefinery.

Today, renewable ethanol production that does not directly compete with food is from lignocellulosic biomass. Producing ethanol in this way requires fermentable substrates derived by hydrolysis [35]. However, in the case of biochar, fermentable substrates cannot be produced by hydrolysis. Instead, the biochar can be valorized through gasification into precursors (synthesis gas or syngas) that can then be used for ethanol production. This syngas can be processed thermochemically using the mixed alcohol synthesis process [63] or biochemically using the syngas fermentation process [108]. The mixed alcohol process operates at elevated temperature and pressure [38, 40], and thorough syngas purification is required to prevent catalyst poisoning. The mixed alcohol process requires a specific syngas composition ratio. The syngas fermentation process, on the other hand, operates near ambient temperature and pressure, does not require elaborate gas cleaning, and is not constrained to a specific syngas composition ratio [38]. Several studies have modelled the production of ethanol from the gasification-fermentation route and assessed it from the technical [58], economic [41] and environmental [40] perspectives. But all the studies consider ethanol production only from biomass, not from biochar, and none assess ethanol production from syngas fermentation integrated into a fast pyrolysis biorefinery.

This biorefinery integration results in added complexity and higher energy consumption because of the additional technologies that are needed. Moreover, the use of NCGs and biochar, which are usually used to supplement the energy needs of the biorefinery, implies that external fuel is

required, thus changing the greenhouse gas (GHG) emissions profile of the process. It is critical for the decision makers to understand the life cycle GHG footprint of the biorefinery. It is also important to understand the implications of the added complexity of the conversion processes on the overall GHG emissions of the biorefinery. Existing studies have assessed the GHG emissions intensity of biomass-based facilities, including fast pyrolysis systems. Fan et al. [28] conducted the life cycle GHG emissions assessment of producing bio-oil from several types of forest biomass. Their life cycle assessment (LCA) encompasses feedstock harvesting up to power generation at a power plant, considering different power generation techniques. Peters et al. [47] simulated the fast pyrolysis system and considered the upgrading of the bio-oil into fungible fuels. Instead of fungible fuels, Zhang et al. [48] conducted an LCA of producing commodity chemicals from the pyrolysis pathway. Although there are several environmental assessments of fast pyrolysis biomass-based facilities, they are based on systems in which the bio-oil material path is of primary interest, thus neglecting the potential use of NCGs and biochar. There is very limited work on the assessment of the life cycle GHG emissions of a biorefinery producing multiple products. In this study, the energy analysis and GHG emissions assessment of a novel, multi-product biorefinery that valorizes both the NCGs and biochar from a fast-pyrolysis biorefinery is presented. This biorefinery integrates thermochemical (fast pyrolysis) and biochemical (syngas fermentation) processes to maximize the use of the original feedstock, increase the product offering of the base case pyrolysis plant, and improve the economy of the base case, as earlier study shows [109]. The following are the objectives of this study:

- To carry out process simulations of various configurations of an integrated, multi-product biorefinery incorporating thermochemical and biochemical technologies to understand the energy and mass balances.

- To develop a life cycle assessment model, from the gathering of the feedstock to end-use application of the products (bio-oil, ethanol, and hydrogen), of a biorefinery.
- To determine the energy consumption, net energy ratio, and GHG emissions intensity of the biorefinery configurations, individual products, and end-use applications, from cradle to grave.
- To assess the life cycle GHG emissions for six different configurations of a biorefinery depending on the use of the NCGs and the external fuel used (natural gas or woodchips) and compare them with the base case fast pyrolysis process.
- To conduct sensitivity and uncertainty analyses to identify important input parameters and the implications of variability in these input parameters on the GHG emissions.

3.2 Method

3.2.1 Goal and scope definition

The aim of this study is to assess the energy consumption, fossil-fuel intensity (net energy ratio), and GHG emissions of integrated biorefineries producing bio-oil, ethanol, and hydrogen. Ethanol is more suitable for mobility, while bio-oil is more suitable for direct combustion. Hydrogen, however, can function in both applications. Because of this mismatch in potential applications of bio-oil and ethanol, two system boundaries were established – cradle-to-gate and cradle-to-grave (see Figure 3-1).

The NER (net energy ratio) (cradle-to-gate) is calculated as the ratio of the total energy content of all products at the biorefinery gate to the total fossil energy consumption. In cradle-to-gate GHG emissions assessments, the functional unit is 1 MJ of product energy. The cradle-to-grave assessment looks at the use of each product in an end-use application. The power generation was considered for bio-oil and hydrogen, as used in a combined cycle power plant, and mobility for ethanol. In the case of ethanol, it was compared with gasoline, and the transportation aspect was not modelled (see Figure 3-1).

These analyses are based on a fast pyrolysis biorefinery processing 2000 dry tonnes per day of spruce woodchips. Apart from a base pathway, six pathways were assessed depending on 1) the use of the NCGs in the biorefining stage and 2) the type of supplemental fuel used in the biorefining stage, which could either be natural gas or woodchips. The terms “configuration” and “pathway” are used throughout this study. These terms may appear to be interchangeable; however, they are

not. In this study, the term “pathway” is associated with a chain of life cycle stages, while the term “configuration” is only applicable to the biorefining stage.

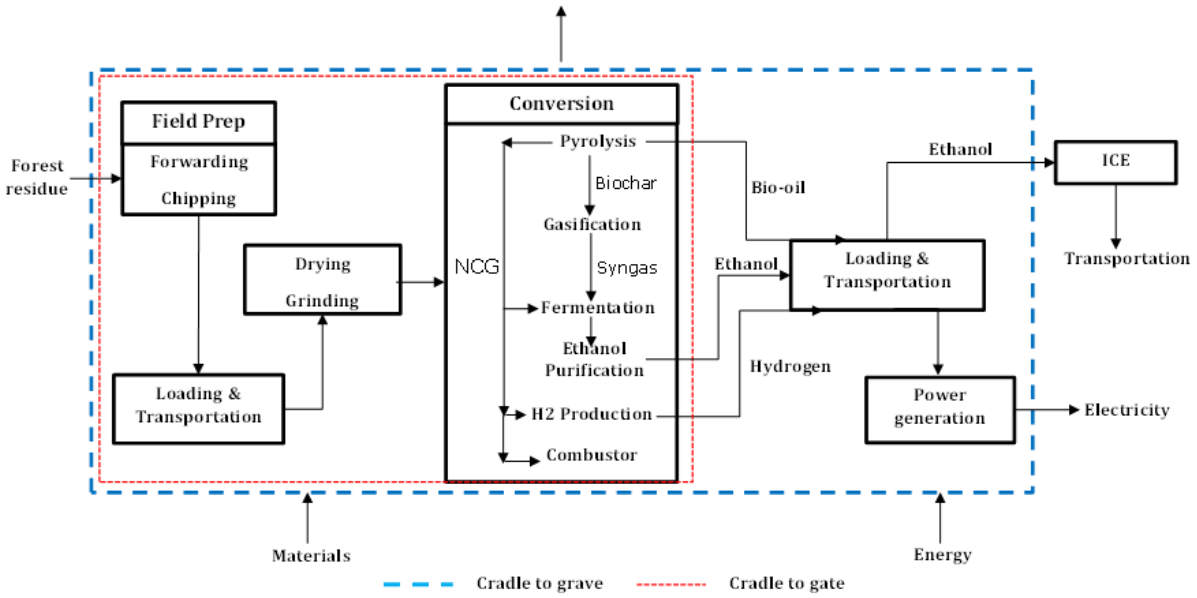

Figure 3-1: Life cycle assessment system boundary of a biorefinery producing ethanol, hydrogen, and bio-oil

3.2.2 Description of pathways

Seven pathways (one base case and six modified pathways) were assessed and are defined by the configurations of the biorefining stage, which is the core of this study. The modification pursued here is that of the biorefining stage. Aside from the base configuration (referred to as configuration 0), there are three major modified biorefining stage configurations (referred to as configurations 1, 2, and 3), and they are based on the use of the NCGs.

Figure 2-2 to Figure 2-4 show the different configurations of the biorefinery. The first configuration (0), shown in

Figure **2-1**, is the conventional fast pyrolysis plant, which was modelled to provide a base configuration to which the modified configurations are compared. The labels "A" and "B" are added, except in configuration 0, to connote the external fuel type used, with "A" and "B" corresponding to natural gas and woodchips, respectively. Hence, there are seven configurations in total, which are summarized in Table 3-1.

Table 3-1: Description of biorefinery configurations

Configuration	Highlights	Final product(s)	Associated figure
0	Base case: conventional fast pyrolysis process	Bio-oil	Figure 2-1
1A	Modified process where NCG is used for heat generation with NG as supplemental fuel	Bio-oil and ethanol	Figure 2-2
1B	Modified process where NCG is used for heat generation with woodchips as supplemental fuel	Bio-oil and ethanol	Figure 2-2
2A	Modified process where NCG is used for ethanol production with NG used as supplemental fuel	Bio-oil and ethanol	Figure 2-3
2B	Modified process where NCG is used for ethanol production with woodchips used as supplemental fuel	Bio-oil and ethanol	Figure 2-3

Configuration	Highlights	Final product(s)	Associated figure
3A	Modified process where NCG is used for hydrogen production with NG used as supplemental fuel	Bio-oil, ethanol, and hydrogen	Figure 2-4
3B	Modified process where NCG is used for hydrogen production with woodchips used as supplemental fuel	Bio-oil, ethanol, and hydrogen	Figure 2-4

The pathways were established by combining a configuration with upstream (feedstock field preparation and transportation to a biorefinery) and downstream (product transportation and power generation) processes. These pathways were named 0, 1, 2, and 3, which correspond to biorefinery configurations 0, 1, 2, and 3. As for the configurations, the labels "A" and "B" are added to the pathways depending on the configuration.

3.2.3 Life cycle stages description

The following sections describe the life cycle stages that were considered, from field preparation to power generation.

3.2.3.1 Field preparation (feedstock production)

Spruce woodchips from forest residues are the chosen feedstock in this study. The spruce tree is an important species in Canada and around the world, making up about 47% of Canada's total

forest inventory [59]. Forest residues are by-products of logging processes that would otherwise be wasted if they are not used. The field preparation stage consists of processes that ready the feedstock for transportation to the biorefinery. These processes are 1) moving residues from the forest area to the roadside, 2) loading the residues into roadside chippers, and 3) chipping the residues at the roadside. These processes consume energy in the form of diesel fuel. The amount of fuel per unit of feedstock processed is given in Table 3-2.

Table 3-2: Energy consumption of field preparation stage processes

Process	**Diesel fuel consumption (L/tonne)**	**References**
Forwarding to roadside	1.92	[110]
Loading residues into chipper	0.82	[111]
Chipping	3.01	[111]

3.2.3.2 Feedstock transportation

Feedstock is transported to a biorefinery by semi-trailer truck. The transportation shipping distance was calculated using the method described in earlier studies [112-114]. The model estimates the transportation distance based on biorefinery capacity and assumes a circular feedstock collection area with the biorefinery located at the center of the circle. Using this model, for the chosen feedstock, an average one-way distance of about 80 km from the field to the biorefinery was estimated. A base value of 1.99 MJ/t.km was used as the fuel consumption efficiency of the semi-truck trailer [111]. The tare weight of a tractor-trailer combination can range between 9 and 16 tonnes [115]. It is also known that trucks are able to carry about twice their unladen weight [116].

Hence, the tare weight of the semi-trailer truck is assumed to be 16 tonnes so that large quantities of feedstock can be moved per trip.

3.2.3.3 Biorefining

This section gives the description of the biorefining stage processes and their modelling, which was carried out in the Aspen Plus process simulator. For the biorefining stage, a processing capacity of 2000 dry tonnes per day of spruce woodchips is considered.

Model validation

The ethanol production process through syngas fermentation is a unique contribution in this study. To verify the reliability and accuracy of the model, literature data was used [41]. The simulated processes were biomass gasification, syngas fermentation, and ethanol purification, and all the process conditions of earlier work were used [41]. The validation was based on the production rate of ethanol. The ethanol production output in earlier work was reported as 71,000 m^3/year versus 71,875 m^3/year output from our model, which shows an error of less than 1.5%. Process conditions specific to this study were subsequently used.

Process model description

Pretreatment

The feedstock, spruce woodchips, received from the field is first processed in the pretreatment area of the biorefinery. This pretreatment includes both grinding to the required particle size for the pyrolysis process and drying to 7% moisture content. For effective operation of the pyrolysis reactor, the particle size and moisture content should be no more than 2 mm and 10%, respectively [60]. The grinding of the feedstock consumes 33 kWh/tonne of feedstock [117]. The drying

operation is carried out using the flue gas generated from the biorefinery. Patel et al. [12] have determined and presented the ultimate and proximate analysis of the feedstock which was considered in this study.

Fast pyrolysis

The pyrolysis process was modelled using the process conditions and results obtained from the pyrolysis experimental study of spruce woodchips in a fluidized bed reactor [12]. The experiment was conducted at a temperature of 490 ^{o}C and at atmospheric pressure. The pyrolysis process was modelled in a RYield reactor. This reactor takes the experimental yields as inputs and estimates the energy consumption of the process. The experimental yields used for this model are taken from an earlier study [12]. Volatile compounds and biochar are the products. The volatile compounds are condensed to extract the compounds that are liquid under ambient condition, which makes up the bio-oil, while non-condensable compounds are directed to the next process depending on the process configuration under consideration. The volatile compounds condense as the temperature decreases to 50 ^{o}C, and the extracted heat is used to generate some of the steam needed for biochar gasification.

Biochar gasification

Biochar needs to be gasified to produce the substrates (CO and H_2) for the syngas fermentation process. Biochar gasification is assumed to be carried out in a dual-fluidized bed gasifier, which has two reactors, one serving as the gasifier and the other the combustor producing heat for the gasifier. Olivine is used as the heat transfer medium between the gasifier and the combustor by continuous circulation at a rate of 12.3 kg/kg of bone dry feed (biochar) as reported by Dutta et al. [63].

The Gibbs energy minimization approach was used in process to model the gasification process using the RGibbs reactor. The gasification reaction occurs at 800 ºC under atmospheric pressure. The steam-to-char ratio of the gasification process is such that the biochar conversion is 80%, as reported by Chaudhari et al. [62]. Biochar is not a conventional compound and was modelled as a non-conventional solid using the ultimate analysis of spruce biochar reported by Burhenne et al. [64].

Syngas fermentation

Ethanol is produced through the fermentation of the syngas produced by the gasification of biochar. The acetogens are the biological workhorses of this process. They are anaerobic micro-organisms that use the acetyl-CoA route for the fixation of CO_2 [66] and other substrates like glucose [67]. Acetogens generally produce two categories of compounds: carboxylic acids and their corresponding alcohols. The former is readily produced. Acetogens have been identified to produce acetic acid, ethanol, butyric acid, butanol, hexanoic acid, hexanol, and 2,3-butanediol [65]. Acetic acid and ethanol are the most common and easily produced compounds. The production of ethanol by acetogens from CO and H_2 is given by Equations 1 and 2 [58].

$$6CO + 3H_2O = C_2H_5OH + 4CO_2 \quad (1)$$

$$6H_2 + 2CO_2 = C_2H_5COOH + 3H_2O \quad (2)$$

The fermentation process was modelled using the equations above with an RStoic block in Aspen Plus. The process conditions of the fermentation process are based on the data from Gaddy et al.'s experiment 15 using the acetogen *Clostridium ljundhalii* [39]. This experiment was selected as it eliminates the net production of acetic acid by recirculating the bottom stream of the ethanol

distillation unit. This recirculation allowed for the achievement of equilibrium concentration of acetic acid in the fermentation medium [39]. This approach was also used in literature [41].

Ethanol purification

The concentration of the ethanol produced in the fermentation process is about 2 wt%. Ethanol must therefore be concentrated to a purity of 99.9% to be used in a fuel application. Ethanol is purified in two steps. In the first step, the diluted ethanol is concentrated to 93 wt% in a distillation column. The distillation unit is modelled with 25 stages, and the feed enters at the 11th stage. A molar reflux ratio of 5 was chosen. In the second step, the concentrated ethanol is further enriched to 99.9% using a molecular sieve separation unit. Further concentration beyond 93% is not feasible due to the azeotropic nature of ethanol-water mixture [68]. The molecular sieve separation unit was included in the process model.

Hydrogen production

The production of hydrogen was assessed only in configuration 3. Pyrolysis gas contains about 75 vol% hydrogen. Hydrogen is produced (separated) from the pyrolysis gas stream using a pressure swing adsorption (PSA) system. The separation of hydrogen from various gas streams using PSA is a common practice today in the process industry [69, 70]. An advantage of PSA is the ability to achieve a high purity of hydrogen (99.9 %) [71]. The PSA system consists of multiple batch-operated columns containing adsorbents such as zeolite and activated carbon [118]. These adsorbents trap unwanted gases and only allow the gas of interest (hydrogen in this case) to pass through. The adsorption process occur at atmospheric temperature [74] and at pressures of 10 and 50 bar [73, 74]. The adsorption of the gas components increases with the adsorption pressure [119]. A pressure of 30 bar was selected for this study as it is the mid-point of the given range. The

pyrolysis gas stream is compressed to this pressure using compressors at a compression ratio of 2.8. The hydrogen recovery from the PSA unit has been reported to be in the range of 80-90 % [74]. A recovery of 90% was used for this study.

3.2.3.4 Product transportation

Product transportation was not considered in the base cradle-to-grave assessment. This is because the actual transportation distance of the product is not predictable. However, its effect was studied through sensitivity analysis for a distance of 200 km [57]. Product transportation links the plant gate and the end-use application considered. Bio-oil is transported by a 30 m^3 tanker trailer. As stated earlier, it is assumed that the tare weight of the tractor-trailer combination is half of the product weight [116]. According to Pootakham et al. [55], petroleum is loaded using pumps operating between 170 and 240 kPa (discharge pressure) and 0.9-1.3 m^3/min (flow). The mid values of these ranges were selected for our assessment. For hydrogen transportation, pipelines are favoured for large amounts and long distances [120]. Small scale (less than one hundred tonne per day) hydrogen transportation is done using liquid tankers and tube trailers [121]. Low hydrogen demand is usually met by tube trailers [122]. Hence, transportation by tube trailers was assessed, using tube trailer specifications [123]. Table 3-3 shows the important characteristics of the tube trailer. Tube trailers are loaded with compressors. Equation 3 models the energy consumption of the compressor as a function of the product capacity of the tube trailer. A drop-and-swap approach for the unloading of the tube trailer at the power generation site was assumed.

$$P = \dot{m}\, ZRT_1 \, \frac{n}{n-1}\left[\left(\frac{p_2}{p_1}\right)^{\frac{n-1}{n}} - 1\right] \times loading\ time \qquad (3)$$

Table 3-3: Hydrogen tube trailer characteristics [124]

Characteristics	Value
Number of tubes	9
Product capacity	~311 kg
Gross weight (including tractor)	~36000 kg
Maximum allowable working pressure	182 bars

3.2.3.5 Power generation

A combined cycle power generation was modelled, consisting of the combustion of each fuel (bio-oil and hydrogen) to generate the electricity through gas turbine. The process operating conditions are the same in all cases. Fuel is supplied to the combustion chamber of the gas turbine at ambient temperature and a pressure of 9 bar. Atmospheric air has been taken in and compressed to 9 bar. Intercoolers are used to cool the air at the exhaust of intermediate stages during compression. For all the fuels used, the air-fuel ratio is such that the combustion temperature is maintained at about 1012 ^{o}C. In the gas turbine, the combustion gases are allowed to expand to near atmospheric pressure. The exhaust gas from the turbine is then used to generate steam to produce more power in the steam turbine. The amount of steam generated is limited to the amount that can satisfy the operating conditions of 350 ^{o}C and 4 bar.

3.3 Life cycle inventory assessment

Table 3-4 gives the life cycle inventory list of the study.

Table 3-4: Life cycle inventory list*

Process	Material/energy	Quantity**	Units
Field preparation			
Residue forwarding to roadside	Diesel		L/day
Pathway 1 (this is biorefinery configuration 1 combined with upstream and downstream life cycle stages)		7,680 (8,987)	
Pathway 2 (this is biorefinery configuration 2 combined with upstream and downstream life cycle stages)		7,680 (10,513)	
Pathway 3 (this is biorefinery configuration 3 combined with upstream and downstream life cycle stages)		7,680 (10,299)	
Residue loading into chipper	Diesel		L/day
Pathway 1		3,280 (3,838)	

Process	Material/energy	Quantity**	Units
Pathway 2		3,280 (4,490)	
Pathway 3		3,280 (4,398)	
Residue chipping at roadside	Diesel		L/day
Pathway 1		12,040 (14,087)	
Pathway 2		12,040 (16,483)	
Pathway 3		12,040 (16,146)	
Feedstock transportation			
Chip loading into semi-trailer truck	Diesel		L/day
Pathway 1		4,080 (4,774)	
Pathway 2		4,080 (5,586)	
Pathway 3		4,080 (5,471)	
Transportation	Diesel		L/day
Pathway 1		35,400 (41,418)	
Pathway 2		35,400 (48,463)	
Pathway 3		35,400 (47,471)	

Process	Material/energy	Quantity**	Units
Biorefinery			
Pretreatment			
Grinding	Electricity	132,000	kWh/day
Drying			
Heat**	Natural gas/woodchips		MW
Configurations 0 & 1 (Configuration 0 is the base case, see Figure 2-1; configuration 1 is the case where ethanol is produced from biochar, see Figure 2-2)		0 (10)	MW
Configuration 2 (Configuration 2 is the case where ethanol is produced from biochar, see Figure 2-3)		31 (53)	MW
Configuration 3 (Configuration 3 is the case where ethanol is produced from biochar, see Figure 2-4)		28 (49)	MW
Pyrolysis			
Heat	Natural gas/woodchips		
Configurations 0 & 1		0	MW

Process	Material/energy	Quantity**	Units
Configuration 2		25	MW
Configuration 3		36	MW
Water consumption	Water	1,187,600	kg/day
Gasification			
Heat	Natural gas/woodchips		
Configuration 1		24	MW
Configuration 2		17	MW
Configuration 3		26	MW
Water consumption	Water	350,000	kg/day
Fermentation			
Water consumption	Water		
Configurations 1 & 3	Water	895,150	kg/day
Configuration 2	Water	1,482,012	kg/day
Ethanol purification			
Heat	Natural gas/woodchips		

Process	Material/energy	Quantity**	Units
Configurations 1 & 3		39	MW
Configuration 2		74	MW
Water consumption	Water		
Configuration 0		-	
Configurations 1 & 3		606,000	kg/day
Configuration 2		1,124,080	kg/day
Hydrogen production	Electricity	148,550	kWh/day
Product hauling			
Loading/unloading			
Bio-oil	Electricity	110.5	kWh/day
Hydrogen	Electricity	122,767.59	kWh/day
Transportation			
Bio-oil	Diesel	22,323.68	L/day
Hydrogen	Diesel	138,043.73	L/day
Power generation			

Process	Material/energy	Quantity**	Units
Water consumption			
Bio-oil	Water	1,449,532.56	kg/day
Hydrogen	Water	316,984.80	kg/day

*Based on 2000 dt/d input feedstock

**Values in parentheses are for the biorefinery configurations in which woodchips are burnt ("B" cases), while those without parentheses are for the configurations in which natural gas is burnt ("A" cases).

3.4 Sensitivity and uncertainty analyses

To understand the significance of the input parameters, a Morris sensitivity analysis was conducted using the Regression, Uncertainty, and Sensitivity Tool (RUST) [88]. The traditional sensitivity analysis discounts the effect of interactions between the input parameters. The Morris method considers these interactions. The result of the analysis is the plot of the Morris standard deviation (ordinate) versus the Morris mean (abscissa). The higher a parameter's Morris mean, the higher its impact on the output. A higher Morris standard deviation indicates that the parameter interacts with other parameters or has a non-linear influence on the output. Uncertainty analysis was also carried out to understand how variations in the input parameters translate into variations in the output. Table 3-5 gives the range of values of the input parameters assessed in this section. Ranges for some of the inputs were taken from the literature. Meanwhile, for other parameters, conservative ranges informed by the authors' judgement were used.

Table 3-5: Range of values for sensitivity analysis input parameters

Parameter	Unit	Base value	Minimum	Maximum	Variation, justification, and sources
Diesel fuel consumption for loading residue into chipper	L/tonne	0.82	0.41	1.23	±50

Parameter	Unit	Base value	Minimum	Maximum	Variation, justification, and sources
Diesel fuel consumption for forwarding	L/tonne	1.92	0.81	2.73	±50
Diesel fuel consumption for chipping	L/tonne	3.01	2.26	4.52	±50
Diesel fuel consumption for loading chips into semi-trailer	L/tonne	1.02	0.51	1.53	±50
Feedstock transportation diesel fuel consumption	L/t.km	1.99	1.41	2.30	Base value is taken from Nie et al. [111], The minimum value is taken from Akbari et al. [125], and the maximum value is calculated from Pootakham et al. [55].

Parameter	Unit	Base value	Minimum	Maximum	Variation, justification, and sources
Diesel fuel heating value	MJ/L	36.00	34.00	38.00	
Density of bio-oil	kg/m^3	1250.00	1100.00	1300.00	This range is taken from another study [126]
Heating value of bio-oil	MJ/kg	18.00	15.00	21.00	
Diesel fuel emission factor	gCO_2eq/L	3771.00	1885.00	5656.00	[127]
Electricity emission factor	gCO_2eq/kWh	544.00	0.00	594.00	Base and minimum values are taken from Davis et al. [128], while and the maximum value is 10% higher than the base value.
Natural upstream gas emission factor	gCO_2eq/GJ	8800.00	6600.00	11000.00	Base value is the 5-year average of the natural gas

Parameter	Unit	Base value	Minimum	Maximum	Variation, justification, and sources
					recovery, processing, transmission, and distribution emissions [129, 130]. The minimum and maximum values are taken as ±25 of the base value.
Water emission factor	gCO_2eq/kg	0.93	0.47	1.40	±50

3.5 Results and discussion

Because the biorefinery stage is both the core and the most intricate aspect of this study, the analysis of biorefinery mass yields and energy consumption is given special attention here. The overall analysis of life cycle energy consumption (the prerequisite for the determination of both the NER and GHG emissions intensity) is discussed. The NER and GHG emissions intensities are also discussed.

3.5.1 Mass yields and energy consumption analysis of biorefinery configurations

The annual production rate of each product is presented in Table 3-6. The base plant assessed capacity production rates are 1023, 303, and 718 tonnes/day for bio-oil, biochar, and NCGs, respectively. In the modified plants, syngas production from biochar is 555 tonnes/day in all cases. The same volume of ethanol is produced from syngas in both configurations 1 and 3, while configuration 2 produces more than double that of configurations 1 and 3. This is because a larger gas stream is processed – syngas plus NCGs. The yields of ethanol were derived to be 857 L/tonne (of biochar) in both configurations 1 and 3, and 743 L/tonne (of biochar plus NCGs) in configuration 2.

The energy consumption distribution (in various sections of the process) for each of biorefinery configuration is depicted in Figure 3-2. It should be noted that the energy demand of the major process equipment shown is the same in all configurations, except for the drying and ethanol purification units. In the case of drying, the energy demand is about 60.8 MW for the configurations that involve burning natural gas as a fuel. In the configurations that involve burning woodchips, the drying energy needs increase over the base value of 60.8 by 10.6, 22.4, and 20.7 MW for configurations 1, 2, and 3, respectively. The difference in the volume of ethanol processed

between configurations 1 and 3 and configuration 2 is the reason the energy demand of the ethanol purification unit is not uniform. As shown in Figure 3-2, the drying process is the highest energy-consuming unit, except in configuration 2, where the high quantity of ethanol produced results in a high energy demand in the purification process. In every configuration, the drying unit makes the difference between the "A" and "B" configurations. Furthermore, configuration 2 is the highest energy-consuming configuration, due to its high energy consumption in ethanol purification. The compression requirement for hydrogen production results in configuration 3 consuming more energy than configuration 1.

In every configuration, the thermal energy requirement is first satisfied by combustible gases available from different units. These combustible gases are the NCGs and off-gases from the fermentation and PSA units. The quantity and source of these combustible gases depends on the configuration. Electrical energy demands are met by grid supply. In configuration 0, the drying and pyrolyzing thermal energies are satisfied by the NCGs and 16% of the biochar. Thus, configuration 0 is self-sufficient in terms of satisfying its thermal energy requirements. Grinding energy is from electricity. In configuration 1, 68% of the required thermal energy is satisfied by NCGs and off-gases from the fermentation unit. This fully satisfies the drying and pyrolyzing thermal energy needs as well as 42% of the thermal energy needs of the gasification process. In configuration 2, off-gases (421 tonnes/day) from the fermentation unit satisfy 38% of the thermal energy requirements, including 58% of the pyrolyzing, 50% of the drying, and 60% of the gasification operations. In configuration 3, the off-gases come from the fermentation and PSA units and satisfy 37% of the heat demand. This includes 42%, 54%, and 39% of the pyrolysis, drying and gasification operations, respectively. The remaining energy consumption of all

configurations is satisfied by supplementing the NCGs and/or off-gases with NG or woodchips (see Table 3-6).

Table 3-6: Yearly product yield and external fuel consumption

	Bio-oil ($L \times 10^3$/yr)	**Ethanol** ($L \times 10^3$/yr)	**H_2** ($kg \times 10^3$/yr)	**External fuel** ($kg \times 10^3$/yr)
Configuration 1A	289,000	85,000	-	45,504
Configuration 1B	289,000	85,000	-	231,647
Configuration 2A	289,000	158,860	-	97,848
Configuration 2B	289,000	158,860	-	492,557
Configuration 3A	289,000	85,000	18,170	90,608
Configuration 3B	289,000	85,000	18,170	454,667

Note: “A” pathways consume NG and “B” pathways woodchips as the external fuel.

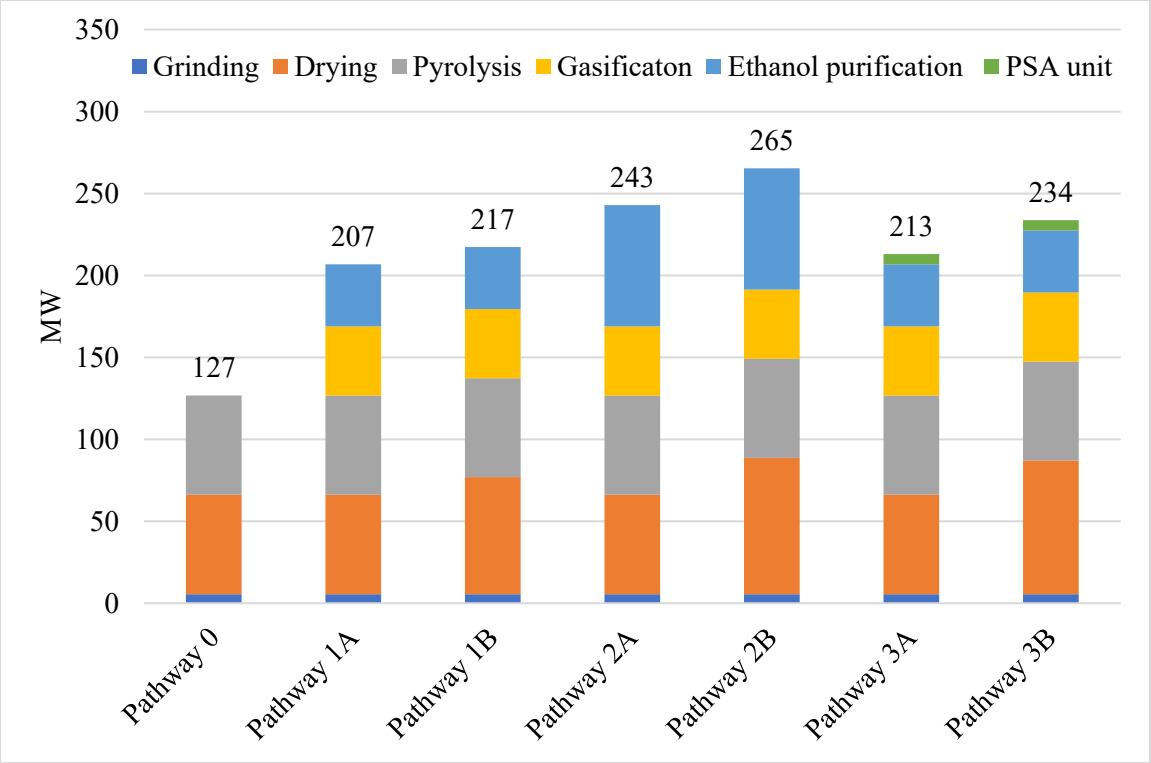

Figure 3-2: Energy demand in the integrated biorefinery configurations (Pathway 1A: Ethanol from biochar; natural gas for supplementary heat | Pathway 1B: Ethanol from biochar; woodchips for supplementary heat | Pathway 2A: Ethanol from biochar and NCG; natural gas for supplementary heat | Pathway 2B: Ethanol from biochar and NCG; woodchips for supplementary heat | Pathway 3A: Ethanol from biochar; Hydrogen from NCG; natural gas for supplementary heat | Pathway 3B: Ethanol from biochar; Hydrogen from NCG; woodchips for supplementary heat)

3.5.2 Overall pathway energy consumption analysis

Figure 3-3 shows the cradle-to-gate energy consumption of the pathways. The most energy intensive of the life cycle stages is the biorefining stage, with its contribution ranging between 84.4% and 91.1%. The breakdown of the biorefining stage energy consumption has been discussed in the previous section. The field preparation and feedstock transportation stages are considerably

less significant than the biorefining stage. The field preparation and feedstock transportation stages contribute between about 3.3% and 5.8%, and 5.6% and 9.8%, of the total life cycle energy consumption, respectively. A comparison of the "A" and "B" pathways reveals that the "B" pathways are more energy intensive than the "A" pathways. This difference comes from the use of wood as the biorefinery fuel in the "B" pathways, which increases the amount of biomass collected and transported, hence increasing the diesel consumption in the field preparation and feedstock transportation stages. Taking pathway 1 as an example, the energy consumption in the field preparation and feedstock transportation for the "A" and "B" pathways are 8.8 and 10.3 MW, and 14.7 and 17.3 MW, respectively. Also, among all the pathways, for both "A" and "B," pathway 2 is the most energy intensive. This higher energy intensity of pathway 2 mainly stems from the higher biorefining stage energy consumption. As might be expected, the quantity of energy required in the base pathway is the lowest. This is because the other pathways have additional processes involved.

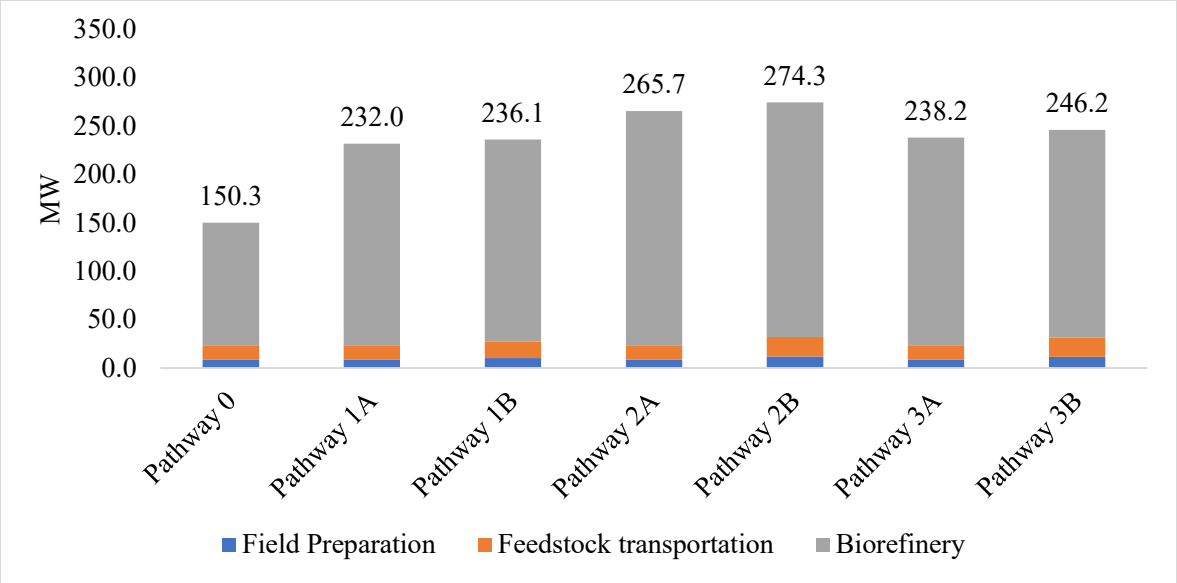

Figure 3-3: Cradle-to-gate energy demand of integrated biorefinery pathways (Pathway 1A: Ethanol from biochar; natural gas for supplementary heat | Pathway 1B: Ethanol from biochar; woodchips for supplementary heat | Pathway 2A: Ethanol from biochar and NCG; natural gas for supplementary heat | Pathway 2B: Ethanol from biochar and NCG; woodchips for supplementary heat | Pathway 3A: Ethanol from biochar; Hydrogen from NCG; natural gas for supplementary heat | Pathway 3B: Ethanol from biochar; Hydrogen from NCG; woodchips for supplementary heat)

3.5.3 Net energy ratio

The NER of each pathway was determined to understand the fossil energy intensity of the pathways. The NERs of the assessed pathways based on the cradle-to-gate analysis are given in Table 3-7. The plant gate was used as the end point for a uniform comparison. The NER calculation discounts the use of renewable energy input. These renewable energy inputs are either from the by-products within the biorefineries system or the use of woodchips as fuel. Hence, with this

discounting, the energy consumption of the configurations burning more renewables appears lower than the gross consumption.

As explained in previous sections, the biorefinery stage is the major energy-consuming stage. Since the "B" pathways consume woodchips, a renewable fuel, in the biorefinery, these have a considerably higher NER than the "A" pathways where natural gas is combusted in the biorefinery. When natural gas is the external fuel of choice in the biorefineries, pathway 1 has the highest NER value, which is about 35 and 27% more than those of pathways 2 and 3, respectively. Although pathways 2 and 3 both have higher total product energy (see Figure 3-4) than pathway 1 (18% and 28% more, respectively), they have much higher fossil energy consumption (81% and 76% more, respectively).

When woodchips ("B" pathways) are the supplemental fuel in the biorefineries, pathway 2 becomes the most favourable, with NER values 3% and 5% higher than those of pathways 1 and 3, respectively. Although pathway 3 has the highest total product energy output, its fossil input is higher than that of pathway 2. Meanwhile, pathway 2 has a total product energy output that is within the range of pathway 3, when both pathways are compared to pathway 1. Overall, the base pathway has the highest NER.

Table 3-7: Net energy ratio of pathways

Pathway	**Net energy ratio**
0	9.43
1A	2.72
1B	8.20
2A	1.78

Pathway	Net energy ratio
2B	8.53
3A	1.98
3B	8.13

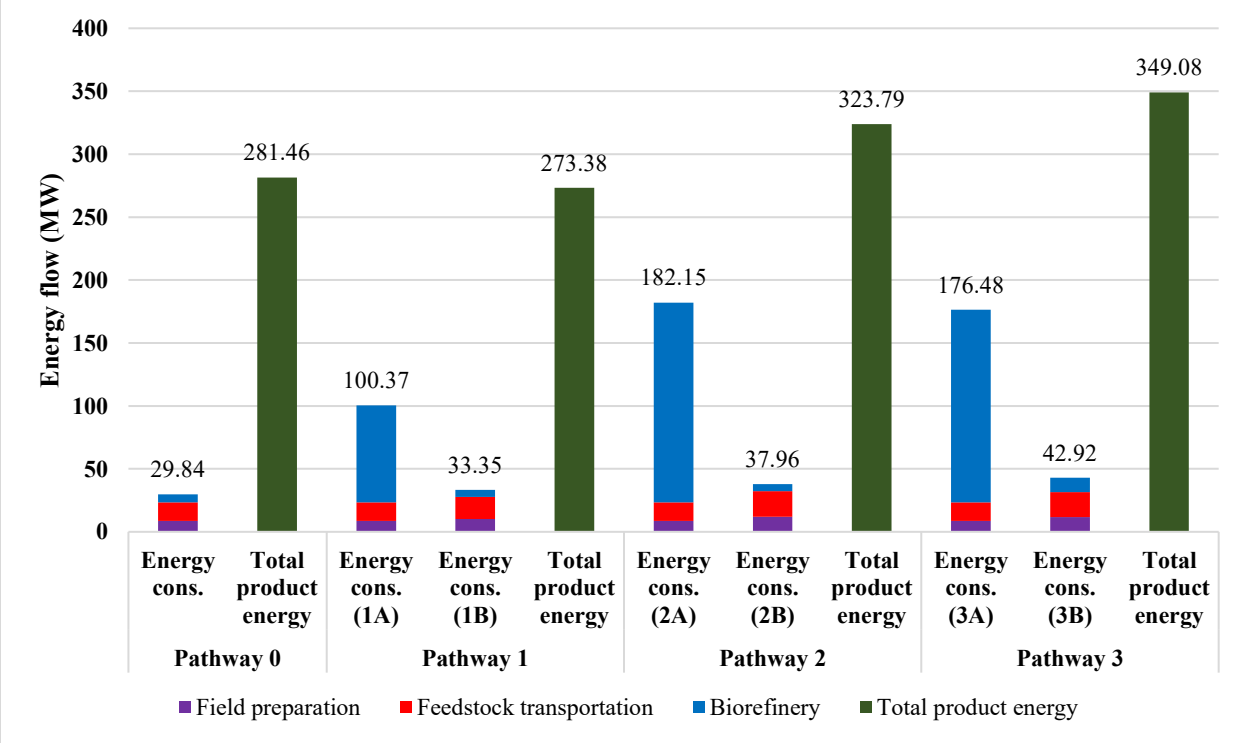

Figure 3-4: Cradle-to-gate energy flow of integrated biorefineries (Pathway 1A: Ethanol from biochar; natural gas for supplementary heat | Pathway 1B: Ethanol from biochar; woodchips for supplementary heat | Pathway 2A: Ethanol from biochar and NCG; natural gas for supplementary heat | Pathway 2B: Ethanol from biochar and NCG; woodchips for supplementary heat | Pathway

3A: Ethanol from biochar; Hydrogen from NCG; natural gas for supplementary heat | Pathway 3B: Ethanol from biochar; Hydrogen from NCG; woodchips for supplementary heat)

3.5.4 Greenhouse gas emissions assessment

This section presents the GHG emissions associated with each of the assessed systems. The emissions are separated into two categories: (i) by pathway (to understand how clean each pathway is) and (ii) by product and end-use application (to understand the emissions intensity range of each product). This was done so that a comparison can be made with the conventional approaches of producing these products. This will also enable us to know how these products perform in an end-use application.

3.5.4.1 By pathway (cradle-to-gate)

This section provides the GHG emissions of each pathway. As in the case of the NER, this cradle-to-gate assessment is done to have a uniform end point for comparison. The results are given in Figure 3-5. As shown, the "B" pathways have lower emissions intensities than the "A" pathways; this is because of the lower fossil energy input, as was found with the NER. The GHG emission intensities of the "B" pathways are about 53, 31, and 49% of those in the "A" pathways, for pathways 1, 2, and 3, respectively. Hence, the use of woodchips, a renewable resource, significantly reduces the emissions intensity of the pathways. With natural gas as the biorefinery fuel, pathway 2 is the most emission intensive. This is because of the large quantity of ethanol being produced, which uses a considerable amount natural gas for heating in the purification step. In these cases, the biorefinery is the major emissions contributor. This is because the biorefinery is the most energy-intensive stage in the life cycle (see section "Overall pathway energy consumption analysis").

When woodchips are burnt instead, pathway 3 is the most emissions-intensive pathway. The lower emissions of pathway 3 in both the field preparation and feedstock transportation stages, compared to pathway 2, are offset by the GHG emissions from pathway 3's higher electrical energy use in the biorefining stage, which is dependent on the carbon-intensity of the selected grid. Unlike the "A" pathways, the biorefinery contribution is significantly reduced in the "B" pathways, as the only source of emissions from the biorefinery is electricity. The contribution of the biorefining stage is now about the same as that of the field preparation stage. In all, the base pathway has a lower emissions intensity than all the improved pathways. This is because pathway 0 has fewer processes and does not require external fuel.

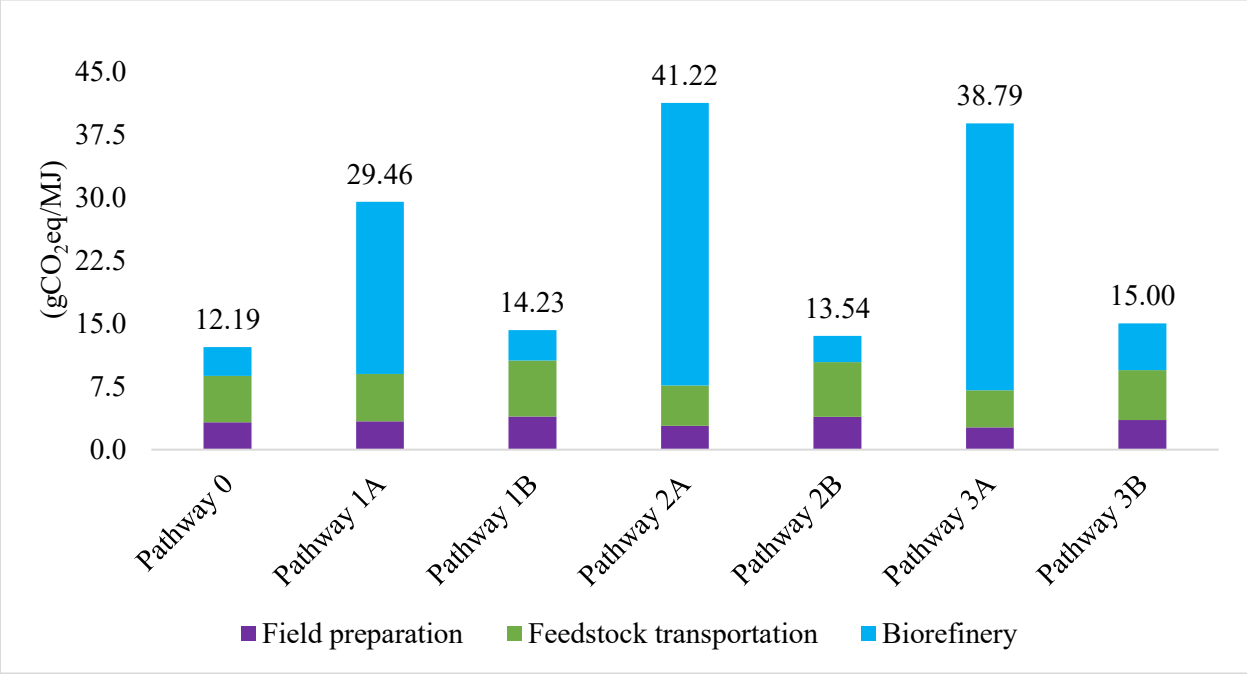

Figure 3-5: Cradle-to-gate GHG emissions intensity of integrated biorefinery pathways (Pathway 1A: Ethanol from biochar; natural gas for supplementary heat | Pathway 1B: Ethanol from biochar; woodchips for supplementary heat | Pathway 2A: Ethanol from biochar and NCG; natural gas for

supplementary heat | Pathway 2B: Ethanol from biochar and NCG; woodchips for supplementary heat | Pathway 3A: Ethanol from biochar; Hydrogen from NCG; natural gas for supplementary heat | Pathway 3B: Ethanol from biochar; Hydrogen from NCG; woodchips for supplementary heat)

3.5.4.2 By product (cradle-to-gate) and end-use application (cradle-to-grave)

It is important to understand the GHG emissions burden of each product. This allows for comparison with other production pathways (both developing and mature). Figure 3-6 shows the GHG emissions intensity of each product for different pathways. The conventional production of hydrogen is from steam reforming of natural gas; this is the most developed and mature technology for hydrogen production today. Autothermal reforming of natural gas is a technology comparable to steam reforming in terms of maturity, but it is less adopted in the industry. As shown in Figure 3-6, the production of hydrogen from proposed pathway is a cleaner production approach. However, when natural gas is burnt in the biorefinery, there is little or no benefit in GHG emissions, when compared with the autothermal reforming technology, coupled with carbon capture and storage, or an emerging low-carbon technology like natural gas decomposition. Furthermore, the proposed approach is more GHG emissions intensive, when compared with a dedicated bio-pathway, such as fast-pyrolysis.

In the case of ethanol, the derived GHG emissions in this study was compared with those of gasoline since ethanol is considered for mobility applications. Ethanol's GHG emissions intensity from our analysis is lower than that of gasoline. There is a significant GHG emissions reduction relative to gasoline for ethanol produced from pathways where wood is burnt in the biorefinery. This is because ethanol purification is the most influential stage in the ethanol production life cycle and its emissions are discounted when woodchips are the fuel of choice. When natural gas is the

fuel of choice, the margin between the GHG emissions intensity of gasoline and ethanol from our proposed method is reduced, especially for pathways 1 and 3. The high GHG emissions intensity of ethanol in these cases is primarily due to the ethanol purification step. While the total GHG emissions associated with ethanol production in pathway 2A are 32% and 25% higher than those in pathways 1A and 3A, respectively, the lower specific GHG emissions of ethanol (as shown in Figure 3-6) in pathway 2A are because the amount of ethanol produced is double that produced in 1A and 3A. In addition, the absolute GHG emissions associated with ethanol in the gasification and drying processes are 67% and 6.7 % higher in pathway 3A than in pathway 2A, respectively. As a result of this, in pathway 3A, the GHG emissions intensity of ethanol is only marginally better than that of gasoline.

For bio-oil, comparison with a petroleum product like heavy fuel oil is apt. There is a clear emission reduction in this case. However, compared to the base case, bio-oil produced from the integrated approaches does not show much benefit, especially in pathways 2A and 3A, where the emissions are much higher. This is because the base case configuration is thermal-energy self-sufficient and burns NCG and some biochar, which are renewable fuels.

It was observed that using hydrogen and bio-oil from these integrated systems provides significant GHG emissions benefit, compared to power generation from natural gas and coal, when their transportation to the power plant is not considered. As seen in Figure 3-7, for bio-oil, this GHG emissions benefit relative to conventional power plants still holds true. However, this is not the case for hydrogen. There is a significant rise in GHG emissions with hydrogen transportation. This is due to hydrogen's low density, which does not allow a large volume to be transported. To put this into perspective, the quantity of hydrogen transported in a tube trailer is about 300 kg and the tare weight of a truck is about 36 tonnes. This is tantamount to transporting an empty truck.

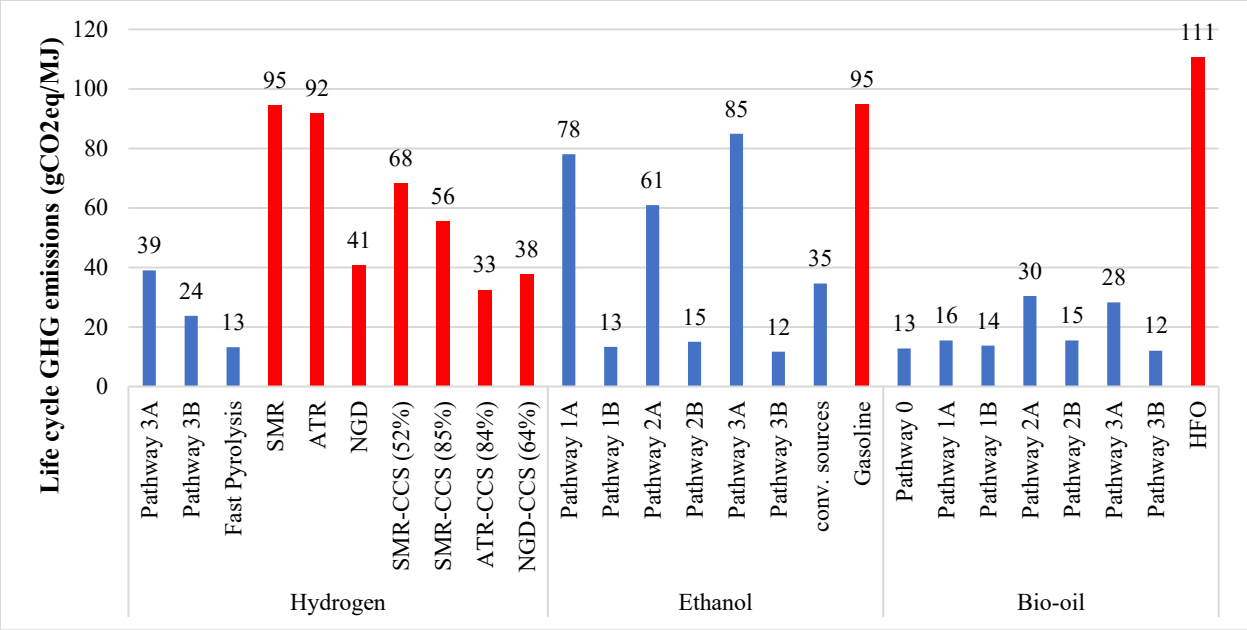

Figure 3-6: Cradle-to-gate emissions intensity of products from integrated biorefineries (Pathway 1A: Ethanol from biochar; natural gas for supplementary heat | Pathway 1B: Ethanol from biochar; woodchips for supplementary heat | Pathway 2A: Ethanol from biochar and NCG; natural gas for supplementary heat | Pathway 2B: Ethanol from biochar and NCG; woodchips for supplementary heat | Pathway 3A: Ethanol from biochar; Hydrogen from NCG; natural gas for supplementary

heat | Pathway 3B: Ethanol from biochar; Hydrogen from NCG; woodchips for supplementary heat)

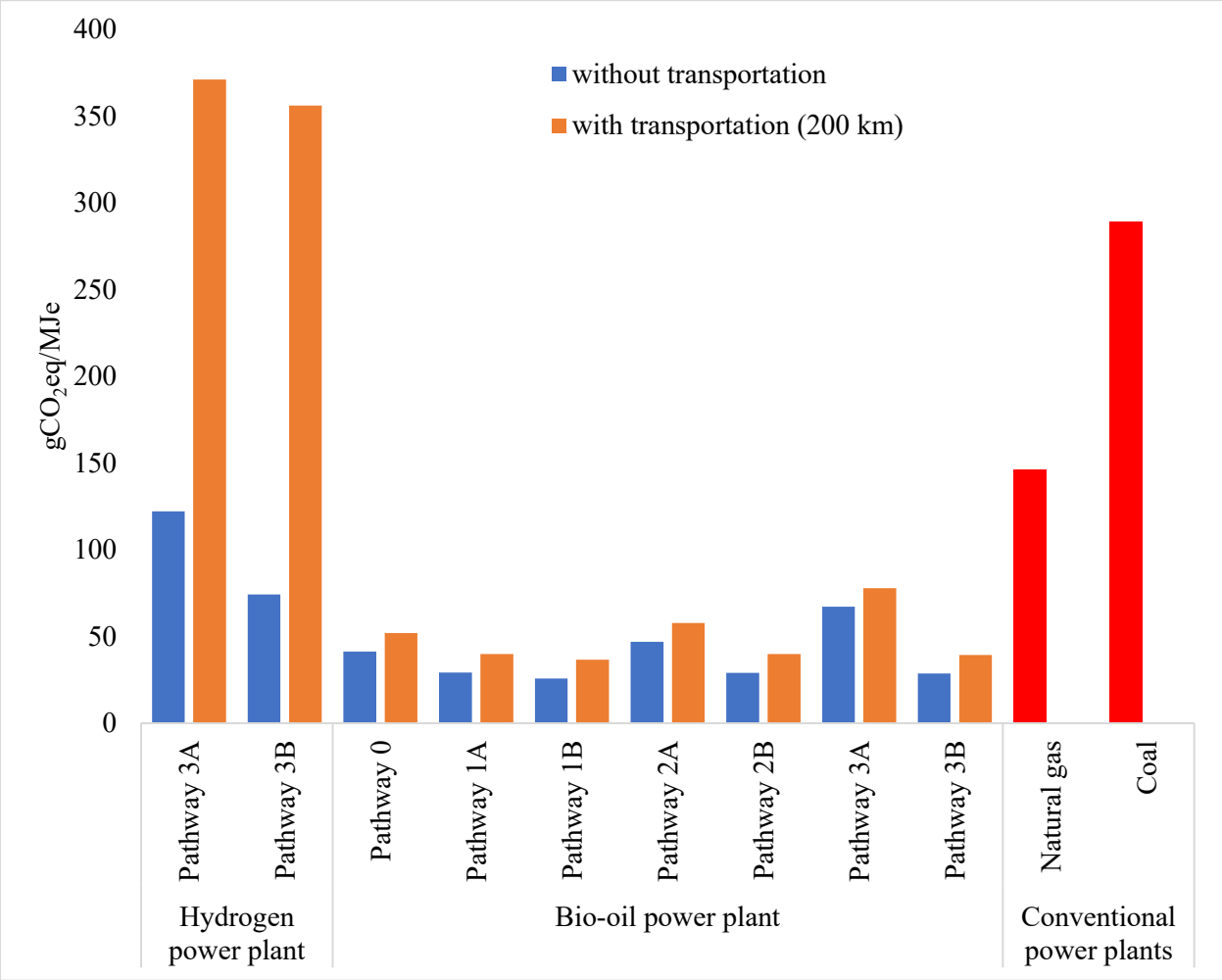

Figure 3-7: Life cycle GHG emissions intensity of power generation from products from integrated biorefineries (Pathway 1A: Ethanol from biochar; natural gas for supplementary heat | Pathway 1B: Ethanol from biochar; woodchips for supplementary heat | Pathway 2A: Ethanol from biochar and NCG; natural gas for supplementary heat | Pathway 2B: Ethanol from biochar and NCG; woodchips for supplementary heat | Pathway 3A: Ethanol from biochar; Hydrogen from

NCG; natural gas for supplementary heat | Pathway 3B: Ethanol from biochar; Hydrogen from NCG; woodchips for supplementary heat)

3.5.5 Sensitivity and uncertainty analyses

3.5.5.1 Effect of feedstock moisture content and produced ethanol concentration

In this study, it was determined that the biorefining stage is a major contributor to the energy and GHG emissions intensities of the integrated biorefineries and their corresponding products. Also, it was observed that the drying process is energy intensive. The moisture content of the input biomass is a parameter that can potentially be tweaked to reduce the energy demand of the drying operation. Similarly, especially for biorefinery configuration 2, ethanol purification is energy intensive. Hence, within the biorefining stage, the effect of biomass moisture content and the ethanol titer produced during the fermentation process was investigated. For brevity, these analyses were only conducted for configuration 2A.

The base case assessment has an assumed biomass moisture content of 50%. Here it was consider that 30% moisture content is a practical amount for feedstock arriving at a biorefinery. Achieving this would require limiting the exposure of the biomass to moisture. Also, a pretreatment process such as torrefaction can be employed for this purpose. At 30% moisture content, the drying energy requirement is reduced by about 39% to 37.1 MW. Figure 3-8 shows the energy consumption of the ethanol purification process as a function of the ethanol titer in the fermentation broth. As this figure shows, higher titers are essential to reduce the energy consumption of the ethanol purification process. For instance, if the ethanol titer could be improved to about 5% from the 2.3% considered in this study, the purification energy will drop by about 42% to 42.8 MW. The production of ethanol from syngas fermentation at higher titers is considerably limited by the microbes' tolerance for high concentrations of ethanol and optimum operating conditions, such as

gas composition, nutrients for microbes, and pH, all of which should be investigated experimentally. The significance of the reduction of both parameters can be seen when they are combined. That is, if the moisture content of the feedstock is reduced to 30% and the ethanol titer is increased to 5%, a gross reduction of about 80 MW in the total energy demand of configuration 2A is observed. This translates to a new cradle-to-gate GHG emission intensity of 30.66 gCO_2eq/MJ (a 26% reduction) for pathway 2A. Meanwhile on a product basis, this translates to 15.35 gCO_2eq/MJ (a 36% reduction) and 35.21 gCO_2eq/MJ (a 39% reduction) for bio-oil and ethanol, respectively, in pathway 2A.

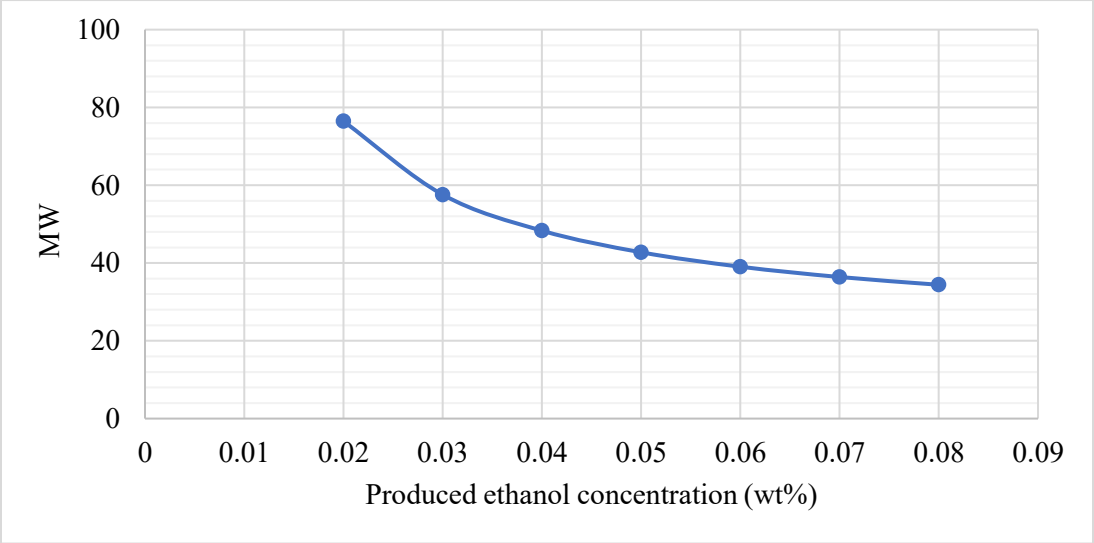

Figure 3-8: Effect of produced ethanol concentration on ethanol purification energy consumption

3.5.5.2 Cradle-to-gate sensitivity analyses

To understand the influence of parameters within the life cycle but outside the biorefinery, a sensitivity analysis of the cradle-to-gate GHG emissions for both the pathways and the products was conducted. This analysis was not done for the end-use application because end-use application GHG emissions follow a similar trend as the products' GHG emissions. The only parameter that could make a difference between the cradle-to-gate and the cradle-to-grave systems is product

transportation, and its influence is discussed in the previous section. Figure 3-9 (a-d) presents the results of the GHG emissions sensitivity analyses. For brevity, the sensitivity analysis results for the other pathways are not shown, as similar trends were observed. The results show that the relative sensitivities are similar, both for the pathways and for the products, and the diesel fuel emission factor and the feedstock transportation fuel consumption are the most important parameters. However, the natural gas emission factor is important in ethanol production. This can be explained by the high energy intensity of the ethanol production process, particularly in the purification steps. With the apparent importance of diesel fuel consumption, the use of higher efficiency equipment in the logistics should be prioritized. Also, a location study to minimize feedstock transportation distance is necessary.

3.5.5.3 Cradle-to-grave uncertainty analyses

Since most of the parameters are probabilistic in nature and can vary from the base values used in the assessment, the results of the effects of the input parameter variabilities on all the outputs considered in depicted in the box plots in Figure 3-10 (a-c) are presented. In Figure 3-10 (a), the degree of variability is roughly equal in all pathways. There is no overlap between the cases when natural gas is burnt and the cases when biomass is burnt. This implies that there is no instance where burning natural gas in the biorefinery produces GHG emissions similar to those from burning biomass. When biomass is burnt and in the base case, the ranges are fairly similar. Meanwhile, in the cases where natural gas is burnt in the biorefinery, pathway 1A is distinctly preferred. In Figure 3-10 (b), the variability in product emissions is highest for hydrogen, followed by bio-oil and then ethanol. In Figure 3-10 (c), the trend is similar.

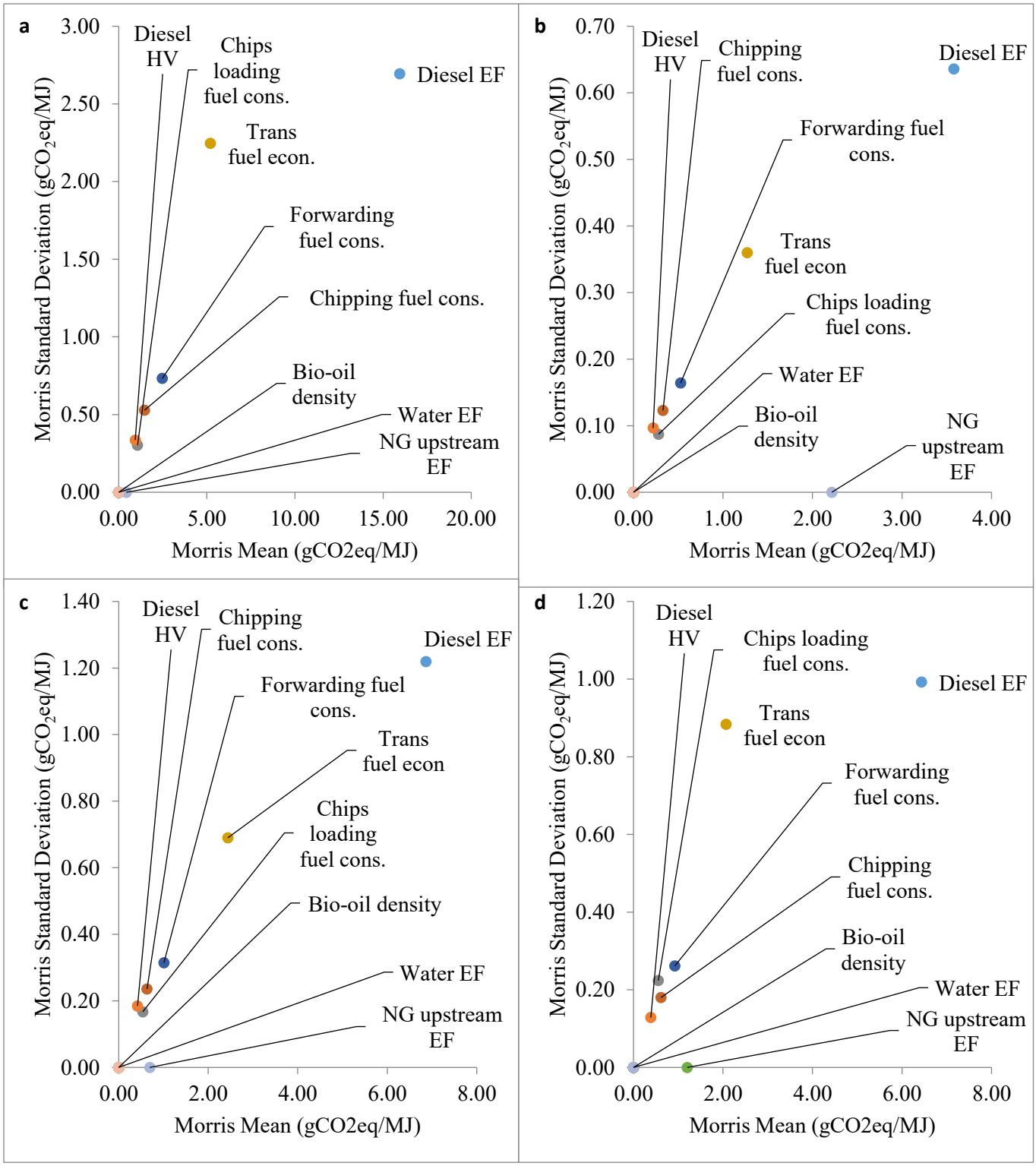

Figure 3-9: Morris sensitivity analysis plots of GHG emissions intensity of (a) pathway 1A (Ethanol from biochar; natural gas for supplementary heat), (b) ethanol from pathway 2A (Ethanol from biochar and NCG; natural gas for supplementary heat), (c) bio-oil from pathway 2A, and (d)

hydrogen from pathway 3A (Ethanol from biochar; Hydrogen from NCG; natural gas for supplementary heat).

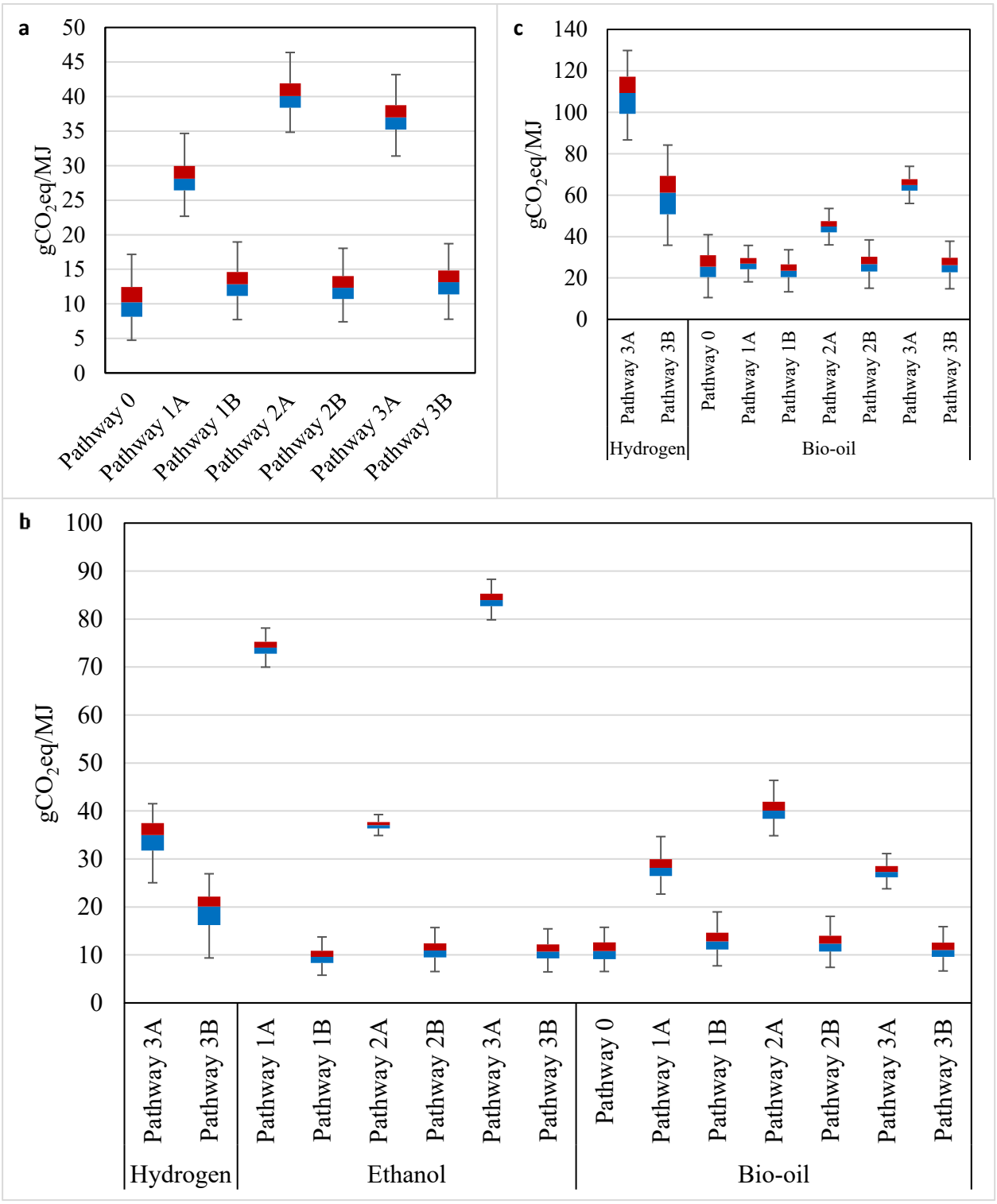

Figure 3-10: Box plots showing variations in GHG emissions of (a) pathways, (b) products, and (c) power generation end use.

3.6 Conclusion

The need to decarbonize the global economy and ensure future energy security has shifted attention towards renewable energy sources over the years. The production of bio-fuels from biomass resources has gained considerable attention because of the possibility to produce fungible transportation fuels. However, the current challenge facing the widespread commercialization of bio-oil and its derivatives is its poor economics. Improvements that valorize and use the by-products of bio-oil production efficiently could be a solution for better economics but come at the expense of increased complexity and energy consumption.

This study, therefore, assessed the energy consumption and environmental implications of a multi-product biorefinery based on a fast pyrolysis process using the NER and GHG emissions as metrics. Specifically, integrated additional technologies to valorize the by-products of the fast-pyrolysis process to produce valuable products, ethanol and hydrogen, in addition to bio-oil were considered. Data-intensive Excel-based models coupled with process simulations were developed for this assessment. Six pathways, defined based on six biorefinery configurations, were assessed and compared to the base fast pyrolysis process.

Based on a deterministic analysis, the NERs of the improved pathways were found to range between 1.78 and 2.72, and 8.13 and 8.53, for the pathways where natural gas and woodchips, respectively, are burnt in the biorefineries. The lower values of the former reveal the high fossil-fuel intensity associated with the use of natural gas. However, the base pathway had an NER value of 9.43, a result of less reliance on fossil energy. The GHG emissions intensity of the assessed pathways ranged between 13.54 and 43.13 gCO_2eq/MJ. Pathway 2A had the highest ethanol production and thus its GHG emission intensity was also high; this is because of the high energy intensity of the ethanol purification process. However, when woodchips are burnt instead, pathway

2 shows the lowest GHG emissions intensity due to its high total product energy. Nonetheless, the GHG emissions intensities of the assessed pathways are all higher than that of the base pathway, which is the conventional fast pyrolysis process. The extra processing involved, especially in the case where natural gas is the fuel of choice, results in more sources of emissions. On a product basis, it can be seen that the GHG emissions intensities of the products produced from the integrated biorefineries are significantly lower than those produced from fossil technologies. However, in the case of ethanol, when natural gas is the fuel of choice, the GHG emissions intensities are not significantly lower than that of gasoline.

Sensitivity analysis results reveal that supplying the feedstock at a lower moisture content reduces the energy consumption and, thus, the GHG emissions intensity of the drying process. Likewise, improving the ethanol titer from the fermentation process can reduce GHG emissions significantly as this reduces the energy consumed during purification. Outside the biorefineries, transportation fuel efficiency is important. Hence, adequate attention should be given to improve transportation efficiency.

Chaper 4 Analysis of the GHG abatement cost of biorefinery products

4.1 Introduction

In the previous chapters, the assessment of the economic and environmental performance of biorefineries was described. In this chapter, how products from biorefineries compare to their conventional counterparts produced from fossil fuels will be explained. The research established that the products from multi-product biorefineries have lower GHG emission intensities than their fossil fuel counterparts. To put the assessment into a clearer context, in this chapter the GHG abatement cost is estimated for producing these products from each of the biorefinery configurations discussed in the previous two chapters.

The objectives of this chapter are:

- To derive the minimum selling price of each product for each of the pathways considered in this study.
- To derive the cost penalty of the GHG emissions savings, that is, the GHG abatement cost of each product relative to a corresponding conventional product.

4.2 Method

4.2.1 Products cost allocation and minimum selling price

The method to derive the costs and emissions associated with the biorefinery configuration was established in the previous two chapters. In this chapter, the method of allocating costs to each product is discussed. This allocation is essential to understand the cost contribution of each product to the overall investment in the biorefineries. To achieve this, costs were allocated to the products based on their market price ratios. The market prices chosen are \$0.32/L [77], \$0.36/L [78], and

$1.5/kg [76], for bio-oil, ethanol, and hydrogen, respectively. Bio-oil was considered as the base product. To carry out the cost allocation, the minimum selling price of bio-oil as a function of the investments in the biorefineries was derived. To derive this minimum selling price, a discount rate of 15% was used. The selection of a discount rate of 15% reflects the low level of development of lignocellulosic biorefineries on a commercial scale; that is, higher risk is involved, and more return would be expected by a potential investor.

4.2.2 Reference products and technologies

Corresponding conventional products and technologies were selected as the reference for the GHG abatement cost calculations. In the case of hydrogen, steam methane reforming (SMR) was selected because it is the most widely used technology for hydrogen production and is commercially mature technology. Today, about 50% of hydrogen produced worldwide is through SMR [131]. GHG emissions from SMR are reported to be about 94.16 $gCO_2eq/MJ\text{-}H_2$ [132]. The cost of producing hydrogen from SMR has been derived to be about $0.94/kg [132]. Ethanol was compared to gasoline because ethanol is being considered for mobility applications and is gradually being blended at higher concentration with gasoline as a transportation fuel, especially in Brazil. Gasoline GHG emissions are reported to be 95 gCO_2eq/MJ [133], and a 10-year average gasoline price of $0.48/L (excluding marketing and distribution, and taxes of combined 34%) [134] was used. For bio-oil, heavy fuel oil is taken as a reference product. Bio-oil can be used for direct combustion in some combined heat and power applications. Heavy fuel oil, a fuel directly combusted, is considered apt as a reference for bio-oil. The price of heavy fuel oil is taken as the one-year average price of very low sulfur fuel oil, which is $0.34/L[135].

4.2.3 GHG abatement cost

The GHG abatement cost is the cost penalty associated with saving the GHG emissions of a process or product. The GHG abatement cost, C_{AB}, expressed in units of \$/tonne-CO_2eq, is calculated as the ratio of the difference between the cost of the product of interest, C_i, as derived from a process of interest, and the cost of the reference product, C_r, as derived from a reference technology, and the difference between the GHG emissions of the reference product, E_r, and the product of interest, E_i. This is expressed mathematically in Equation 4.1.

$$C_{AB} = \frac{C_i - C_r}{E_r - E_i} \quad 4.1.$$

4.3 Results and discussion

The results of the cost allocation for the biorefineries products are presented in Table 4-1. The cost trend follows the rate of return trends discussed in Chapter 2. Configuration 3 has the lowest costs for both bio-oil and ethanol, followed by configuration 2 and 1 (please see section 3.2.3 in Chapter 2 for a detailed explanation). Figure 4-1 shows the GHG abatement cost expressed in \$/tonne-CO_2eq. Bio-oil shows the lowest GHG abatement cost of all the products, and pathway 3A is the least costly (in terms of GHG abatement), despite having a GHG emissions saving value that falls in the lower extreme of the range (see Table 4-2). However, pathway 3A is favoured because it has the lowest minimum selling price of bio-oil. Ethanol shows a wide variability in GHG abatement costs among the different pathways. Generally, the GHG abatement cost of ethanol in the pathways where woodchips were used to provide supplementary process heat are lower than the pathways where natural gas was used. However, it is noteworthy that pathway 2A has a significantly lower abatement cost than the other natural gas pathways, due to its lower GHG emissions intensity and relatively low minimum selling price. Hydrogen also shows a high GHG

abatement cost. This is mainly due to the higher cost of hydrogen from the biorefineries compared to the price of hydrogen from SMR. It is worthy of note that these GHG abatement costs would vary with time because of the volatility of fossil fuel prices. At higher fossil fuel prices, GHG abatement costs would be much lower and may even become negative in some cases, indicating a net cost savings achieved by switching to bioenergy. Overall, the results of these analyses are instructive to decision makers as a guide for setting the cost of CO_2 emissions for fossil technologies.

Table 4-1: The cost of individual products from the studied biorefineries

Pathway	Bio-oil ($/L)	Ethanol ($/L)	Hydrogen ($/kg)
1A	0.382	0.430	-
1B	0.391	0.438	-
2A	0.354	0.396	-
2B	0.391	0.438	-
3A	0.343	0.395	1.60
3B	0.375	0.420	1.74

Table 4-2: GHG emissions savings in gCO_2eq/MJ of biorefinery products relative to the reference products (SMR hydrogen, gasoline, and heavy fuel oil)

Pathway	Bio-oil	Ethanol	Hydrogen
1A	95.08	8.94	-

Pathway	Bio-oil	Ethanol	Hydrogen
1B	96.87	73.69	-
2A	80.11	26.09	-
2B	95.10	71.96	-
3A	82.31	2.12	55.53
3B	98.53	75.29	70.84

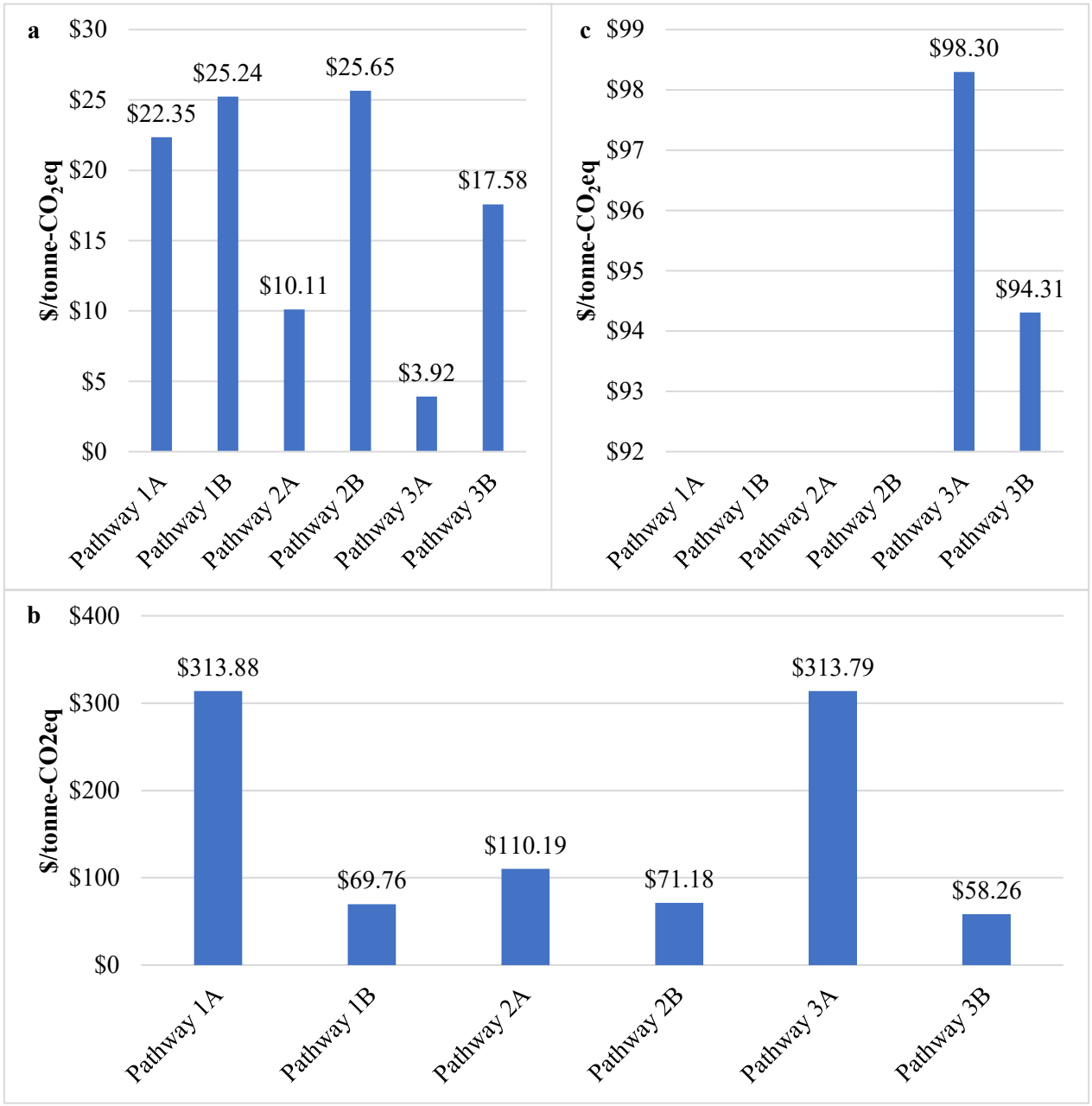

Figure 4-1: GHG abatement cost of (a) bio-oil, (b) ethanol, and (c) (Pathway 1A: Ethanol from biochar; natural gas for supplementary heat | Pathway 1B: Ethanol from biochar; woodchips for supplementary heat | Pathway 2A: Ethanol from biochar and NCG; natural gas for supplementary heat | Pathway 2B: Ethanol from biochar and NCG; woodchips for supplementary heat | Pathway 3A: Ethanol from biochar; Hydrogen from NCG; natural gas for supplementary heat | Pathway 3B: Ethanol from biochar; Hydrogen from NCG; woodchips for supplementary heat)

4.4 Conclusion

In this chapter, the cost penalty associated with the GHG emissions savings were quantified from producing renewable fuels in a novel, integrated, multi-product biorefinery relative to the production of corresponding conventional fossil-based fuels that can be replaced by these products. The minimum selling price of each product was derived for each pathway, and the GHG abatement costs were calculated. The GHG abatement costs are between \$3.92 and \$25.65/tonne-CO_2eq, \$58.26 and \$333.88/tonne-CO_2eq, and \$94.31 and \$98.30/tonne-CO_2eq, for bio-oil, ethanol, and hydrogen, respectively. The results of this assessment are useful for decision makers in determining the price of CO_2 emissions from fossil fuel technologies.

Chaper 5 Conclusion and recommendations for future works

5.1 Conclusion

This study was conducted to understand the economic, energetic, and environmental implications of adopting a multi-product approach towards biorefining. Such an approach encourages the complete valorization of the original biomass feedstock and increases the number of value-added products within the biorefinery product portfolio and, hence, the revenue of the biorefinery. The study determined that fast pyrolysis is suitable for a multi-product approach because of the availability of side streams, biochar, and non-condensable gases (NCGs), that usually end up in low-value applications, mainly combustion. A novel biochar valorization approach (gasification followed by syngas fermentation) was integrated into the conventional fast pyrolysis process to convert biochar into syngas and syngas, in turn, into ethanol. Six different configurations of the biorefinery concept were assessed. These configurations were based on the three different uses of the non-condensable gases: combustion, ethanol production, and purification for hydrogen production. To simulate this integrated biorefinery, the biorefinery was modelled in the Aspen Plus simulation program to obtain all the mass and energy balances associated with the system. To estimate the associated economic implications, a data-intensive techno-economic model was developed.

The biorefineries, in addition to about 289,000 m^3/year of bio-oil, produced between 85,000 (in configuration 1 and 3) and 158,000 m^3/year (in configuration 2) of ethanol, and about 18,000 tonnes/year of hydrogen (in configuration 3). In configuration 1, biochar was converted to ethanol through gasification and subsequent fermentation of the syngas. The non-condensable gases were used to generate heat for the process. In configuration 2, both syngas generated from biochar and

the non-condensable gases were converted into ethanol. Configuration 3 is similar to configuration 1and 2 in the use of biochar. However, in configuration 3, the non-condensable gases were purified to produce hydrogen. These biorefineries consume about 700,000 dry tonnes of biomass per year. The overall mass conversion of the original feedstock was 61%, 69%, and 64% for configurations 1, 2, and 3, respectively. Meanwhile, the base configuration has an overall mass yield of 64%. Hence, only configuration 2 has a better mass yield than the base configuration. However, it is important to note that ethanol and hydrogen have better market prospects than biochar. Furthermore, a higher profitability was achieved in the novel biorefinery configurations than the base case; the IRR of these biorefinery configurations is between 7.46 and 13.01% (see Figure 5-1). The profitability of the biorefineries in which natural gas was burnt was higher than the corresponding biorefineries that burnt woodchips, due to the lower cost and higher heating value of natural gas relative to woodchips. The biorefinery configuration in which biochar is converted to ethanol and hydrogen is produced from the hydrogen-rich non-condensable gases was the most profitable configuration. The profitability of the base case was 7%, if biochar is not sold, but could match the highest profitability among the biorefineries if biochar could be sold at the rate of $236/tonne. However, it is worth noting that the ethanol and hydrogen considered in this study are more strategically integrated into the operations of the biorefinery than biochar and have better market prospects. Sensitivity analysis revealed that the sales price of the products is the most important parameter affecting the profitability of the biorefineries. In addition to the sales price, the capital investment and feedstock cost are important parameters. Higher capacities are preferred because they lower the marginal cost of added capacity. These results prove that a multi-product approach to biorefinery has the potential to return higher profits for investors in the biorefining industry.

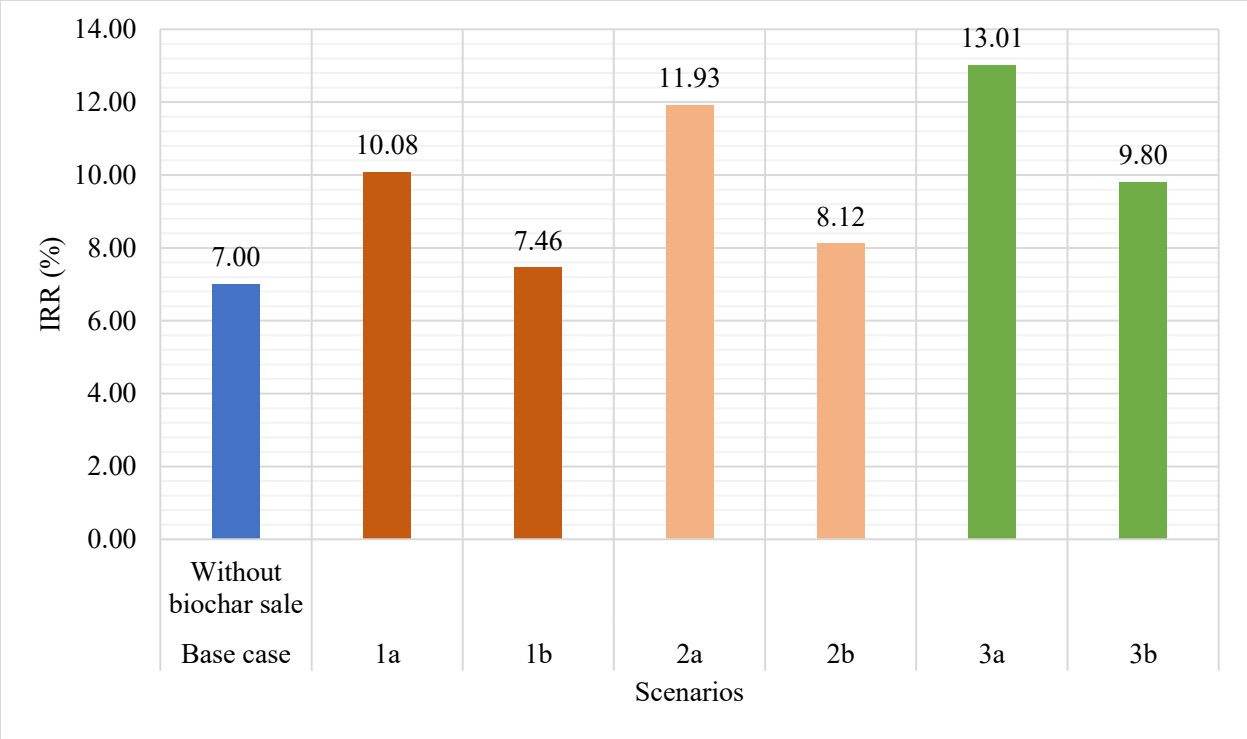

Figure 5-1: Internal rate of return of biorefinery scenarios

Having assessed the economics of the multi-product approach to biorefining, the energetic and environmental implications of the added complexity of the biorefineries from different life cycle perspectives (cradle-to-gate and cradle-to-grave) were assessed. A data-intensive life cycle greenhouse gas emissions assessment model was built for each pathway, starting from field preparation to end-use application. Energy analyses of the biorefineries reveal that energy consumption in the modified life cycle pathways is higher than in the base case and is dominated by the biorefining stage. Thus, it follows that in the biorefining stage, the energy consumption in the base biorefinery configuration is lower than that of the modified configurations. Generally, in the biorefining stage and among the modified configurations, the drying and pyrolysis operations are the significant energy-consuming operations. In addition, this energy consumption is more significant in the "B" pathways, where woodchips are the external fuel of choice. In configuration

2, the high energy intensity of the ethanol purification operation and the larger quantity of ethanol produced makes ethanol purification more energy-intensive than drying and pyrolysis. For the same reason, configuration 2 and, hence, pathway 2 had the highest energy consumption.

The fossil fuel intensity of the biorefinery configurations was estimated using the net energy ratio. As expected, the pathways in which natural gas was burnt in the biorefinery had a much lower net energy ratio than the pathways in which woodchips were burnt. Among the pathways in which natural gas is burnt, pathway 1 had the lowest fossil fuel intensity with an NER value of 2.71. Meanwhile, pathway 2 was the least fossil fuel-intensive configuration, having an NER value of 8.40 when woodchips is the fuel. It might be expected that pathway 1 is the least fossil fuel-intensive pathway when woodchips are burnt; however, the higher total product energy from pathway 2 dominated, relative to the lower fossil energy consumption of pathway 1. The base case had the lowest fossil fuel intensity, with an NER value of 9.43, since energy requirements in the biorefining stage were completely satisfied by the produced non-condensable gases and biochar. The GHG emissions assessments result showed similar trends as the NER (see Figure 5-2). The pathways (and their products) in which woodchips were burnt had lower GHG emissions intensities than the pathways in which natural gas was burnt. Among the pathways in which natural gas was burnt, pathway 2A had the highest GHG emissions intensity, and this stems from its high energy and fossil fuel intensities.

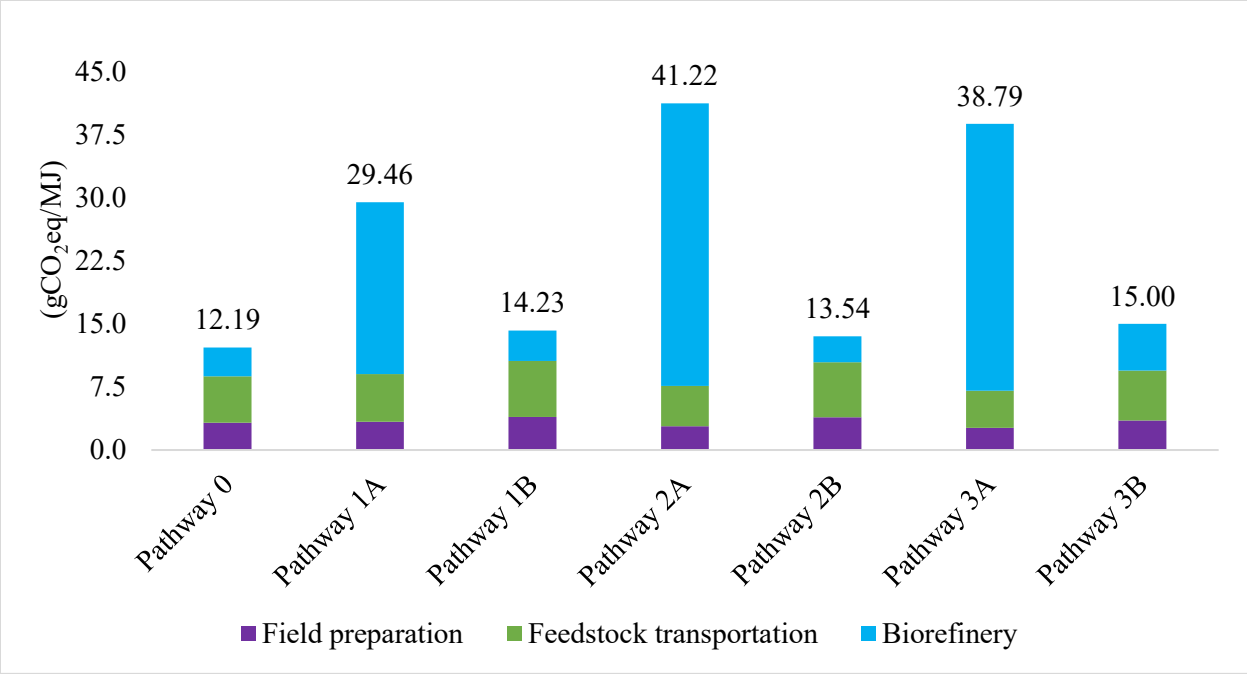

Figure 5-2: Cradle-to-gate GHG emissions intensity of integrated biorefinery pathways

Generally, in the case of product emissions (see Figure 5-3), hydrogen production from the accessed biorefineries proved to be a cleaner approach than producing hydrogen from natural gas production technologies. For instance, hydrogen production from the biorefinery configuration 3 saves between 17 and 71 gCO_2eq/MJ compared to SMR without carbon capture and storage, the conventional hydrogen production technology. In the case of ethanol, when compared to gasoline, the emissions intensities are lower. However, the difference is marginal when natural gas is burnt in the biorefineries for ethanol production. Likewise, when bio-oil GHG emissions intensities are compared to those from heavy fuel oil, there are significant emissions savings of between 81 and 99 gCO_2eq/MJ. Furthermore, when hydrogen and bio-oil are used for power generation, significant cradle-to-grave GHG emissions savings are also observed, relative to power generation from coal and natural gas power plants, when the transportation of these products to the power plants is not considered. When product transportation is considered, the emissions intensity savings still holds

true for bio-oil, but not for hydrogen power generation. The cradle-to-grave GHG emissions intensity of hydrogen power generation is about five times higher when a 200 km transportation distance is considered, compared to when no product transportation is considered. This high impact of hydrogen transportation is due to the low volumetric density of hydrogen.

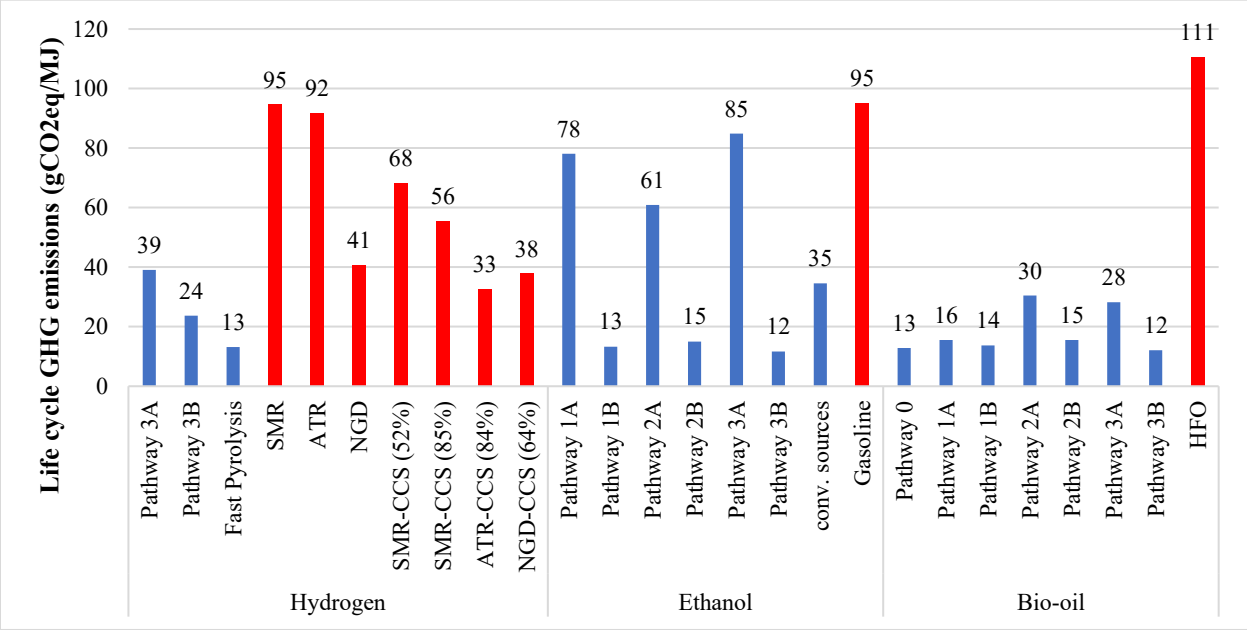

Figure 5-3: Cradle-to-gate emissions intensity of products from integrated biorefineries

Having established the profitability of the multi-product approach to bio-refining relative to the base case and the emissions savings of the derived products relative to their fossil counterparts, the cost penalties associated with these emissions savings for the products were derived. Cost allocation using the ratio of the market prices of the products was done. The results showed GHG abatement costs of between \$3.92 and \$24.81/tonne-CO_2eq, \$64.45 and \$1495.17/tonne-CO_2eq, and \$94.31 and \$98.30/tonne-CO_2eq, for bio-oil, ethanol, and hydrogen, respectively. These derived abatement costs serve as a guide for policy makers in setting a CO_2 emissions tax for

corresponding products from fossil fuel technologies to encourage the development of biorefineries.

5.2 Recommendations for future work

- This study can be expanded to include the further processing of the bio-oil into a transportation fuel to fully understand the impact of the modification on the production of renewable transportation fuels.
- The syngas fermentation process can be used to valorize by-products of other thermochemical processes. Future work can integrate this modification into other processes for by-products that would have otherwise been used for less valuable applications such as combustion. Such technologies include slow pyrolysis, the thermo-catalytic reforming (TCR) process, etc. TCR is a promising technology that can be used to produce high-quality bio-oil. It also generates a large amount of biochar that can be valorized into various products.
- This study accessed the use of spruce woodchips (woody biomass) as the feedstock. A comparative assessment looking at other feedstock categories like municipal solid wastes and agricultural residues would provide information on the effect of the feedstock choice on the profitability of the biorefinery configurations.
- Considering that the method of cost allocation in this study relied substantially on the ratio of the market prices of the products, it is suggested that future studies should look at cost allocation alternatives that reflect the cost contribution of the products within the multi-product biorefinery.

References

1. Anderson D. Chapter 11: Energy and economic prosperity. World Energy Assessment: Energy and the Challenge of Sustainability: United Nations Development Programme; 2000.

2. Ritchie H, Max R. Energy Production and Consumption: Ourwoldindata.org; 2020 [cited 2022 January 28]. Available from: https://ourworldindata.org/energy-production-consumption#citation.

3. Thorbecke W. How oil prices affect East and Southeast Asian economies: Evidence from financial markets and implications for energy security. Energy Policy. 2019;128:628-38.

4. Scheffran J, Felkers M, Froese R. Economic Growth and the Global Energy Demand. Green Energy to Sustainability2020. p. 1-44.

5. Global electricity generation mix, 2010-2020: IEA; [cited 2021 November 19]. Available from: https://www.iea.org/data-and-statistics/charts/global-electricity-generation-mix-2010-2020.

6. de Blas I, Mediavilla M, Capellán-Pérez I, Duce C. The limits of transport decarbonization under the current growth paradigm. Energy Strategy Reviews. 2020;32:100543.

7. Agrawal R, Singh NR, Ribeiro FH, Delgass WN. Sustainable fuel for the transportation sector. Proceedings of the National Academy of Sciences. 2007;104(12):4828.

8. Reitz RD, Ogawa H, Payri R, Fansler T, Kokjohn S, Moriyoshi Y, et al. IJER editorial: The future of the internal combustion engine. International Journal of Engine Research. 2019;21(1):3-10.

9. Mandys F. Electric vehicles and consumer choices. Renewable and Sustainable Energy Reviews. 2021;142:110874.

10. Ioannou I, D'Angelo SC, Galán-Martín Á, Pozo C, Pérez-Ramírez J, Guillén-Gosálbez G. Process modelling and life cycle assessment coupled with experimental work to shape the future sustainable production of chemicals and fuels. Reaction Chemistry & Engineering. 2021;6(7):1179-94.

11. Patel M, Oyedun AO, Kumar A, Gupta R. A techno-economic assessment of renewable diesel and gasoline production from aspen hardwood. Waste and Biomass Valorization. 2019;10(10):2745-60.

12. Patel M, Oyedun AO, Kumar A, Gupta R. What is the production cost of renewable diesel from woody biomass and agricultural residue based on experimentation? A comparative assessment. Fuel Processing Technology. 2019;191:79-92.

13. Dien BS, O'Bryan PJ, Hector RE, Iten LB, Mitchell RB, Qureshi N, et al. Conversion of switchgrass to ethanol using dilute ammonium hydroxide pretreatment: influence of ecotype and harvest maturity. Environmental Technology. 2013;34(13-14):1837-48.

14. Hossain SMZ. Biochemical conversion of microalgae biomass into biofuel. Chemical Engineering & Technology. 2019;42(12):2594-607.

15. Zhu Y, Jones SB. Techno-economic analysis for the thermochemical conversion of lignocellulosic biomass to ethanol via acetic acid synthesis. Pacific Northwest National Lab.(PNNL), Richland, WA (United States); 2009.

16. Skorek-Osikowska A, Martín-Gamboa M, Dufour J. Thermodynamic, economic and environmental assessment of renewable natural gas production systems. Energy Conversion and Management: X. 2020;7:100046.

17. Czernik S, Evans R, French R. Hydrogen from biomass-production by steam reforming of biomass pyrolysis oil. Catalysis Today. 2007;129(3):265-8.

18. Jang Y-S, Malaviya A, Cho C, Lee J, Lee SY. Butanol production from renewable biomass by clostridia. Bioresource Technology. 2012;123:653-63.

19. Hu W, Dang Q, Rover M, Brown RC, Wright MM. Comparative techno-economic analysis of advanced biofuels, biochemicals, and hydrocarbon chemicals via the fast pyrolysis platform. Biofuels. 2016;7(1):57-67.

20. Oh Y-K, Hwang K-R, Kim C, Kim JR, Lee J-S. Recent developments and key barriers to advanced biofuels: A short review. Bioresource Technology. 2018;257:320-33.

21. Maity SK. Opportunities, recent trends and challenges of integrated biorefinery: Part I. Renewable and Sustainable Energy Reviews. 2015;43:1427-45.

22. Li B, Ou L, Dang Q, Meyer P, Jones S, Brown R, et al. Techno-economic and uncertainty analysis of in situ and ex situ fast pyrolysis for biofuel production. Bioresource Technology. 2015;196:49-56.

23. Wright MM, Daugaard DE, Satrio JA, Brown RC. Techno-economic analysis of biomass fast pyrolysis to transportation fuels. Fuel. 2010;89:S2-S10.

24. Brown TR, Thilakaratne R, Brown RC, Hu G. Techno-economic analysis of biomass to transportation fuels and electricity via fast pyrolysis and hydroprocessing. Fuel. 2013;106:463-9.

25. Zhang YHP. Reviving the carbohydrate economy via multi-product lignocellulose biorefineries. Journal of Industrial Microbiology and Biotechnology. 2008;35(5):367-75.

26. Zhao X, Liu D. Multi-products co-production improves the economic feasibility of cellulosic ethanol: A case of Formiline pretreatment-based biorefining. Applied Energy. 2019;250:229-44.

27. Rahmati S, Doherty W, Dubal D, Atanda L, Moghaddam L, Sonar P, et al. Pretreatment and fermentation of lignocellulosic biomass: reaction mechanisms and process engineering. Reaction Chemistry & Engineering. 2020;5(11):2017-47.

28. Fan J, Kalnes TN, Alward M, Klinger J, Sadehvandi A, Shonnard DR. Life cycle assessment of electricity generation using fast pyrolysis bio-oil. Renewable Energy. 2011;36(2):632-41.

29. Yuan Z, Eden MR. Superstructure optimization of integrated fast pyrolysis-gasification for production of liquid fuels and propylene. AIChE Journal. 2016;62(9):3155-76.

30. Jones SB, Meyer PA, Snowden-Swan LJ, Padmaperuma AB, Tan E, Dutta A, et al. Process design and economics for the conversion of lignocellulosic biomass to hydrocarbon fuels: fast pyrolysis and hydrotreating bio-oil pathway. Pacific Northwest National Lab.(PNNL), Richland, WA (United States); 2013.

31. Hiroyuki F, Paul L, Simon B. Hydrogen: Tracking Clean Energy Progress: International Energy Agency; 2019 [Available from: https://www.iea.org/tcep/energyintegration/hydrogen/.

32. Singh B, Singh BP, Cowie AL. Characterisation and evaluation of biochars for their application as a soil amendment. Soil Research. 2010;48(7):516-25.

33. Tan X-f, Liu S-b, Liu Y-g, Gu Y-l, Zeng G-m, Hu X-j, et al. Biochar as potential sustainable precursors for activated carbon production: Multiple applications in environmental protection and energy storage. Bioresource Technology. 2017;227:359-72.

34. Hidalgo P, Navia R, Hunter R, Coronado G, Gonzalez M. Synthesis of carbon nanotubes using biochar as precursor material under microwave irradiation. Journal of Environmental Management. 2019;244:83-91.

35. Zabed H, Sahu JN, Boyce AN, Faruq G. Fuel ethanol production from lignocellulosic biomass: An overview on feedstocks and technological approaches. Renewable and Sustainable Energy Reviews. 2016;66:751-74.

36. Tenenbaum DJ. Food vs. fuel: diversion of crops could cause more hunger. Environ Health Perspect. 2008;116(6):A254-A7.

37. Villanueva Perales AL, Reyes Valle C, Ollero P, Gómez-Barea A. Technoeconomic assessment of ethanol production via thermochemical conversion of biomass by entrained flow gasification. Energy. 2011;36(7):4097-108.

38. Stoll IK, Boukis N, Sauer J. Syngas Fermentation to Alcohols: Reactor Technology and Application Perspective. Chemie Ingenieur Technik. 2020;92(1-2):125-36.

39. Gaddy JL, Arora DK, Ko C-W, Phillips JR, Basu R, Wikstrom CV, et al. Methods for increasing the production of ethanol from microbial fermentation. BIOENGINEERING RESOURCES, INC.; 2007.

40. Roy P, Dutta A, Deen B. Greenhouse gas emissions and production cost of ethanol produced from biosyngas fermentation process. Bioresource Technology. 2015;192:185-91.

41. de Medeiros EM, Posada JA, Noorman H, Osseweijer P, Filho RM. Hydrous bioethanol production from sugarcane bagasse via energy self-sufficient gasification-fermentation hybrid route: Simulation and financial analysis. Journal of Cleaner Production. 2017;168:1625-35.

42. Modisha PM, Ouma CNM, Garidzirai R, Wasserscheid P, Bessarabov D. The Prospect of Hydrogen Storage Using Liquid Organic Hydrogen Carriers. Energy & Fuels. 2019;33(4):2778-96.

43. Benalcázar EA, Deynoot BG, Noorman H, Osseweijer P, Posada JA. Production of bulk chemicals from lignocellulosic biomass via thermochemical conversion and syngas fermentation: a comparative techno-economic and environmental assessment of different site-specific supply chain configurations. Biofuels, Bioproducts and Biorefining. 2017;11(5):861-86.

44. Pourbafrani M, McKechnie J, MacLean HL, Saville BA. Life cycle greenhouse gas impacts of ethanol, biomethane and limonene production from citrus waste. Environmental Research Letters. 2013;8(1):015007.

45. Kumar D, Murthy GS. Life cycle assessment of energy and GHG emissions during ethanol production from grass straws using various pretreatment processes. The International Journal of Life Cycle Assessment. 2012;17(4):388-401.

46. Amaya-Santos G, Chari S, Sebastiani A, Grimaldi F, Lettieri P, Materazzi M. Biohydrogen: A life cycle assessment and comparison with alternative low-carbon production routes in UK. Journal of Cleaner Production. 2021;319:128886.

47. Peters JF, Iribarren D, Dufour J. Simulation and life cycle assessment of biofuel production via fast pyrolysis and hydroupgrading. Fuel. 2015;139:441-56.

48. Zhang Y, Hu G, Brown RC. Life cycle assessment of commodity chemical production from forest residue via fast pyrolysis. The International Journal of Life Cycle Assessment. 2014;19(7):1371-81.

49. IEA Data and statistic: Total energy supply (TES) by source, World 1990-2018: International Energy Agency; [cited 2021 February 17]. Available from: https://www.iea.org/data-and-statistics?country=WORLD&fuel=Energy%20supply&indicator=TPESbySource.

50. Hannah R. Energy Production and Consumption [cited 2021 February 17]. Available from: https://ourworldindata.org/energy-production-consumption.

51. Morales M, Quintero J, Conejeros R, Aroca G. Life cycle assessment of lignocellulosic bioethanol: Environmental impacts and energy balance. Renewable and Sustainable Energy Reviews. 2015;42:1349-61.

52. Dassanayake GDM, Kumar A. Techno-economic assessment of triticale straw for power generation. Applied Energy. 2012;98:236-45.

53. Williams CL, Emerson RM, Hernandez S, Klinger JL, Fillerup EP, Thomas BJ. Preprocessing and Hybrid Biochemical/Thermochemical Conversion of Short Rotation Woody Coppice for Biofuels. 2018;6(74).

54. Patel M, Zhang X, Kumar A. Techno-economic and life cycle assessment on lignocellulosic biomass thermochemical conversion technologies: A review. Renewable and Sustainable Energy Reviews. 2016;53:1486-99.

55. Pootakham T, Kumar A. Bio-oil transport by pipeline: A techno-economic assessment. Bioresource Technology. 2010;101(18):7137-43.

56. Brassard P, Godbout S, Lévesque V, Palacios JH, Raghavan V, Ahmed A, et al. 4 - Biochar for soil amendment. In: Jeguirim M, Limousy L, editors. Char and Carbon Materials Derived from Biomass: Elsevier; 2019. p. 109-46.

57. Akbari M, Oyedun AO, Kumar A. Techno-economic assessment of wet and dry torrefaction of biomass feedstock. Energy. 2020;207:118287.

58. Pardo-Planas O, Atiyeh HK, Phillips JR, Aichele CP, Mohammad S. Process simulation of ethanol production from biomass gasification and syngas fermentation. Bioresource Technology. 2017;245:925-32.

59. Statistical data: Forest inventory Canada [cited 2021 July 23]. Available from: https://cfs.nrcan.gc.ca/statsprofile/inventory/canada.

60. Rogers JG, Brammer JG. Estimation of the production cost of fast pyrolysis bio-oil. Biomass and Bioenergy. 2012;36:208-17.

61. Jafari Naimi L. A study of cellulosic biomass size reduction: University of British Columbia; 2016.

62. Chaudhari ST, Bej SK, Bakhshi NN, Dalai AK. Steam gasification of biomass-derived char for the production of carbon monoxide-rich synthesis gas. Energy & Fuels. 2001;15(3):736-42.

63. Dutta A, Talmadge M, Hensley J, Worley M, Dudgeon D, Barton D, et al. Process design and economics for conversion of lignocellulosic biomass to ethanol: thermochemical pathway by indirect gasification and mixed alcohol synthesis. National Renewable Energy Lab.(NREL), Golden, CO (United States); 2011.

64. Burhenne L, Damiani M, Aicher T. Effect of feedstock water content and pyrolysis temperature on the structure and reactivity of spruce wood char produced in fixed bed pyrolysis. Fuel. 2013;107:836-47.

65. Phillips JR, Huhnke RL, Atiyeh HKJF. Syngas fermentation: a microbial conversion process of gaseous substrates to various products. 2017;3(2):28.

66. Liberato V, Benevenuti C, Coelho F, Botelho A, Amaral P, Pereira N, et al. Clostridium sp. as Bio-Catalyst for Fuels and Chemicals Production in a Biorefinery Context. Catalysts. 2019;9(11).

67. Drake HL, Gößner AS, Daniel SL. Old Acetogens, New Light. Annals of the New York Academy of Sciences. 2008;1125(1):100-28.

68. Peng Y, Lu X, Liu B, Zhu J. Separation of azeotropic mixtures (ethanol and water) enhanced by deep eutectic solvents. Fluid Phase Equilibria. 2017;448:128-34.

69. Bernardo G, Araújo T, da Silva Lopes T, Sousa J, Mendes A. Recent advances in membrane technologies for hydrogen purification. International Journal of Hydrogen Energy. 2020;45(12):7313-38.

70. Nordio M, Wassie SA, Van Sint Annaland M, Pacheco Tanaka DA, Viviente Sole JL, Gallucci F. Techno-economic evaluation on a hybrid technology for low hydrogen concentration separation and purification from natural gas grid. International Journal of Hydrogen Energy. 2020.

71. Fahim MA, Alsahhaf TA, Elkilani A. Chapter 11 - Hydrogen Production. In: Fahim MA, Alsahhaf TA, Elkilani A, editors. Fundamentals of Petroleum Refining. Amsterdam: Elsevier; 2010. p. 285-302.

72. Banu A-M, Friedrich D, Brandani S, Düren T. A Multiscale Study of MOFs as Adsorbents in H2 PSA Purification. Industrial & Engineering Chemistry Research. 2013;52(29):9946-57.

73. Speight JG. Chapter 15 - Hydrogen Production. In: Speight JG, editor. Heavy Oil Recovery and Upgrading: Gulf Professional Publishing; 2019. p. 657-97.

74. Allevi C, Collodi G. 12 - Hydrogen production in IGCC systems. In: Wang T, Stiegel G, editors. Integrated Gasification Combined Cycle (IGCC) Technologies: Woodhead Publishing; 2017. p. 419-43.

75. Akbari M, Oyedun AO, Kumar A. Ammonia production from black liquor gasification and co-gasification with pulp and waste sludges: A techno-economic assessment. Energy. 2018;151:133-43.

76. Recharge: Green hydrogen' on sale in open market at 80% higher price than grey H2 2020 [cited 2020 October 21].

77. Argusmedia: US VGO touches six-month high 2020 [cited 2021 December 13]. Available from: https://www.argusmedia.com/en/news/2138029-us-vgo-touches-sixmonth-high.

78. Ethanol Commodity: Markets Insider [cited 2021 October 21]. Available from: https://markets.businessinsider.com/commodities/ethanol-price.

79. Akbari M, Oyedun AO, Jain S, Kumar A. Options for the conversion of pulp and paper mill by-products in Western Canada. Sustainable Energy Technologies and Assessments. 2018;26:83-92.

80. Multi-residential and commercial rates: EPCOR 2019 [cited 2019 November 1]. Available from: https://www.epcor.com/products-services/water/rates-terms-conditions/Pages/commercial-multi-residential-rates.aspx.

81. Canada Energy Regulator. Canada's Energy Future Data Appendices 2017 [cited 2020 January 1]. Available from: https://apps.cer-rec.gc.ca/ftrppndc/dflt.aspx?GoCTemplateCulture=en-CA.

82. Spath P, Aden A, Eggeman T, Ringer M, Wallace B, Jechura J. Biomass to hydrogen production detailed design and economics utilizing the Battelle Columbus Laboratory indirectly-heated gasifier. National Renewable Energy Lab., Golden, CO (US); 2005.

83. Canada salary calculator: CanadaVisa 2016 [cited 2020 November 20]. Available from: http://www.canadavisa.com/canada-salary-wizard.html.

84. Akbari M, Oyedun AO, Kumar A. Comparative energy and techno-economic analyses of two different configurations for hydrothermal carbonization of yard waste. Bioresource Technology Reports. 2019;7:100210.

85. Humbird D, Davis R, McMillan JD. Aeration costs in stirred-tank and bubble column bioreactors. Biochemical Engineering Journal. 2017;127:161-6.

86. Kreutz T, Williams R, Consonni S, Chiesa P. Co-production of hydrogen, electricity and CO2 from coal with commercially ready technology. Part B: Economic analysis. International Journal of Hydrogen Energy. 2005;30(7):769-84.

87. Larson ED, Jin H, Celik FE. Large-scale gasification-based coproduction of fuels and electricity from switchgrass. 2009;3(2):174-94.

88. Di Lullo G, Gemechu E, Oni AO, Kumar A. Extending sensitivity analysis using regression to effectively disseminate life cycle assessment results. The International Journal of Life Cycle Assessment. 2020;25(2):222-39.

89. Piccolo C, Bezzo F. A techno-economic comparison between two technologies for bioethanol production from lignocellulose. Biomass and Bioenergy. 2009;33(3):478-91.

90. Michailos S, Parker D, Webb C. Design, Sustainability Analysis and Multiobjective Optimisation of Ethanol Production via Syngas Fermentation. Waste and Biomass Valorization. 2019;10(4):865-76.

91. Shabangu S, Woolf D, Fisher EM, Angenent LT, Lehmann J. Techno-economic assessment of biomass slow pyrolysis into different biochar and methanol concepts. Fuel. 2014;117:742-8.

92. Dickinson D, Balduccio L, Buysse J, Ronsse F, van Huylenbroeck G, Prins W. Cost-benefit analysis of using biochar to improve cereals agriculture. GCB Bioenergy. 2015;7(4):850-64.

93. Campbell RM, Anderson NM, Daugaard DE, Naughton HT. Financial viability of biofuel and biochar production from forest biomass in the face of market price volatility and uncertainty. Applied Energy. 2018;230:330-43.

94. Shemfe MB, Gu S, Ranganathan P. Techno-economic performance analysis of biofuel production and miniature electric power generation from biomass fast pyrolysis and bio-oil upgrading. Fuel. 2015;143:361-72.

95. Draper K, Groot H, Miles T, Twer M. Survey and Analysis of the US Biochar Industry Preliminary Report Draft; August 16, 2018, WERC Project MN17-DG-230.

96. Biochar Market Size, Share & Trends Analysis Report By Technology (Gasification, Pyrolysis), By Application (Agriculture (Farming, Livestock)), By Region, And Segment Forecasts, 2019 - 2025: Grand View Research; [cited 2021 February 19]. Available from: https://www.grandviewresearch.com/industry-analysis/biochar-market#:~:text=The%20global%20biochar%20market%20size,be%20the%20key%20growth%20driver.

97. Towler G, Sinnott R. Chapter 7 - Capital Cost Estimating. In: Towler G, Sinnott R, editors. Chemical Engineering Design (Second Edition). Boston: Butterworth-Heinemann; 2013. p. 307-54.

98. Franczyk A. Using the Morris sensitivity analysis method to assess the importance of input variables on time-reversal imaging of seismic sources. Acta Geophysica. 2019;67(6):1525-33.

99. IEA Data and statistics: Total energy supply (TES) by source, World 1990-2018: International Energy Agency; [cited 2021 February 17]. Available from: https://www.iea.org/data-and-statistics?country=WORLD&fuel=Energy%20supply&indicator=TPESbySource.

100. Ritchie H, Roser M. Why did renewables become so cheap so fast? : Our World In Data; 2021 [Available from: https://ourworldindata.org/cheap-renewables-growth.

101. Ajao O, Benali M, Faye A, Li H, Maillard D, Ton-That MT. Multi-product biorefinery system for wood-barks valorization into tannins extracts, lignin-based polyurethane foam and cellulose-based composites: Techno-economic evaluation. Industrial Crops and Products. 2021;167:113435.

102. Dávila I, Gullón B, Labidi J, Gullón P. Multiproduct biorefinery from vine shoots: Bio-ethanol and lignin production. Renewable Energy. 2019;142:612-23.

103. Liu Z, Wan X, Wang Q, Tian D, Hu J, Huang M, et al. Performances of a multi-product strategy for bioethanol, lignin, and ultra-high surface area carbon from lignocellulose by PHP (phosphoric acid plus hydrogen peroxide) pretreatment platform. Renewable and Sustainable Energy Reviews. 2021;150:111503.

104. Hu X, Gholizadeh M. Progress of the applications of bio-oil. Renewable and Sustainable Energy Reviews. 2020;134:110124.

105. Acar C, Dincer I. 4.24 Hydrogen Energy Conversion Systems. In: Dincer I, editor. Comprehensive Energy Systems. Oxford: Elsevier; 2018. p. 947-84.

106. Bruun EW. Application of Fast Pyrolysis Biochar to a Loamy soil-Effects on carbon and nitrogen dynamics and potential for carbon sequestration. 2011.

107. Liu P, Liu W-J, Jiang H, Chen J-J, Li W-W, Yu H-Q. Modification of biochar derived from fast pyrolysis of biomass and its application in removal of tetracycline from aqueous solution. Bioresource Technology. 2012;121:235-40.

108. Phillips JR, Huhnke RL, Atiyeh HK. Syngas Fermentation: A Microbial Conversion Process of Gaseous Substrates to Various Products. Fermentation. 2017;3(2).

109. Giwa T, Akbari M, Kumar A. Techno-economic assessment of an integrated biorefinery producing bio-oil, ethanol, and hydrogen. Under review. 2022.

110. Dias AC. Life cycle assessment of fuel chip production from eucalypt forest residues. The International Journal of Life Cycle Assessment. 2014;19(3):705-17.

111. Nie Y, Bi X. Life-cycle assessment of transportation biofuels from hydrothermal liquefaction of forest residues in British Columbia. Biotechnology for Biofuels. 2018;11(1):23.

112. Sultana A, Kumar A, Harfield D. Development of agri-pellet production cost and optimum size. Bioresource Technology. 2010;101(14):5609-21.

113. Sarkar S, Kumar A. Biohydrogen production from forest and agricultural residues for upgrading of bitumen from oil sands. Energy. 2010;35(2):582-91.

114. Wang Z, Dunn JB, Han J, Wang MQ. Material and energy flows in the production of cellulosic feedstocks for biofuels for the GREET model. Argonne National Lab.(ANL), Argonne, IL (United States); 2013.

115. Hawley D. How Much Does a Semi Truck Weigh? USA: J.D. POWER; 2021 [cited 2021 October 5]. Available from: https://www.jdpower.com/cars/shopping-guides/how-much-does-a-semi-truck-weigh#:~:text=The%20unladen%20weight%20of%20a,weight%20of%20about%2035%2C000%20pounds.

116. Fact #621: May 3, 2010 Gross Vehicle Weight vs. Empty Vehicle Weight: Office of Energy Efficiency and Renewable Energy; 2010 [cited 2021 September 5]. Available from:

https://www.energy.gov/eere/vehicles/fact-621-may-3-2010-gross-vehicle-weight-vs-empty-vehicle-weight.

117. Jafari Naimi L. A study of cellulosic biomass size reduction [PhD Thesis]. Vancouver: University of British Columbia; 2016.

118. Banu A-M, Friedrich D, Brandani S, Düren TJI, Research EC. A multiscale study of MOFs as adsorbents in H2 PSA purification. 2013;52(29):9946-57.

119. Idris I, Abdullah A, Shamsudin IK, Othman MR. Optimizing purity and recovery of hydrogen from syngas by equalized pressure swing adsorption using palm kernel shell activated carbon adsorbent. AIP Conference Proceedings. 2019;2124(1):020059.

120. Dagdougui H, Sacile R, Bersani C, Ouammi A. Chapter 4 - Hydrogen storage and distribution: implementation scenarios. In: Dagdougui H, Sacile R, Bersani C, Ouammi A, editors. Hydrogen Infrastructure for Energy Applications: Academic Press; 2018. p. 37-52.

121. Aakko-Saksa PT, Cook C, Kiviaho J, Repo T. Liquid organic hydrogen carriers for transportation and storing of renewable energy – Review and discussion. Journal of Power Sources. 2018;396:803-23.

122. Yang C, Ogden J. Determining the lowest-cost hydrogen delivery mode. International Journal of Hydrogen Energy. 2007;32(2):268-86.

123. Hydrogen tube trailer - 9 tubes, DOT 3AAZ, 2400 psi, 40ft: City Machine & Welding Inc.; 2021 [cited 2021 September 21]. Available from: http://cmwelding.com/configuration/hydrogen-h2-tube-trailer-9-tubes-dot-3aax-2400psi-40-ft.

124. HYDROGEN TUBE TRAILER - 9 TUBES DOT 3AAX 2400 PSI 40 FT: City Machine & Welding, Inc; 2021 [cited 2021 September 20]. Available from: http://cmwelding.com/configuration/hydrogen-h2-tube-trailer-9-tubes-dot-3aax-2400psi-40-ft.

125. Akbari M, Oyedun AO, Gemechu E, Kumar A. Comparative life cycle energy and greenhouse gas footprints of dry and wet torrefaction processes of various biomass feedstocks. Journal of Environmental Chemical Engineering. 2021;9(4):105415.

126. Xu Y, Hu X, Li W, Shi YJPib, production b. Preparation and characterization of bio-oil from biomass. 2011:197-222.

127. Nimana B, Verma A, Di Lullo G, Rahman MM, Canter CE, Olateju B, et al. Life Cycle Analysis of Bitumen Transportation to Refineries by Rail and Pipeline. Environ Sci Technol. 2017;51(1):680-91.

128. Davis M, Moronkeji A, Ahiduzzaman M, Kumar AJEfSD. Assessment of renewable energy transition pathways for a fossil fuel-dependent electricity-producing jurisdiction. 2020;59:243-61.

129. National Inventory Report 1990–2018: Greenhouse Gas Sources and Sinks in Canada Environment and Climate Change Canada; 2020 [Available from: http://publications.gc.ca/site/eng/9.816345/publication.html.

130. Canada's Energy Future 2020: Energy Supply and Demand Projections to 2050 2020: Canada Energy Regulator; 2020 [Available from: https://www.cer-rec.gc.ca/en/data-analysis/canada-energy-future/2020/index.html.

131. Masoudi Soltani S, Lahiri A, Bahzad H, Clough P, Gorbounov M, Yan Y. Sorption-enhanced steam methane reforming for combined CO_2 capture and hydrogen production: A state-of-the-art review. Carbon Capture Science & Technology. 2021;1:100003.

132. Oni AO, Anaya K, Giwa T, Di Lullo G, Kumar A. Comparative assessment of blue hydrogen from steam methane reforming, autothermal reforming, and natural gas decomposition technologies for natural gas-producing regions. Energy Conversion and Management. 2022;254:115245.

133. Di Lullo G, Zhang H, Kumar A. Evaluation of uncertainty in the well-to-tank and combustion greenhouse gas emissions of various transportation fuels. Applied Energy. 2016;184:413-26.

134. Petroleum & Other liquids: Weekly Retail Gasoline and Diesel Prices: U.S. Energy Information Agency; [cited 2021 February 26]. Available from: https://www.eia.gov/dnav/pet/pet_pri_gnd_dcus_nus_a.htm.

135. Global 20 Ports Average: Shipandbunker.com; [cited 2022 January 28]. Available from: https://shipandbunker.com/prices/av/global/av-g20-global-20-ports-average.